

**Implementation and validation of
in vitro methodologies for phototoxicity
evaluation of raw materials of
pharmaceutical and cosmetic products**

Bruna Catarina de Freitas Maciel

Dissertation of the 2nd Cycle of Studies Conducive to Master
Degree in Analytical, Clinical and Forensic Toxicology.

Project realized under the supervision of:

Professor Doctor Isabel Almeida- Laboratory of Pharmaceutical Technology

Professor Doctor Helena Carmo- Laboratory of Toxicology

Porto, October 2016

It is allowed the complete reproduction of this dissertation only for research purposes through a written declaration of the person concerned that such pledge.

Acknowledgements

O sucesso de um grande trabalho nunca se obtém por conta própria, existem pessoas que muito nos apoiam, nos ajudam, nos devolvem a esperança nos momentos certos e não nos deixam desistir. Os momentos de desespero, alegria e angústia foram passados juntos de pessoas às quais não poderia deixar de agradecer.

Em primeiro lugar às minhas orientadoras Prof. Dr. Isabel Almeida e Prof. Dr. Helena Carmo por todo o conhecimento científico, por apoiarem o meu trabalho, por me fazerem crescer quer a nível científico quer a nível pessoal, por partilharem a sua vasta experiência e conhecimento comigo, por me ouvirem nos momentos de desespero, não me deixarem desanimar e ouvirem as minhas dúvidas. Aprendi muito com elas e levo os seus ensinamentos para a vida.

Ao Prof. Dr. Domingos Ferreira e ao Prof. Dr. José Sousa Lobo, os mais sinceros agradecimentos por me proporcionarem as melhores condições laboratoriais para a realização de todo trabalho laboratorial e a todos os Professores e técnicos do laboratório de Tecnologia Farmacêutica da Faculdade de Farmácia da Universidade do Porto por me acolherem da melhor forma. À Professora Doutora Emília Sousa e à Professora Doutora Marta Correia-da-Silva agradeço a cedência dos compostos obtidos por síntese química.

À Mestre Verónica Rocha e Dr. Diana Silva por serem um pilar no trabalho prático, por estarem sempre disponíveis para me ajudarem em qualquer dúvida ou problema, por me terem acompanhado e passado o testemunho do seu vasto conhecimento, sem estas duas pessoas não teria conseguido ter o trabalho que tenho hoje. Também à Beatriz Santos e Catarina Silva pela preciosa ajuda na prestada.

Aos meus colegas e amigos de Laboratório Ana Afonso, Jéssica Lopes, Alexandra Costa, Beatriz Santos, Carolina Peneda, Isabel Malta e Ogbonna John por estarem sempre presentes, ouvirem as minhas angústias e me darem conselhos que me fizeram seguir em frente e nunca desistir perante as adversidades. Um especial agradecimento à Bárbara Pereira e Rui Faria por me aturarem, ouvirem, ajudarem e acima de tudo por todas as boas memórias que me proporcionaram, levo-as para a vida!

À Daniela Correia um “obrigada!” do tamanho do mundo pelo grande caminho que percorremos juntas até à entrega de uma dissertação de mestrado, foi uma licenciatura, dúvidas, alegrias, sucessos, tristezas, mas acima de tudo uma amizade para a vida. Além

disto, por sempre me ajudar a ver os resultados de outra perspectiva e por partilharmos a nossa experiência científica.

À Inês Mateus, à Cientuna e a todos os demais amigos que me acompanharam, um agradecimento não chega porque sem eles não teria a força que tenho para enfrentar os problemas e encara-los com boa disposição.

Por fim, mas não menos importante, agradeço à minha família, em especial aos meus pais, a quem dedico esta dissertação. Por todo o esforço que sempre fizeram para me proporcionar o melhor futuro possível, pois sem eles não teria as oportunidades que tenho, como a realização de um mestrado. Além disso, agradeço também por toda a paciência e compreensão que demonstram para comigo, mesmo em momentos mais difíceis.

“The only way to do great work
is to love what you do”
Steve Jobs

Abstract

The skin is the largest organ and the main barrier between the environment and the internal organs. Therefore, it is constantly exposed to deleterious effects of solar radiation which might be exacerbated by photosensitizer compounds. These compounds are capable of absorbing radiation between 290 and 700 nm, causing dermal reactions, through phenomena known as photosensitivity. It is known that ROS generation is one of the mechanisms involved in photosensitivity events. Several *in vitro* methods have been developed to assess phototoxicity including the 3T3 neutral red uptake phototoxicity test (3T3 NRU-PT) which is conducted with mouse fibroblasts. However, when a compound is applied on the skin, it is firstly exposed to keratinocytes and therefore testing phototoxicity in a human keratinocyte cell line would be more appropriate for a feasible methodology.

The aim of the present study was to implement a phototoxicity assay in a human keratinocyte cell line (HaCaT) based on the 3T3 Neutral Red Uptake Phototoxicity assay (3T3 NRU-PT), using a UVA/UVB Osram lamp, and to evaluate the phototoxic potential of a series of raw materials for cosmetic and pharmaceutical products with the developed methodology. A complementary aim was to perform preliminary tests regarding the implementation of a phototoxicity test using oxidative stress measures (total glutathione-tGSH- and reactive oxygen species –ROS- generation) as endpoints. In order to optimize the NRU-PT assay, some parameters were analyzed such as optimal cell density and the neutral red dye concentration and incubation time. The irradiation dose and temperature, and HaCaT sensitivity to radiation were also evaluated. For validation purposes, chlorpromazine, quinine and 5-methoxypsoralen (5-MOP) were used as positive controls while sodium lauryl sulphate, hexachlorophene and acetylsalicylic acid were used as negative controls. The ability of the test compounds to generate ROS was analyzed using the 2',7'-dichlorodihydrofluorescein diacetate (DCFH-DA) probe assay after 24h compound exposures, following optimization of probe concentration and incubation time. Using the test conditions previously optimized, generation of ROS and tGSH were studied as putative predictors of phototoxic potential after irradiation.

The radiation intensity recommended by the Organisation for Economic Co-operation and Development (OCDE) 432 guideline is 1.7mW/cm², which corresponded to the irradiation obtained with the lamp positioned at 46.5cm height. The keratinocyte cell line was sensitive to UV exposure and irradiation times longer than 15 min were cytotoxic. A period of 10 min, corresponding to cell viability of $77 \pm 2.94\%$, was established as the optimal irradiation time. The optimization of the NR assay demonstrated that the ideal

concentration of the NR was 50 µg/mL (with 3h incubation time) and HaCaT cell density of 2×10^5 cell/well. For chlorpromazine, 5-MOP and quinine the calculated photo irritation factor (PIF) values were 23.30 ± 2.69 , 78.8 ± 5.11 and 2.09 ± 0.85 , respectively. Regarding negative controls, sodium lauryl sulphate and hexachlorophene PIF values corresponded to 1.25 ± 0.53 and 1.03 ± 0.08 , respectively and acetylsalicylic acid PIF could not be obtained. When analyzing the phototoxicity of a series of test compounds, all were found to be non-phototoxic ($PIF \geq 2$) except the *C. sativa* extract that can be classified as a probable phototoxic ($PIF = 2.18 \pm 0.42$). Noteworthy, in some cases the PIF values could not be calculated and therefore the calculation of mean photo effect (MPE) should be performed for the elucidation of the phototoxic effect.

Regarding ROS generation assay, the optimal cell density and the DCFH-DA concentration and incubation time were optimized. Therefore, 2×10^5 cells/well, a concentration of 50 µM DCFH-DA and 30min incubation time appear to be the ideal conditions to this assay, since the fluorescence signal was high enough to ensure appropriate sensitivity. None of the compounds showed a marked ability to generate ROS in HaCaT cells after 24h compound exposure. With respect to the implementation of a phototoxicity test using oxidative stress measures (tGSH and ROS generation) as endpoints, the exploratory study performed puts in evidence the complexity of this evaluation and the need for further optimizations tests.

The modified neutral red assay developed here in was found to be a simple and reliable method for detecting phototoxic effects of reference agents and raw materials of topical formulations. Based on our data, the HaCaT-NRU-PT is a valuable *in vitro* model for the phototoxicity evaluation.

Resumo

A pele é o maior órgão do corpo e a principal barreira entre o ambiente circundante e os órgãos internos. Por isso, a pele está constantemente exposta à radiação solar podendo causar efeitos deletérios, que podem aumentar quando a exposição solar é combinada com compostos fotosensibilizadores. Estes compostos são compostos capazes de absorver radiação entre 290 e 700 nm, originando reações dérmicas num fenómeno denominado como fotossensibilidade. Está relatado que a formação de ROS é um dos mecanismos envolvido na ocorrência da fotossensibilidade. Muitos métodos *in vitro* têm sido desenvolvidos para avaliação da fototoxicidade, incluindo o ensaio 3T3 NRU-PT que é realizado em fibroblastos de rato. Contudo, quando um composto é aplicado na pele, primeiramente entra em contacto com os queratinócitos e assim, testes de fototoxicidade usando linhas celulares de queratinócitos humanos são metodologias viáveis.

O objetivo da presente dissertação foi a implementação de um ensaio de fototoxicidade numa linha celular de queratinócitos humanos (HaCaT) baseado no ensaio 3T3 NRU-PT com uma lâmpada UVA/UVB (Osram) e utilizando o método assim desenvolvido, avaliar o potencial fototóxico de uma série de matérias-primas e produtos farmacêuticos. Um objetivo complementar foi a realização de testes preliminares para a implementação de um teste de fototoxicidade usando a determinação do stresse oxidativo (formação de tGSH e ROS) como *endpoint*. No que diz respeito à otimização do ensaio NRU-PT, alguns parâmetros foram analisados, tais como, a densidade celular ideal, concentração do corante NR e o respetivo tempo de incubação. A dose e temperatura da irradiação e a sensibilidade da HaCaT à mesma, foram também parâmetros avaliados. Para fins de validação, a clorpromazina, quinina e 5-MOP foram usados como controlos positivos, enquanto o lauril sulfato de sódio, hexaclorofeno e ácido acetilsalicílico foram usados como controlos negativos. A capacidade destes compostos para formar ROS foi analisada usando um ensaio com a sonda DCFH-DA depois de uma exposição de 24h com o composto. Para tal, uma prévia otimização da concentração da sonda e do seu tempo de incubação foi realizada. Usando as condições otimizadas anteriormente, a formação de ROS e tGSH foram estudadas como uma predição putativa do potencial fototóxico depois da irradiação.

A intensidade de radiação recomendada na norma 432 da OCDE é $1,7\text{mW}/\text{cm}^2$, o que corresponde à radiação obtida quando a lâmpada é colocada a 46,5 cm de altura. A linha celular de queratinócitos mostrou-se sensível à exposição UV e tempos superiores ou iguais a 15 min demonstraram citotoxicidade. Assim, um período de 10 min que corresponde a $77 \pm 2,94\%$ de viabilidade celular foi estabelecido como o tempo de irradiação ideal. A

otimização do ensaio NR demonstrou que a concentração ideal de NR é 50 µg/mL (com um tempo de incubação de 3h) e uma densidade celular da HaCaT de 2×10^5 células/poço. Para a clorpromazina, 5-MOP e quinina os valores de PIF calculados foram $23,30 \pm 2,69$, $78,8 \pm 5,11$ e $2,09 \pm 0,85$, respetivamente. No que diz respeito aos controlos negativos, os valores de PIF do lauril sulfato de sódio e hexaclorofeno foram $1,25 \pm 0,53$ e $1,03 \pm 0,08$, respetivamente e não foi possível obter o PIF do ácido acetilsalicílico. Quando foi analisada a fototoxicidade de uma série de compostos, todos se mostraram como não fototóxicos ($PIF \geq 2$), exceto o extrato de *C. sativa* que pode ser classificado como provavelmente fototóxico ($PIF = 2,18 \pm 0,42$). Deve ser levado em conta que em alguns casos o valor de PIF não pôde ser calculado e assim, o cálculo do MPE seria um importante fator para elucidar o efeito fototóxico destes compostos.

Relativamente ao ensaio da formação de ROS, foram avaliados alguns parâmetros, como por exemplo, a densidade celular ideal, a concentração de DCFH-DA e o respetivo tempo de incubação. Assim, 2×10^5 células/poço, uma concentração de DCFH-DA de 50 µM e um tempo de incubação de 30 min aparentam ser as condições ideais para este ensaio, uma vez que o sinal da fluorescência é alto o suficiente para assegurar uma sensibilidade apropriada do ensaio. Nenhum dos compostos mostrou uma capacidade relevante para formar ROS depois de uma exposição de 24h aos compostos em células HaCaT. No que diz respeito à implementação de um teste de fototoxicidade avaliando a quantidade de stresse oxidativo (formação de tGSH e ROS) como *endpoints*, o estudo exploratório evidencia a complexidade desta avaliação e a necessidade de testes de otimização mais aprofundados no futuro.

O ensaio de NR modificado desenvolvido nesta dissertação mostrou ser um método simples e confiável para detetar os efeitos fototóxicos dos referidos agente e matérias-primas de formulação tópica. Além disso, com base nos nossos dados, o HaCaT NRU-PT é uma modelo *in vitro* mais realista para a avaliação da fototoxicidade.

Index

1. Introduction.....	1
1.1. Skin.....	1
1.1.1. Epidermis.....	2
1.1.2. Dermis.....	4
1.1.3. Hypodermis.....	5
1.2. Solar radiation.....	5
1.3. Photosensitivity.....	6
1.3.1. Phototoxicity/photoirritation.....	6
1.3.2. Photoallergy.....	8
1.3.3. Photogenotoxicity/photomutagenicity.....	8
1.3.4. Photocarcinogenicity.....	8
1.4. Mechanisms of photosensitivity reactions.....	8
1.5. Photosensitizers.....	10
1.5.1. Cosmetics.....	11
1.5.2. Drugs.....	12
1.6. Photosafety evaluation.....	13
1.6.1. Regulatory aspects.....	15
1.7. Phototoxicity evaluation.....	18
1.7.1. Spectral absorption.....	18
1.7.2. Light source and irradiation conditions.....	18
1.7.3. Phototoxicity testing.....	19
1.7.4. <i>In vitro</i> assays.....	20

1.7.5.	<i>In vivo</i> assays	25
1.8.	Analyzed compounds	26
1.8.1.	Positive controls	27
1.8.2.	Negative controls	29
1.8.1.	Raw compounds.....	31
2.	Aim.....	36
3.	Materials and methods	36
3.1.	Materials.....	36
3.1.1.	Raw materials.....	36
3.1.2.	Laboratory materials.....	37
3.2.	Methods.....	37
3.2.1.	Cell culture	37
3.2.2.	Implementation and optimization of phototoxicity <i>in vitro</i> test.....	38
3.2.3.	Phototoxicity study	40
3.2.4.	Statistical analysis	45
4.	Results and discussion	46
4.1.	HaCat cell line characterization	46
4.2.	ROS generation assay	46
4.2.1.	Solvent control	46
4.2.2.	ROS generation assay optimization	47
4.2.3.	ROS generation using DCFH-DA.....	48
4.3.	Neutral red uptake assay	54
4.3.1.	Solvent control	54
4.3.2.	Neutral red uptake assay optimization	55

4.3.3.	Neutral red uptake cytotoxicity test.....	56
4.4.	Implementation and validation of a phototoxicity assay using HaCaT	61
4.4.1.	Solvent control	61
4.4.2.	Spectral absorption	61
4.4.3.	Optimization of irradiation conditions	63
4.4.4.	Neutral red uptake phototoxicity test	64
4.4.5.	Optimization of UV-mediated ROS generation assay using DCFH-DA with a positive control	77
4.4.6.	Validation of UV-mediated ROS generation assay using DCFH-DA with a positive control	80
4.4.7.	Study of quinine HCL in total glutathione (tGSH)) by DTNB-GSSG reductase recycling assay with irradiation	81
5.	Conclusions	82
6.	References	84

Figure Index

Figure 1. Skin structure.....	1
Figure 2. Structure of epidermis.....	2
Figure 3. Histological section of human skin epithelium.....	3
Figure 4. Structure of dermis.....	4
Figure 5. Solar spectrum.....	5
Figure 6. Mechanisms involved in photosensitivity	9
Figure 7. Energy states involved in mechanisms of phototoxicity	10
Figure 8. Hazard identification of photosensitivity.....	14
Figure 9. Experimental test procedure of the 3T3 NRU phototoxicity	22
Figure 10. Conversion of DCFH-DA into DCF.....	24
Figure 11. Chemical structure of 5-MOP.....	27
Figure 12. Chemical structure of CPZ.	28
Figure 13. Chemical structure of H ₂ O ₂	28
Figure 14. Chemical structure of Quinine HCl	29
Figure 15. . Chemical structure of ASA	29
Figure 16. Chemical structure of hexachlorophene.	30
Figure 17. Chemical formula of SLS.....	30
Figure 18. Chemical structure of 1,2-DHX	31
Figure 19. Chemical structure of Avobenzone.	32
Figure 20. A) Chemical structure of CA; B) Chemical structure of CAP	32
Figure 22. Chemical structure of Diclofenac	33
Figure 23. Chemical structure of EHMC	34

Figure 24. A) Chemical structure of RSV; B) Chemical structure of RGS.....	35
Figure 24. Determination of HaCaT cells doubling time	46
Figure 25. Fluorescence of HaCaT cell line exposed to solvent control by the Neutral Red by the DCFH-DA assay	47
Figure 26. Optimization of ROS generation assay with fluorescence regarding cell density, DCFH-DA concentration, incubation time and positive control (H ₂ O ₂) concentration	47
Figure 27. ROS detection in HaCaT cell line exposed to H ₂ O ₂ by the DCFH-DA assay	48
Figure 28. ROS detection in HaCaT cell line exposed to Quinine HCl by the DCFH-DA assay.	48
Figure 29. ROS detection in HaCaT cell line exposed to 1,2-DHX by the DCFH-DA assay.	49
Figure 30. ROS detection in HaCaT cell line exposed to 5-MOP by the DCFH-DA assay ..	49
Figure 31. ROS detection in HaCaT cell line exposed to ASA by the DCFH-DA assay	50
Figure 32. ROS detection in HaCaT cell line exposed to Avobenzone by the DCFH-DA assay	50
Figure 33. ROS detection in HaCaT cell line exposed to <i>C. sativa</i> extract by the DCFH-DA assay	51
Figure 34. ROS detection in HaCaT cell line exposed to CPZ by the DCFH-DA assay	51
Figure 35. ROS detection in HaCaT cell line exposed to Diclofenac by the DCFH-DA assay	52
Figure 36. ROS detection in HaCaT cell line exposed to EHMC by the DCFH-DA assay...	52
Figure 37. ROS detection in of HaCaT cell line exposed to Hexachlorophene by the DCFH-DA assay.....	53
Figure 38. ROS detection in HaCaT cell line exposed to RSV by the DCFH-DA assay.....	53
Figure 39. ROS detection in HaCaT cell line exposed to SLS by the DCFH-DA assay.....	54
Figure 40. Cell viability of HaCaT cell line exposed to solvent control by the Neutral Red assay.....	54

Figure 41. Observation under inverted microscope of HaCaT cells incubated with 100 µg/mL NR solution	55
Figure 42. Optimization of NR uptake assay with absorbance regarding cell density, NR concentration and incubation time	55
Figure 43. Cell viability of HaCaT cell line exposed to 5-MOP by the Neutral Red assay....	56
Figure 44. Cell viability of HaCaT cell line exposed to ASA by the Neutral Red assay	56
Figure 45. Cell viability of HaCaT cell line exposed to Avobenzone by the Neutral Red assay	57
Figure 46. Cell viability of HaCaT cell line exposed to CPZ by the Neutral Red assay	57
Figure 47. Cell viability of HaCaT cell line exposed to Diclofenac by the Neutral Red assay	58
Figure 48. Cell viability of HaCaT cell line exposed to EHMC by the Neutral Red assay ...	58
Figure 49. Cell viability of HaCaT cell line exposed to Hexachlorophene by the Neutral Red assay	59
Figure 50. Cell viability of HaCaT cell line exposed to H ₂ O ₂ by the Neutral Red assay	59
Figure 51. Cell viability of HaCaT cell line exposed to Quinine HCl by the Neutral Red assay	60
Figure 52. Cell viability of HaCaT cell line exposed to SLS by the Neutral Red assay	60
Figure 53. Cell viability of HaCaT cell line exposed to solvent control at plate A) not irradiate and B) irradiate by the Neutral Red assay	61
Figure 54. <i>C. sativa</i> spectral absorption.....	61
Figure 55. CPZ spectral absorption.....	61
Figure 56. Quinine HCl spectral absorption.....	62
Figure 57. SLS spectral absorption.....	62
Figure 58. Hexachlorophene spectral absorption.....	62
Figure 59. ASA spectral absorption.....	62

Figure 60. Diclofenac spectral absorption.....	62
Figure 61. EHMC spectral absorption.....	62
Figure 62. 1,2-DHX spectral absorption.....	62
Figure 63. 5-MOP spectral absorption.....	62
Figure 64. Avobenzone spectral absorption.....	63
Figure 65. RSV spectral absorption.	63
Figure 66. H ₂ O ₂ spectral absorption.....	63
Figure 67. RGS spectral absorption.....	63
Figure 68. UVA/UVB Osram lamp	64
Figure 69. Temperature achieved using a water-cooling. and radiometer used in this work	64
Figure 70. Viability of HaCaT cells exposed to UVA/UVB radiation, determined by the Neutral Red assay	64
Figure 71. Cell viability of HaCaT cell line exposed to 5-MOP, determining the phototoxicity by the Neutral Red assay	65
Figure 72. Cell viability of HaCaT cell line exposed to CPZ, determining the phototoxicity by the Neutral Red assay	66
Figure 73. Cell viability of HaCaT cell line exposed to Quinine HCl, determining the phototoxicity by the Neutral Red assay	67
Figure 74. Cell viability of HaCaT cell line exposed to ASA, determining the phototoxicity by the Neutral Red assay.	68
Figure 75. Cell viability of HaCaT cell line exposed to Hexachlorophene, determining the phototoxicity by the Neutral Red assay	68
Figure 76. Cell viability of HaCaT cell line exposed to SLS, determining the phototoxicity by the Neutral Red assay	69
Figure 77. Cell viability of HaCaT cell line exposed to 1,2-DHX, determining the phototoxicity by the Neutral Red assay	70

Figure 78. Cell viability of HaCaT cell line exposed to Avobenzone, determining the phototoxicity by the Neutral Red assay	70
Figure 79. Cell viability of HaCaT cell line exposed to <i>C.sativa</i> , determining the phototoxicity by the Neutral Red assay	71
Figure 80. Cell viability of HaCaT cell line exposed to CA, determining the phototoxicity by the Neutral Red assay	71
Figure 81. Cell viability of HaCaT cell line exposed to CAP, determining the phototoxicity by the Neutral Red assay	72
Figure 82. Cell viability of HaCaT cell line exposed to Diclofenac, determining the phototoxicity by the Neutral Red assay	73
Figure 83. Cell viability of HaCaT cell line exposed to EHMC, determining the phototoxicity by the Neutral Red assay	73
Figure 84. Cell viability of HaCaT cell line exposed to first analysed samples encoded in table 9, by the Neutral Red assay.....	74
Figure 85. Cell viability of HaCaT cell line exposed to second analysed samples encoded in table 10, by the Neutral Red assay.....	74
Figure 86. Cell viability of HaCaT cell line exposed to H ₂ O ₂ , determining the phototoxicity by the Neutral Red assay	75
Figure 87. Cell viability of HaCaT cell line exposed to RSV, determining the phototoxicity by the Neutral Red assay	75
Figure 95. Cell viability of HaCaT cell line exposed to RGS, determining the phototoxicity by the Neutral Red assay	76
Figure 89. Fluorescence of HaCaT cell line exposed to positive control by the DCFH-DA assay with and without fresh medium replacement steps. DCFH-DA incubated before irradiation	78
Figure 90. Fluorescence of HaCaT cell line exposed to positive control by the DCFH-DA assay with and without fresh medium replacement steps. DCFH-DA incubated after irradiation	78

Figure 91. Fluorescence of HaCaT cell line exposed to positive control by the DCFH-DA assay with and without fresh medium replacement steps. DCFH-DA incubated for 1h30 after irradiation.....	79
Figure 92. Fluorescence of HaCaT cell line exposed to positive control by the DCFH-DA assay A) before and B) after the DCFH-DA incubation.....	79
Figure 93. Fluorescence of HaCaT cell line exposed to Quinine HCl by the DCFH-DA assay	80
Figure 94. tGSH of HaCaT cell line exposed to 1260 μ M of Quinine HCl normalized by protein using Lowry Protocol	81

Table Index

Table 1. Main clinical manifestations of phototoxicity	7
Table 2. Photosensitizer drugs.....	12
Table 3. Summary of the photosafety testing regulation.....	16
Table 4. Comparison of four commonly used <i>in vitro</i> phototoxicity test.....	20
Table 5. Evaluation of phototoxicity depending of the PIF and MPE	23
Table 6. A comparison of different <i>in vivo</i> phototoxicity test.	26
Table 7. Summary of used compounds and their molecular weight.	35
Table 8. Summary of used compounds, their solvents and concentrations.....	41
Table 9. Summary of phototoxicity, cytotoxicity and ROS generation results.....	77

Abbreviations

1,2- DHX: 1,2-Dihydroxyxanthone

3-D: tree-dimensional

3R: Replace, Reduce and Refine

3T3 NRU PT: 3T3 Neutral Red Uptake Phototoxicity Test

5-MOP: 5-Methoxypsoralen, bergapten

8-MOP: 8-Methoxypsoralen, xanthotoxin

ACN: acetonitrile

ADME: absorption, distribution, metabolism and elimination

ASA: Acetylsalicylic acid

AUC: area under the curve

C. sativa: *Castanea sativa*

CA: Chlorogenic acid

CAP: Chlorogenic acid persulfate

CDER: Centre for Drug Evaluation and Research

COX: cyclooxygenase

CPZ: Chlorpromazine

DCF: 2',7'-dichlorofluorescein

DCFH: 2',7'-dichlorodihydrofluorescein

DCFH-DA: 2',7'-dichlorodihydrofluorescein diacetate

DMEM: Dulbecco's Modified Eagles's Medium

DMSO: Dimethyl sulfoxide

DNA: deoxyribonucleic acid

DPBS: Dulbecco's Phosphate Buffered Saline

DPBS: Dulbecco's Phosphate Buffered Saline

DTNB: 5,5'-dithiobis(2-nitrobenzoic acid)

EC: Cosmetics Regulation

ECVAM: European Centre for the Validation of Alternative Methods

EDTA: trypsin-ethylenediaminetetraacetic Acid

EHMC: Ethylhexyl Methoxycinnamate

EMA: European Medicine Agency

E-RSV: E-resveratrol

EU: European Union

FBS: fetal bovine serum

FDA: Food and Drug Administration

GLP: Good Laboratory Practice

GSH: reduced and

GSSG: glutathione oxidised

H₂O₂: Hydrogen peroxide

HCl: hydrochloride

HClO₄: perchloric acid

IC₅₀: the half maximal inhibitory concentration

ICDRG: International Contact Dermatitis Research Group

ICH: International Conference on Harmonisation

IR: infrared

KHCO₃: potassium bicarbonate

MPE: mean photo effect

NADPH: nicotinamide adenine dinucleotide phosphate

NaOH: sodium hydroxide

NR: neutral red

NRU: neutral red uptake

NSAIDs: non-steroidal anti-inflammatory drugs

OECD: Organisation for Economic Co-operation and Development

OMC: octylmethoxycinnamate

PHF: photohaemolysis- factor

PIF: photo irritation factor

PIL: Patient Information Leaflet

PT: phototoxicity test

RBC-PT: Red Blood Cell Phototoxicity Test

RGS: Resveratrol glycoside sulfate, 3, 5, 4' -trihydroxy stilbene-3- β -D-glucopyranoside persulfate

RHE-PT: reconstructed human epidermis phototoxicity test

ROS: reactive oxygen species

RSV: Resveratrol

SBC: Sunburn cell

SCCS: European Commission Scientific Committee on Consumer Safety

SD: standard deviation

SLS: Sodium Lauryl Sulphate

SOP: Standard Operating Procedure

SPCs: Summaries of Product Characteristics

tGSH: total glutathione

TNB: 5-thio-2-nitrobenzoic acid

USA: United States of America

UV: ultraviolet

UVA: ultraviolet A

UVB: ultraviolet B

UVC: ultraviolet C

UV-vis: Ultraviolet-visible

Vis: visible

Z-RSV: Z-resveratrol

1. Introduction

1.1. Skin

The skin is known as the larger organ of the body and the main barrier between the organism and the external environment (1). Its primary function is the defense of the organism against pathogens invasion, minimizing chemical and physical aggressions, preventing this way an unregulated loss of water and solutes (2). Skin is also responsible for thermoregulation as it is a highly irrigated organ (3).

Defined as an optically heterogeneous medium, skin controls the amount of radiation that can penetrate and reach the deepest dermal structures by mechanisms of reflection, refraction, scattering and absorption (4, 5). However, changes in its optical properties can result in a greater ultraviolet (UV) penetration, increasing the dose that reaches the viable skin layers (4), thus promoting skin damage (4, 6).

The skin is divided in three different layers (Figure 1). The most external layer is denominated by epidermis. The middle layer is the structural component of the skin, the dermis. The inner layer, the hypodermis is composed by adipocytes, representing a support of fat between the skin and the organs (1). These layers will be described briefly in the following sections.

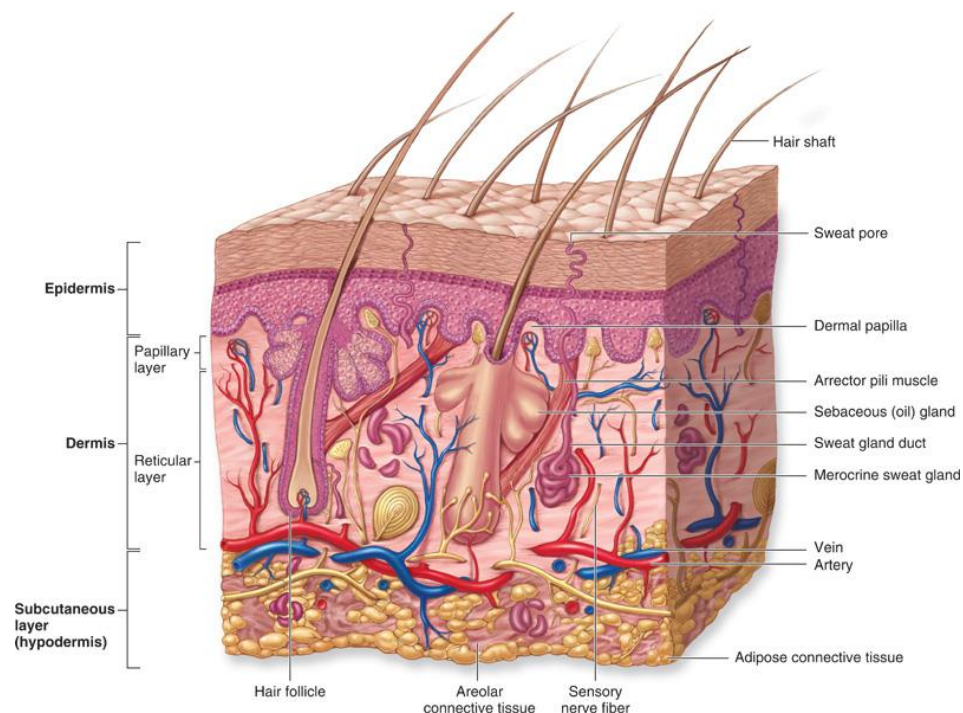


Figure 1. Skin structure, highlighting the layers, cells, arteries, venules and other components (7).

1.1.1. Epidermis

The epidermis corresponds to the outermost skin barrier (2). For that reason it is where topical products are applied. Its thickness is thus an important factor in photosensitivity study and it may vary from 0.5 mm on the thinnest areas, such as eyelids, to 4-6 mm on the thicker ones, such as the palm of the hand and the sole of the foot. After skin contact, chemicals can penetrate the cutaneous barrier, and at the application point, the absorption is directly proportional to the thickness of the skin (1).

The epidermal layer is a stratified, squamous, keratinized and avascular tissue of ectodermal origin, that contains epithelial cells in five morphologically distinct layers, which are named, according to the direction dermis-epidermis: basal layer, spinous layer, granular layer, lucid layer and stratum corneum (Figure 2) (8).

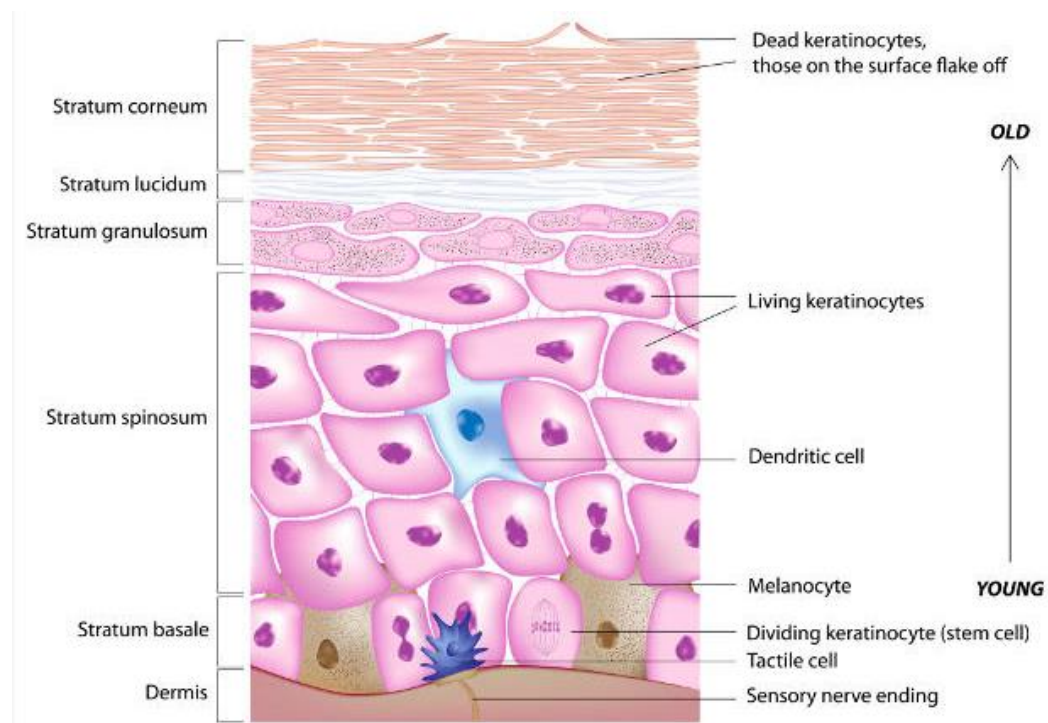


Figure 2. Structure of epidermis depicting the layers, the cells and the direction of development (9).

The highest metabolic activity is found in the basal layer, where cells present high mitotic rate, which is important to produce enough cells to replace surface cells, as these are continually lost by desquamation (1, 10).

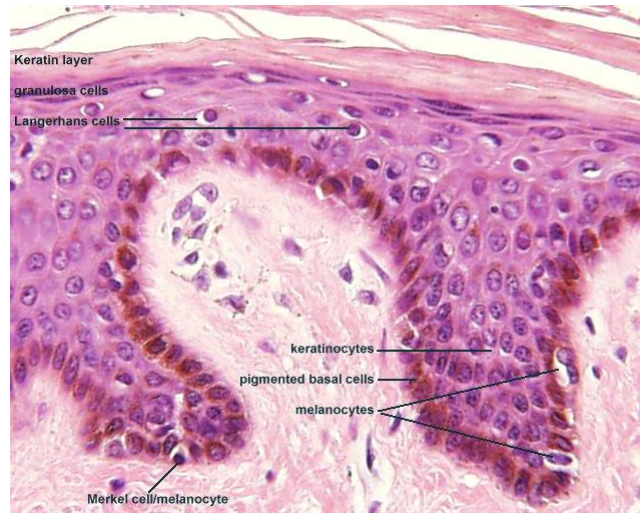


Figure 3. Histological section of human skin epithelium (11).

The most abundant epidermal cells are the keratinocytes (1), corresponding to 90% of its cells (12). Keratinocytes owe their name to the fact that they produce "keratin" (1), a protein responsible for maintaining the epidermis integrity (1), since their chemical structure provides water resistance (12), making the epidermis impermeable to some chemical contact with the skin and resistant to environmental attacks (1). Melanocytes, Langerhans cells and Merkel cells are the other cells present in this layer (Figure 3) (1, 12).

Skin oxidative stress

It is known that the skin is constantly exposed to environmental damage, undergoing reactive oxygen species (ROS) generation and consequently oxidative stress, which may lead to cellular death and related skin diseases (13). As the keratinocytes are the most external barrier of the skin (1), they act as the main environmental barrier, defending the skin against damage such as UV radiation, bacteria, viruses, heat, parasites and fungi (13).

ROS include the oxygen radicals (superoxide and hydroxyl) and the non-radical molecular oxygen derivatives (hydrogen peroxide and singlet oxygen) (14, 15). The cells have the capacity to generate ROS, especially in mitochondria, reducing molecular oxygen through nicotinamide adenine dinucleotide phosphate (NADPH) oxidase and xanthine oxidase (16). It is known that ROS production in keratinocytes is stimulated by sunlight radiation (13), through NADPH oxidase and cyclooxygenase (COX) (17, 18). The NADPH quinone reductases have high activity in epidermis (19), increasing their rate when exposed to UV light (20) and the reduction on proteasome activity in human keratinocytes is also

associated with UV radiation (21). However, the elucidation of the cellular and molecular mechanisms involved in ROS generation in the skin warrants further research (22).

The skin has several antioxidant defenses against ROS (10, 13, 23), including glutathione (GSH), superoxide dismutase (SOD), catalase, glutathione peroxidase-1 (GPx-1), metallothionein-2 (MT-2) (10), NADPH quinone oxidoreductase 1 (NQO1), and the phase 2 enzyme heme oxygenase-1 (HO-1) (13, 23, 24). GSH is the major cellular antioxidant and participates in an enzymatic system that is capable of eliminating hydrogen peroxide. In live cells, 98% of the GSH pool remains in the reduced state due to glutathione reductase (25, 26) (22), and the intracellular levels of GSH determine the cell capacity to cope with oxidative stress (25, 26).

1.1.2. Dermis

Dermis is the tissue that supports the skin and its appendages, such as hair, nails, etc. Furthermore, it is highly innervated and vascularized, in opposite to the epidermis (1).

The dermis is divided into two layers: the most superficial, the papillary dermis (27), which has a rich capillaries network, providing nutrients for the overlying epidermis and skin appendages (1); and a thick bottom layer, the reticular dermis (27), composed of connective tissue a large collagen fiber, supporting the skin (1).

The main cells of the dermis are the fibroblasts (1, 27) which are responsible for the synthesis of connective tissue components of the dermis, namely collagen, elastin, structural glycoproteins and glycosaminoglycans (27). In the dermis, mast cells, lymphocytes, and histiocytes, which are associated with the immunosystem, can also be found (Figure 4) (1).

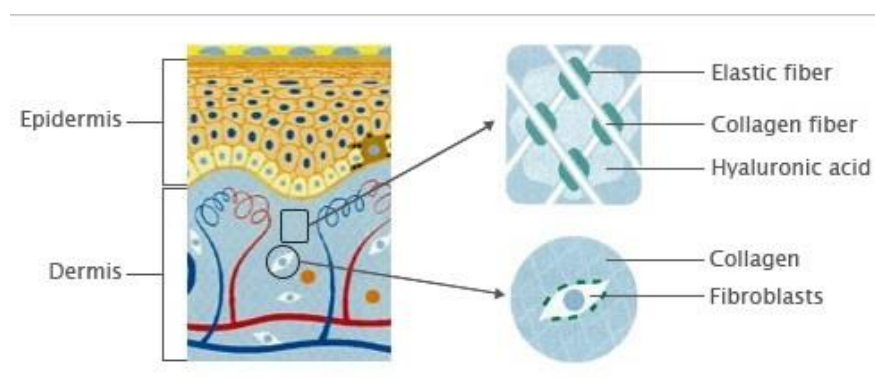


Figure 4. Structure of dermis, depicting the presence of connective tissue and blood vessels in reticular dermis (28).

1.1.3. Hypodermis

The hypodermis is composed of adipocytes, grouped into "lobes", which are separated by connective tissue. It has arterioles and venules to easily nourish the hypodermis (1). In addition to the adipocytes, macrophages and fibroblasts are also present in this layer (29). The hypodermis serves as a "cushion" of fat between the skin and the organs that lie underneath (1), serving also as support to the other skin layers (29).

1.2. Solar radiation

Sunlight emits in all electromagnetic spectrum: X-rays, UV, visible light (vis), infrared and radio waves (in small amounts) (30). The most probable wavelengths to cause phototoxicity are the UV and the vis (31). The first wavelength is between 100nm-400nm, subdivided into ultraviolet A (UVA-315-400nm (23, 24)), ultraviolet B (UVB- 280-315nm (23, 24)) and ultraviolet C (UVC- 100-280nm (23, 24)) (3, 32) and the second comprises wavelength from 400 nm to 760 nm (33), the latter corresponding to the peak of radiation power that reaches the Earth surface (Figure 5) (30).

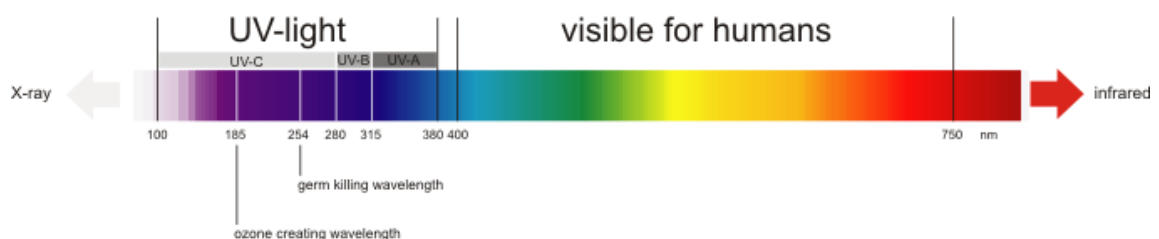


Figure 5. Solar spectrum is divided into UV (UVA, UVB and UVC), visible light, infrared and x-rays (34).

It is known that UV exposure is potentially dangerous to health. UVA affects directly the dermis leading to photoaging and DNA damage, inducing ROS generation (35, 36). Besides this, it represents the larger responsible for the phototoxic and photoallergic reactions (31, 37). This fact is due to several reasons, such as: 95% of UV radiation that reaches the Earth surface corresponds to UVA (32); it penetrates the skin more easily and has the capability to pass through many materials, including some windows (37). Regarding UVB radiation, sunburn is the most probable phototoxic reaction to be caused by UVB (32, 35), although only 5% of it can penetrate the ozone layer of the earth's atmosphere (32). UVC is almost

completely absorbed by stratospheric ozone, so there is no evidence that it causes phototoxic reactions (31).

Ultimately, visible light represents 50% of sunlight that arrives the Earth surface (3) easily penetrate the skin, although it is not energetic enough to cause severe damages. The reactions induced by visible light goes beyond the damage caused to the skin, such as eyes injuries and aging of the eye due to oxidative stress in the tissue (31).

1.3. Photosensitivity

Photosensitivity corresponds to the photobiology study of the cutaneous reaction (38). Photobiology studies the effects of UVA, UVB, visible and infrared (IR) radiation on living systems (39). For a photosensitivity reaction to occur, a photochemical event must occur. This event happens when UV/vis light is absorbed (40) by endogenous or exogenous chemicals (3), called photosensitizers (41). A photosensitizer is a chemical capable of entering the body through ingestion, injection, topical application (36, 41) or inhalation (36, 42), and transferring energy to the cellular components (3). Furthermore, according to the Center for Drug Evaluation and Research (CDER), for a compound to be photoactivated it should absorb radiation between 290 and 700 nm (4).

When a photoactivated compound, capable of reaching the skin by dermal penetration or through the systemic circulation, is applied and subsequently excited by UV or visible light, photoirritation, photoallergy, (4) photogenotoxicity or/and photocarcinogenicity phenomena (41) can occur (4). Further, eyes can also suffer ocular injury after being irradiated, resulting in oxidative stress (3, 43).

1.3.1. Phototoxicity/photoirritation

Phototoxicity is the most common manifestation of photosensitivity (44). The difference between phototoxicity and photoirritation is inconsistent (3) but most authors consider it the same (45, 46). Therefore, phototoxicity is characterized by an induction or enhancement of an acute response, independent of the immune system, after topical or systemic photosensitizer administration, which will reach the skin and subsequently be exposed to UV/vis radiation (4, 41, 45, 47, 48). Thus, it can be concluded that chemicals that absorb light in UV/vis region may cause phototoxicity if they absorb energy and produce ROS

(including singlet oxygen), or change to more toxic species (49, 50). Ultimately, phototoxicity reactions depend on several factors, such as the radiation dose and the concentration of the photosensitizer (47) and it can be induced by a single exposure, not requiring an induction period (4, 47, 50).

Clinical manifestations of phototoxicity

The phototoxic reaction is, usually, associated with immediate symptoms (41), so it is possible to detect effects minutes to hours after exposure to a photosensitizer and UV/vis radiation (51).

The phototoxic reaction symptoms depend on the photosensitizer and radiation doses that reach the skin and can vary from asymptomatic phase to serious sunburn (51). The most exposed areas to the sun, such as the nose, forehead, ears, V area of the neck and back of hands are the first to present symptoms, usually an exaggerated sunburn, followed by erythema, edema (51-53), blistering and prolonged hyperpigmentation (52). Vesicles and blisters appear in more severe reactions (51) with subsequent peeling (41, 50). Sometimes, similar signs of porphyria, such as the fragility of the skin and vesicles may appear as well as eczematous characteristics or lichenoid features (Table 1) (41, 50).

Table 1. Main clinical manifestations of phototoxicity (51, 53).

Acute phototoxicity	Subacute phototoxicity	Delayed phototoxicity
Similar to exaggerated sunburn	Pseudoporphyria	Chronic actinic dermatitis
Urticaria	Photoonycholysis	
Erythema	Dyschromia	
Edema	Lichenoid features	
Tingling	Eczematous characteristics	
Burning	Telangiectasia	
Residual hyperpigmentation	Pellagra	
Exfoliation	Phytophotodermatitis	
Fever		

1.3.2. Photoallergy

Contrary to phototoxicity, photoallergy is defined as an immune reaction to a UV/vis radiation activated chemical (4, 45) having an idiosyncratic response. However, photosensitizers that cause a phototoxicity reaction can also cause a photoallergic reaction (4). Since the photoallergic reaction is an immune reaction (4, 45), it does not occur in the first exposition, requiring an induction period of one or two weeks before the skin reactivity becomes remarkable (4, 41). For this reason, photoallergy is usually defined as a delayed photosensitivity reaction (50).

1.3.3. Photogenotoxicity/photomutagenicity

Photogenotoxicity, or photomutagenicity, is a genotoxic response (41, 45) observed after the exposure to a photosensitizer and UV/vis radiation (41), that cause damage in the genetic information and consequently the formation of mutations (45, 54). This damage can affect the somatic and germ cells and this way it may be transmitted to future generations (54).

1.3.4. Photocarcinogenicity

Photocarcinogenicity can occur when an organism is exposed to a chemical and repeated exposure to light/UV radiation (3, 41), inducing tumors (45). This can be due to two types of photocarcinogenicity: the photo co-carcinogenicity, which is an indirect increase of carcinogenic effects induced by UV, and the photochemical carcinogenesis, which is a carcinogenic effect of a drug when photoactivated by exposure to UV (41, 45).

1.4. Mechanisms of photosensitivity reactions

As mentioned above, all photosensitizers absorb in 290-700 nm range, which indicates the ability of a molecule to become in an excited state (41), i.e., the ability of a molecule to pass from the ground state to an excited electronic state (3, 31). This change in a molecule's state can occur by two mechanisms: oxygen-dependent or not-dependent (3, 47). In oxygen-dependent processes, denominated type II reactions, the energy is transferred to oxygen, producing a singlet oxygen (3), an excited molecule that can react with unsaturated fatty acids, nucleic acid molecules, proteins (47), plasma or membrane organelles (3) and

dissipate energy in several ways, such as by photolysis or photodegradation, originating toxic photo products (Figure 6) (41). In type I reaction (not-oxygen dependent mechanism), the transfer of electrons originates radicals which can, or not, involve oxygen (41, 44). When the energy transfer happen between biomolecules, photosensitizer and oxygen, ROS formation is induced (41, 55) which is the cause of most photosensitizers (56, 57). Since ROS are unstable and highly reactive molecules, when these molecules capture electrons from another molecules or biomolecules (DNA, proteins or lipids) they became stable but lead to oxidative damage and endogenous antioxidant system dysfunction, promoting skin damage (Figure 6) (58, 59).

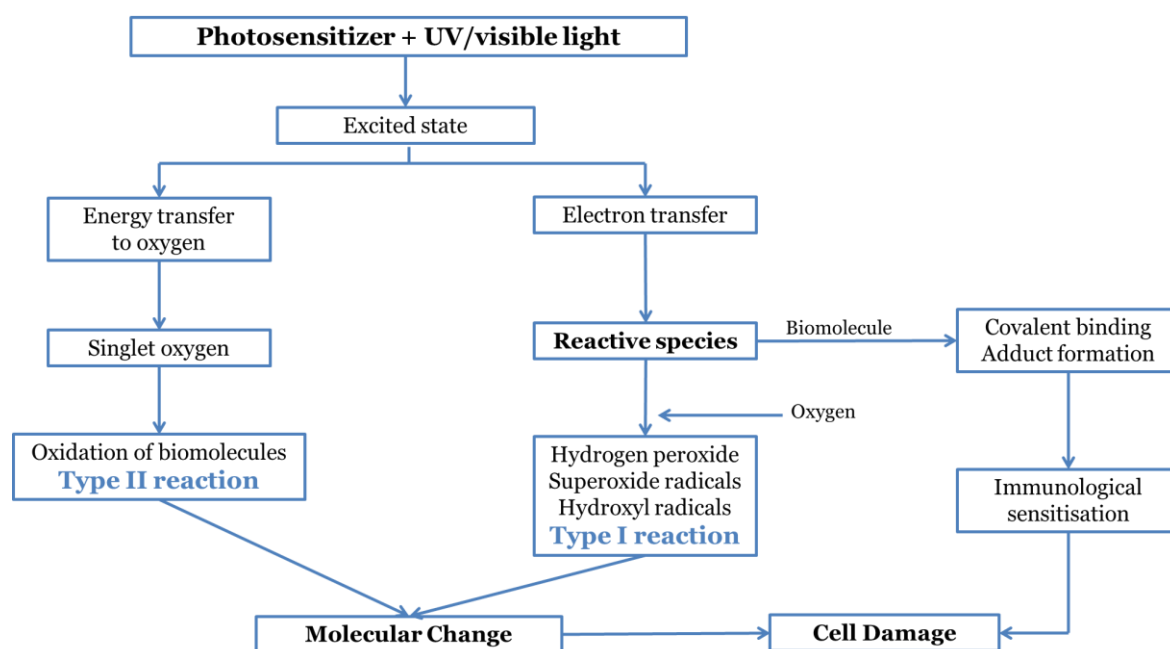


Figure 6. Mechanisms involved in photosensitivity (41).

When the excited singlet state or the excited triplet state transfers energy to another molecule, light emission (fluorescence or phosphorescence) and/or heat release occur (Figure 7) (3, 31). The singlet state is usually short-lived (10^{-8} to 10^{-9} s), however, it can cross to form a triplet state, which has a longer lifetime (10^{-4} to 10^1 s) (31, 41). Generally, photosensitized oxidations proceed in the triplet state, thus, the most powerful photosensitizers are those that provide a high yield of a long-lived state (41). Triplet state has a sub-millisecond lifetime, so the photosensitization process is more powerful if the photosensitizer is excited close to the biological target (31, 41) or if, before absorption of light, it is formed a complex between the chromophore and the target (31).

Plasma membrane, cytoplasmic organelles and nucleus are the most probable cellular targets for photosensitizing oxidation, depending on the radiation absorption and photosensitizer location (41). The phototoxic potential of a compound depends of several factors, such as photosensitizer chemical nature, substrate chemical nature, light absorption (31, 41), excited states nature (3), reaction conditions (solvent, pH, photosensitizer concentration, substrate and oxygen), among others. (31, 41).

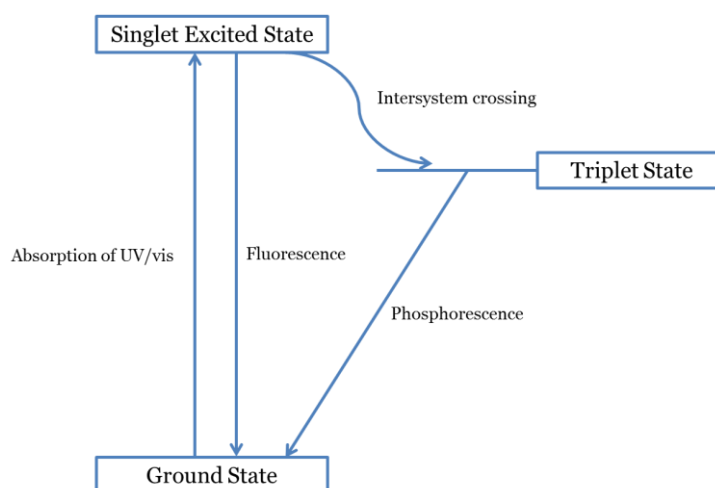


Figure 7. Scheme demonstrative of energy states involved in mechanisms of phototoxicity (3).

At histological level sunburn cells (SBC) are formed (60), which are apoptotic keratinocytes (61) that appear 24-48 hours after UVB irradiation (62) and can persist during 1 week or more. However, this phenomenon is still poorly understood (3).

1.5. Photosensitizers

A photosensitizer is a chemical capable to absorb radiation between 290 and 700nm causing damage in living organism. A large number of photosensitizers has been recognized as industrial or therapeutic agents (41) forming part of plants, foods, pharmaceuticals or cosmetics composition (47, 59). Regarding pharmaceutical products, a photosensitizer can be the drug itself, an excipient, a metabolite, an impurity or a degradation product (4). The photosensitizers have differences in their structures, with only one common aromatic system and/or conjugated multiple bonds (47).

The vehicles used in the pharmaceutical and cosmetic industries have been reported with capacity to modify the optical properties of the skin (4), increasing, for example, the

cutaneous absorption of drugs (63, 64), reducing/increasing the amount of light reflected/scattered/absorbed in the skin (4, 65, 66) or modifying drugs photoproperties (67, 68) and their photostability (4, 69-71). Besides that, the photosensitizer can still be photosensitizers by themselves (4, 72).

In addition to drugs and cosmetic ingredients, certain proteins and environmental pollutants were described to have photosensitizer potential. Hereupon, photosensitizers are present in everyday life and the living organism can be exposed by several routes, so it becomes important to implement photosafety studies in several fields such as food, pharmaceutical and cosmetic industries and ecology (47).

Since, cosmetics and medicines are possibly the best known photosensitizers and responsible for most phototoxicity reactions, they will be described in more detail below.

1.5.1. Cosmetics

A cosmetic product is any substance or preparation for topical application, either in the epidermis, hair, nails, lips, the external genitals or teeth and mucous membranes of the oral cavity, that is used to clear, perfume or protect them (73).

It is known that cosmetics frequently cause adverse reactions, but not very severe health hazard (36). Nevertheless, the risks that cosmetic products carry to health must have special attention in chronic exposure and application over a large area of the skin (36, 59). Some cosmetics are referred to cause phototoxic reaction due to the active ingredients, fragrances and stabilizers. To assess the safety of cosmetics products, an important factor is how it is used the substance amount and concentration used, and the penetration rate. Some may contain “penetration enhancers”, which increase the skin penetration (36). Therefore, it is extremely important to ensure their photosafety as much as possible, creating regulations for cosmetic products (59, 74). Examples of cosmetic ingredients known to be phototoxic are 5-methoxypsoralen (5-MOP, bergapten) (3, 75, 76), 8-methoxypsoralen (xanthotoxin; 8-MOP) (3, 75), angelicin (77).

Sunscreens

Sunscreens are considered cosmetic products in most countries and their use is an effective and inexpensive solution for preventing the skin damage induced by UV radiation (78). Since, they are in constant exposure to sunlight, they should not contain phototoxic

active ingredients (79) (which normally are the UV-filters (80)). For this reason, phototoxicity test must also be performed in sunscreens final formulation (79).

Therefore, the cosmetic industry has made many efforts to develop sunscreens with a large absorption spectrum and few chemicals, since the presence of different UV filters can lead to synergistic effects in the sunscreens final performance and photostabilization (35). More and more UV filters and other active antioxidant substances as vitamin A derivatives have been found in the environment, which promote recovery and protection of photodamaged skin (81). Besides that, some UV-filters or combinations can be photodegraded, resulting in photo-products that can be toxic (35, 81). Thus, the study of the phototoxic potential of new UV-filters combinations and antioxidant substances is a priority (81). Due to their presence in environment, bioaccumulation and toxicological properties, including the photo-reaction, UV-filters have been considered as potentially harmful pollutant and it is mandatory to use stable UV-filters under UV exposure. Therefore, the study of UV-filters photostability, including photodegradation and phototoxicity is crucial (82).

1.5.2. Drugs

A drug is defined as a compound used to diagnose, cure, mitigate, treat or prevent a disease and to affect the structure or any function of animals or human's body (83). A list with many different classes of drugs implicated in skin photosensitivity phenomena in humans was created in 2002 (Table 1) (47, 50, 84, 85).

Table 2. Photosensitizer drugs (52).

Antibiotics	Fluoroquinolones
	Nalidixic acid
	Tetracyclines
	Sulphonamides
Antifungals	Griseofulvin
Diuretics and cardiovascular agents	Thiazides
	Frusemide
	Amiodarone
	Quinidine

Non-steroidal anti-inflammatory drugs	Naproxen Tiaprofenic acid Piroxicam Azapropazone
Calcium channel antagonists	Nifedipine Benoxaprofen (now discontinued)
Psoralens	8-MOP 5-MOP
Psychoactive drugs	Phenothiazines (chlorpromazine, thioridazine) Protriptyline
Retinoids	Isotretinoin Etretinate Acitretin
Photodynamic therapy agents	Foscan Photofrin

The most common mechanism of drug-induced photosensitivity is, undoubtedly phototoxicity (50), which may require a metabolic conversion to become photoactive (3). However, some drugs can cause photosensitivity that does not involve UV absorption through the formation of endogenous molecules that absorb UV via secondary mechanisms (e.g. disruption of heme synthesis) (4).

1.6. Photosafety evaluation

The principal features that characterize a photosensitizer and support the recommendation to be submitted to photosafety testing are: ability to absorb radiation in the range of natural sunlight (290-700 nm) (4, 45, 57); capacity to generate reactive species following UV/vis absorption and distribution in a relevant degree to light-exposed tissues namely skin and eyes (57). In accordance with the Organisation for Economic Co-operation and Development (OECD), prior to *in vivo* or *in vitro* biological testing, the absorption spectrum in the UV/vis range should be determined for the substance in study (41, 48), which corresponding to the first step of photosafety tests (4, 45, 57). Preclinical photosafety tests serve to support clinical studies (86) and to determine if effects such as phototoxicity, photoallergy, photogenotoxicity or photocarcinogenesis are produced or improved by the presence of chemical and sunlight simulated radiation (Figure 8) (45). These tests should be performed only *in vitro* for cosmetics and *in vitro* or *in vivo* for drugs (86, 87). For most

pharmaceuticals, it is usually recommended that only the drug (not excipients) undergo testing for adverse photoeffects. However, for topical products which will be applied to the sun-exposed skin, Food and Drug Administration (FDA) recommends that the active ingredient and the drug product must be subjected to evaluation under conditions of simulated solar light (4). For ocular phototoxicity evaluation, there are no specific *in vitro* assays, and therefore the only possible conclusion is to consider the compound with little risk of being phototoxic (57).

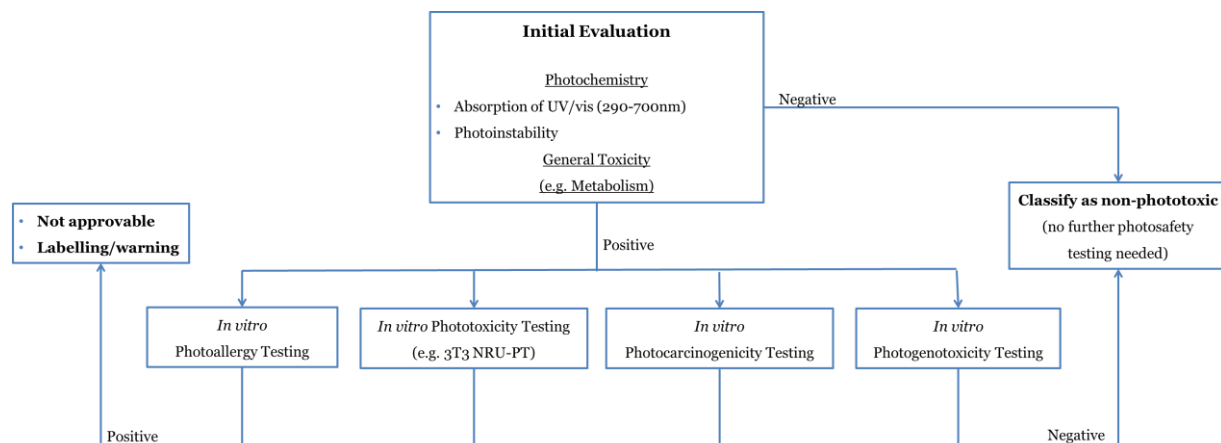


Figure 8. Hazard identification of photosensitivity (41).

Some animal tests are allowed, but the main goal of the current research is the development and validation of 3Rs principles (Replace, Reduce and Refine) - alternative methods to animals use (88). The principles of the 3Rs advice researchers to use alternative or to upgrade the animal experiment conditions. The first R relates to the Replacement of the animal model. If this is not possible, researchers should consider the refining (Refinement) of the experiment, using, for example, anti-pain medication before and after the operation, better housing, better management conditions of the animals before experiments, reducing stress on-experiment. Finally, the last R (reduction) refers to the reduction of the number of animals used (89). In 2010, the European Union (EU) adopted the Directive 2010/63/EU, which updated and replaced the 1986 Directive 86/609/EEC on the protection of animals used for scientific purposes following the 3R guidelines (90).

1.6.1. Regulatory aspects

The “Note for guidance on non-clinical local tolerance testing of medicinal products” of European Medicine Agency (EMA) referring photosafety testing, was adopted in 1990 and updated in 2001 ([91](#), [92](#)). In 1995, the OECD supported the first initiative which referred to the importance of defining a regulatory environment for photosafety testing, proposing a new guideline denominated: “Acute dermal photoirritation screening test” (TGP951). In this guideline, for the first time, are included general principles for rabbit or guinea pig use ([92](#), [93](#)). In 2002, the EMA released the “Note for guidance on photosafety testing” ([45](#), [92](#), [93](#)), where the photoallergy, photogenotoxicity and photocarcinogenicity were addressed, in addition to phototoxicity ([45](#)), defining photosafety tests as the adverse effects detection of medicinal product in the presence of UV/vis. Moreover, phototoxicity (photoirritation), photoallergy, photogenotoxicity and photocarcinogenesis are considered the 4 photosafety tests and conditions are advised, as well as, information about testing procedures for each type of photosensitivity, experimental procedure for photosafety in general, sources/light irradiation conditions and metabolic activation. In general, the performance of methods validated *in vitro* in all photoreactive compound bioavailable to the skin or eye is recommended ([45](#), [92](#), [93](#)).

In United States of America (USA), once the FDA published in 2003 the “Guidance for industry on photosafety testing”, regulations for performing photosafety tests in medicines manufacture were developed ([92](#), [93](#)). The FDA guidance is very similar to European guidance mentioned above on photosafety testing. However the FDA guidance does not recommend non-clinical test models to test photoallergy ([4](#)) and does not recommend specific tests ([92](#)). The *in vitro* assay 3T3 Neutral Red Uptake Phototoxicity Test (3T3 NRU-PT) is also recommended for phototoxicity test, but it is not recommended for products insoluble in water or for evaluation of complete formulations ([4](#)). Therefore, in contrast with the EMA guideline, the use of animal testing is encouraged ([4](#), [92](#), [93](#)), because *in vitro* assays are considered not predictive of the *in vivo* situation ([4](#)), and clinical studies are reported using photoreactive compounds in the skin or eyes at levels sufficient to cause photoirritation ([92](#)).

The OECD test guideline 432 (2004) has the main objective to define the *in vitro* 3T3 NRU phototoxicity test conditions, giving orientations of cell preparation, media and culture conditions, preparation of tests substances, irradiation conditions and final test conditions of 3T3 NRU-PT ([92](#)).

The adoption in 2008 of the “Concept paper on the need for revision of the note for guidance on photosafety testing” of EMA was the first specific step towards consensus of photosafety tests regulation, resulting in the International Conference on Harmonization (ICH) consensus ([92](#), [93](#)), denominated guideline ICH topic M3 (R2) of 2009: “Guideline on non-clinical safety studies for the conduct of human clinical trials and marketing authorization for pharmaceuticals” presenting several phototoxicity tests conditions ([92](#)). Finally, the ICH S10 of 2012, “Guidance on photosafety evaluation of pharmaceuticals” contained in more detail the strategies for photosafety evaluation ([46](#)).

Table 3. Summary of the photosafety testing regulation.

Name	Year	Type	Institution responsible	Region	Type of photosensitivity
“Acute dermal photoirritation screening test” (TGP951)	1995	Guidance	OECD	Europe	Phototoxicity
“Guidelines for the Safety Assessment of a Cosmetic Product”	1997	Guideline	Colipa	Europe	Phototoxicity Photomutagenicity.
“Note for guidance on non-clinical local tolerance testing of medicinal products” (final version)	2001	Guidance	EMA	Europe	Phototoxicity
“Note for guidance on photosafety testing”	2002	Guidance	EMA	Europe	Phototoxicity Photoallergy Photogenotoxicity Photocarcinogenicity
“Guidance for industry on photosafety testing”	2003	Guidance	FDA	USA	Phototoxicity Photoallergy Photogenotoxicity Photocarcinogenicity
“ <i>In Vitro</i> 3T3 NRU phototoxicity test”	2004	Guidance	OECD	Worldwide	Phototoxicity
“Guideline on non-clinical safety studies for the conduct of human clinical trials and marketing authorization for pharmaceuticals” topic M3(R2)	2009	Guideline	ICH	Worldwide	Phototoxicity Photocarcinogenicity General photosafety
“Non-clinical evaluation for anticancer pharmaceuticals” topic S9	2009	Guideline	ICH	Worldwide	Phototoxicity
Cosmetics Regulation (EC) No 1223/2009, Annexe I	2009	Regulation	European Commission	Europe	Phototoxicity
“Guidance on the safety assessment of nanomaterials in cosmetics”	2010	Guidance	SCCS	Europe	Phototoxicity Photogenotoxicity Photoclastogenicity
“Guidance on photosafety evaluation of pharmaceuticals” S10	2012	Guidance	ICH	Worldwide	Phototoxicity Photoallergy Photogenotoxicity Photocarcinogenicity

Cosmetics

For cosmetics and personal care products industry, the identification of phototoxic potential of each individual chemicals present in final formulations is a priority (49), being essential to test phototoxicity of compounds for sales authorization (94), testing and identifying chemicals risk (49).

According to the Cosmetics Regulation (EC) No 1223/2009, Annexe I "A particular focus on local toxicity evaluation (skin and eye irritation), skin sensitization, and in the case of UV absorption photo-induced toxicity shall be made" (95) and to evaluate the potential phototoxic of a substance the European Commission Scientific Committee on Consumer Safety (SCCS) in "Guidance on the safety assessment of nanomaterials in cosmetics" it is referred that there are several important points to consider, for example the applied method, the finished product concentration, the amount of product used in each application, the frequency at which the product should be used, the consumers target groups and their characteristics, the quantity that enter the body (absorbed fraction) and the exposure routes (96).

In Europe, in 2003, the sales of cosmetics that have been tested in animals was prohibited by directive 2003/15/EC of the European Commission (59, 97). subsequently, in 2009, the sales of cosmetics products, the final formulation, ingredients or their combination that have been tested on animals anywhere in the world, became banned in the European Union (EU) under the 7th amendment (EU Regulation 1223/2009) to the Cosmetics Directive (Directive 76/768/EEC) (95). This directive had the objective of protect and improve life conditions of experimental animals, with alternative *in vitro* tests and the implementation of 3R principle (59).

In 2010, the European Commission SCCS published the "Guidance on the safety assessment of nanomaterials in cosmetics" stating that, for nanomaterials, no specific alternative method has been validated. Also, *in vitro* tests presently available are not suitable for the characterization of their dose-response, which means that the quantitative risk assessment of cosmetic products that use nanomaterials is presently not possible (96).

Drugs

Formerly, most of systemically administered drugs were not subject to controlled trials to determine their phototoxic potential. Later it was observed that some drugs were

phototoxic in humans. Dermatologic drugs applied topically were tested for phototoxicity *in vivo* to verify if that these absorbed light in the UVA, UVB or visible spectrum (4).

In case of lack in data on *in vivo* testing for phototoxicity and photoallergy, warnings about potential phototoxic must be added on product labels, and adverse clinical reactions reported (4). Nevertheless, some drugs identified as photoirritants can obtain marketing authorization, but the FDA recommends that in the Summaries of Product Characteristics (SPCs) and Patient Information Leaflet (PIL) should not only be indicated the communication of risks (adverse reactions observed), but also a warning to avoid unprotected exposure to the sun during treatment with the drug (4, 45). There are also cases in which even if the compound is not referred to have toxic effects on the skin, it must be tested for damage in eye, observing in animals or in clinical trials (94).

1.7. Phototoxicity evaluation

1.7.1. Spectral absorption

As referred above, a potential phototoxic compound must absorb photons to initiate the photochemical event. Thus, before evaluating the phototoxic potential of a compound, its spectral absorption must be evaluated and only when the compound absorbs between 290 and 700 nm should the phototoxic assays be performed (48, 93). Using a spectrophotometer, the absorption spectra of the chemicals are measured in aqueous medium or in a suitable organic solvent (usually methanol) if aqueous medium is not appropriate (48, 59, 93).

1.7.2. Light source and irradiation conditions

As sunlight simulator, a xenon arc lamp with appropriate filters to remove the UVC and attenuate the UVB part of the emission spectrum is usually used, in order to simulate the type and dose of radiation which reaches the skin in a real situation. The irradiation dose should be high to ensure the efficient activation of a broad spectrum of potential photosensitizers, but without causing any, or hardly any, deleterious effects (45). When the irradiation is equal to or greater than 10 J/cm², phototoxic reactions can be seen and below 1-2 J/cm² of UVA false negatives may occur (98).

The types of light sources most commonly used in phototoxicity testing are: emission spectra limited to UV radiation, such as fluorescent lamps for UVA or UVB radiation, or mercury arc lamps; and emission spectrum of the sunlight simulator since they emit a reproducible UVA spectrum with high stability and are easily accessible (98).

Phototoxic testing of compound for skin application is mainly evaluated with UVA (3). However, there are phototoxic compounds that are activated by visible light (99) and UVB (100), or enhanced by UVB (3, 101). UVA doses ranging from 5 to 20 J/cm² have been successfully used in current *in vitro* and *in vivo* phototoxicity assays (57, 98).

1.7.3. Phototoxicity testing

After the determination of the UV/vis absorption spectrum of the compound, the drug photochemical properties and the photochemical reactions that the active molecule may suffer are evaluated (4, 47). As mentioned above, *in vitro* tests to replace *in vivo* tests are highly encouraged (45) and *in vitro* methods such as the 3T3 neutral red uptake (NRU) phototoxicity tests are increasingly used instead of animal models, due to ethical aspects (94). However, many substances that have shown phototoxic activity *in vitro* may not show an effect *in vivo*, and vice versa. This phenomenon is caused by the physicochemical properties of the substance and also by the nature of the living organism. From this point of view some authors argue that test on vertebrate animals should not be replaced (47).

The phototoxicity testing in animals, sometimes followed by phototoxic studies in humans, should be considered for all drugs and formulation components that absorb UVB, UVA or visible radiation and which are applied directly on the skin or eyes, which may affect these areas when administered systemically or are known to affect its stability (4). The ICH S10 divides the photosafety evaluation in to three steps: UV spectral analysis for evaluating UV-absorbing properties, ROS assay for photoreactivity and 3T3 NRU PT (59).

Notably, a compound that does not reveal phototoxic effects may reveal other adverse effects when exposed to sunlight. Thus, other tests such as photoallergic, photogenotoxic and photocarcinogenic tests should be performed to confirm the photosensitizers effect of the compound (Figure 8) (41).

1.7.4. In vitro assays

Several *in vitro* assays to determine the phototoxicity of chemical compounds are frequently described in the literature. A summary table (table 4) with the comparison of four different *in vitro* assays is shown below, presenting their advantages and disadvantages, the cellular model used and what it is possible to determine with each assay.

Table 4. Comparison of four commonly used *in vitro* phototoxicity test.

Test	Advantages	Disadvantages	Model	Determinations
3T3 NRU PT	<ul style="list-style-type: none"> - The only test that predicts correctly the phototoxic potential of test chemicals in humans - First tested <i>in vitro</i> according to the OECD 432 guideline 	<ul style="list-style-type: none"> - Does not foresee other adverse effects - Does not foresee effects of metabolites or mixtures 	<ul style="list-style-type: none"> - mice BALB/c 3T3 fibroblasts - Human keratinocyte cell line (HaCaT) 	Phototoxicity
RHE-PT	<ul style="list-style-type: none"> - Pure chemicals or complex mixtures can be applied as in a <i>in vivo</i> situation - Concentrations applied are closer to real exposure conditions - Exposure time and spectrum of simulated sunlight similar to the <i>in vivo</i> situation - Simulating adsorption and penetration of the skin 	<ul style="list-style-type: none"> - The number of commercial suppliers is limited - Lack of skin appendices that can influence the sensitivity of the skin - Very expensive 	<ul style="list-style-type: none"> - Skin fibroblasts (dermal models) - Skin keratinocytes and a stratum corneum (epidermal models) - Fibroblasts, keratinocytes and a stratum corneum (full skin models) 	Phototoxicity
RBC-PT	<ul style="list-style-type: none"> - Includes photochemically induced met-Hb formation - Mammalian erythrocytes are readily available - Erythrocytes can be exposed to more-intensive UV irradiation - Erythrocytes do not contain a nucleus - Cells can be exposed to the entire solar spectrum for prolonged periods 	<ul style="list-style-type: none"> - Low specificity and low negative prediction - Not a stand-alone test 	<ul style="list-style-type: none"> - Mammalian erythrocytes 	Phototoxicity (Photohaemolysis)
Yeast assay	<ul style="list-style-type: none"> - Ability to withstand quite long exposures to UVB, UVA, solar simulated or solar radiation - Useful for testing reciprocity between light exposure and drug concentration and dose-rate effects 	<ul style="list-style-type: none"> - Lack of data in the literature - Inadaptability to some antibiotics 	<ul style="list-style-type: none"> -Facultative anaerobic yeast such as <i>S. cerevisiae</i> 	<ul style="list-style-type: none"> - Phototoxicity - Photomutagenic - Genotoxicity - Photogenotoxicity

The *in vitro* 3T3 NRU-PT is an alternative to *in vivo* tests, being the first *in vitro* test included in the OECD guideline 432 ([94](#)). In addition, it was also officially accepted by the EU Commission and by the EU member states in the Directive 2010/63/EU ([102](#)). For this reason, the use of this assay is recommended, as described in more detail below.

3T3 Neutral Red Uptake Phototoxicity Test (3T3 NRU-PT)

The phototoxicity assay 3T3 NRU consists in comparing the cytotoxicity of a chemical compound in the presence and absence of a non-cytotoxic dose of UV/vis in order to identify its phototoxic potential induced by chemical excitation after radiation exposure ([45](#), [48](#)). In this assay, cytotoxicity is assessed by the reduction of vital dye (neutral red) absorption and consequent reduction of its concentration, 24 hours after treatment with test compound and irradiation ([103](#)) (Figure 9). The neutral red (NR) is a weak cationic dye that readily penetrates cell membranes of living cells by active transport, being accumulated in lysosomes ([48](#), [104](#)). Thus, it is possible to distinguish between viable, damaged, or dead cells ([48](#), [104](#)).

To validate the assay, 11 laboratories have tested 30 blind-coded chemicals, and based on the validation protocol used, a highly detailed OECD test guideline which includes the use and procedures of the test (OECD 432) was adopted ([49](#)).

Since some excipients may affect the photosensitive properties of the active substance, the test should be conducted with the final product formulation. However, due to solubility problems, that may not be possible in cell culture. As a solution to this problem, and since *in vitro* tests, such as three-dimensional skin models (3-D) are not yet validated, the *in vivo* studies can be performed in this situation ([45](#)).

Advantages and disadvantages

The comparison between 3T3 NRU and *in vivo* photopatch tests showed that the first is able to predict correctly the phototoxic potential of chemicals ([41](#)). Thus, substances identified as phototoxic with this assay are considered as such *in vivo* (animal and human), after systemic application and distribution to the skin, or after topical application ([45](#)).

The disadvantages reported in literature for this assay consist, mainly, in the fact that it does not provide information about other adverse effects, such as photogenotoxicity,

photoallergy or photocarcinogenicity. However, there are other weak points described, such as being able to not determine the phototoxic potency or the effect of metabolites or mixtures (48). Moreover, for some insoluble substances or complete drug formulations, this assay is not adequate (4).

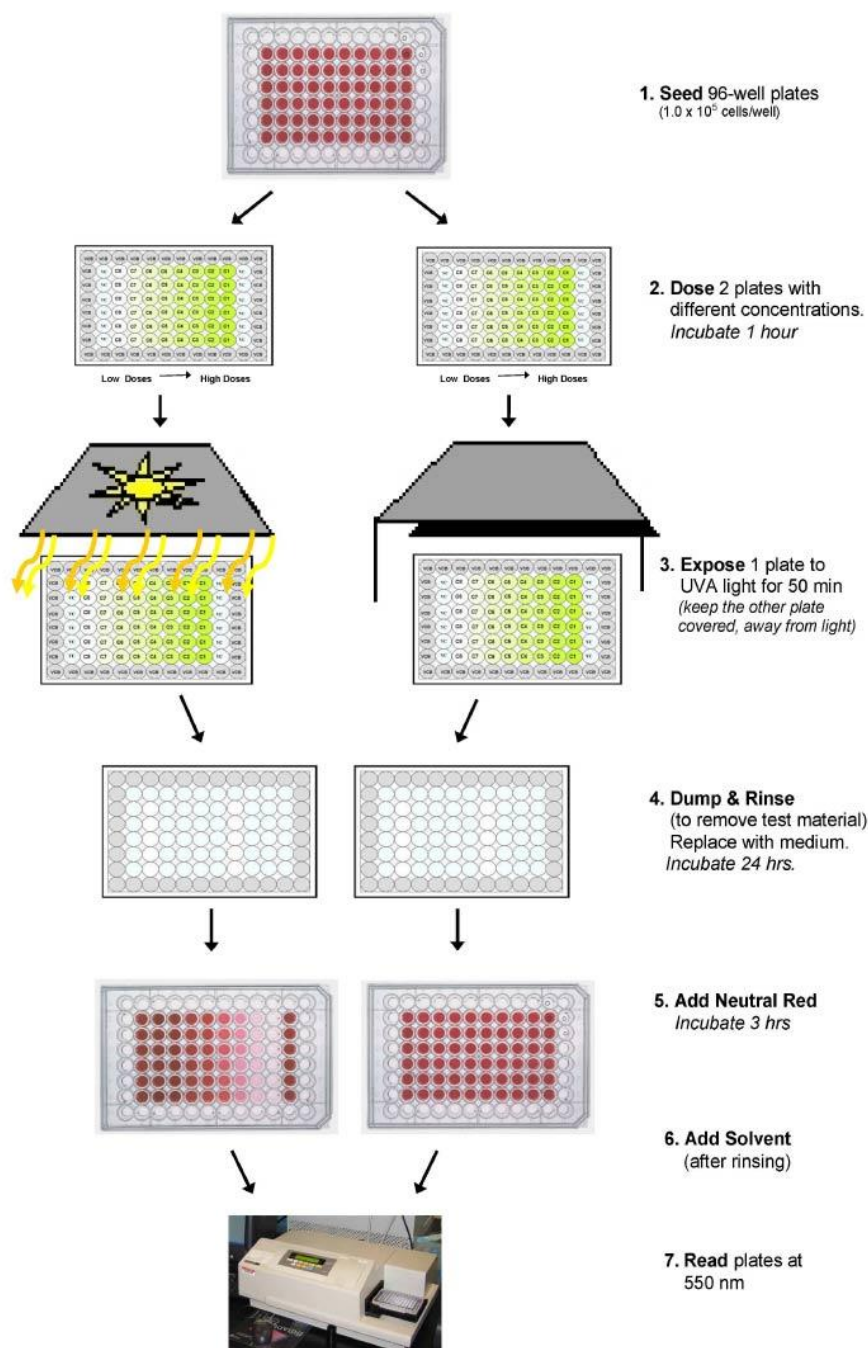


Figure 9. Schematic representation of the experimental test procedure of the 3T3 NRU phototoxicity (105).

OECD Test Guideline 432 provides the following parameters for predicting phototoxicity: the photo irritation factor (PIF) and mean photo effect (MPE) (49, 58):

- Photo irritation factor (PIF) – compares the half maximal inhibitory concentration (IC₅₀) values, i.e., 50% reduction in the uptake of NR for the cells exposed to UVA radiation compared with the unexposed (49). To calculate this, the ratio between the IC₅₀ without UVA and the IC₅₀ with UVA is used (106), as the following calculation:

$$PIF = \frac{IC_{50} (-Irr)}{IC_{50} (+Irr)} \quad (48)$$

- Mean photo effect (MPE) – statistical comparison of the dose response curve of cells exposed and not exposed to UVA radiation (49, 106), i.e., a comparison of the area under the curve (AUC) of the concentration response curves obtained from cells exposed and not exposed to UVA radiation (107) (Table 3).

The compounds are considered not phototoxic, probably phototoxic or phototoxic according to the criteria defined on table 5.

Table 5. Evaluation of phototoxicity depending of the PIF and MPE (106).

	PIF	MPE
¹⁾ No Phototoxicity	<2	<0.1
²⁾ Probable Phototoxicity	2 – 5	0.1 - 0.15
³⁾ Phototoxicity	>5	>0.15

The use of the BALB/c mice fibroblast cell line 3T3 is recommended in the standard protocol of the EU and OECD guideline. However, other cell lines can be used with the same test protocol, if the culture conditions are adapted to the specific cell needs (45) producing equivalent results (48). The protocol was successfully used with human keratinocytes in a blind study conducted with chemicals in EU/COLIPA validation study (108). Since keratinocytes represent the major cell type in the epidermis and this layer is the most relevant to induce epidermal irritation in humans, the human keratinocyte cell line (HaCaT) can also be used. Furthermore, this cell line provides a source of cells practically inexhaustible, allowing large laboratory reproducibility (106).

ROS generation (DCFH-DA) assay

As referred above, ROS generation is one of the phototoxic reaction consequences. The toxicity is due to the formation of oxidizing agents, such as $O_2 \cdot$, H_2O_2 , $HOCl$, NO , NO_2 , NH_2Cl . To detect the production of reactive oxygen species in the cells, 2',7'-dichlorodihydrofluorescein diacetate (DCFH-DA) is frequently used. This assay is based in fluorescent compound production when ROS are present in the medium (109). DCFH-DA, a nonfluorescent molecule can permeate cell membranes and accumulate in the cytoplasm, where esterases remove the acetate to produce 2',7'-dichlorodihydrofluorescein (DCFH) a polar compound that does not permeate cells (109, 110). Finally, DCFH is quickly oxidized to 2',7'-dichlorofluorescein (DCF), the measured fluorescent compound (excitation at 485 nm and emission at 530 nm) (109) (Figure 10).

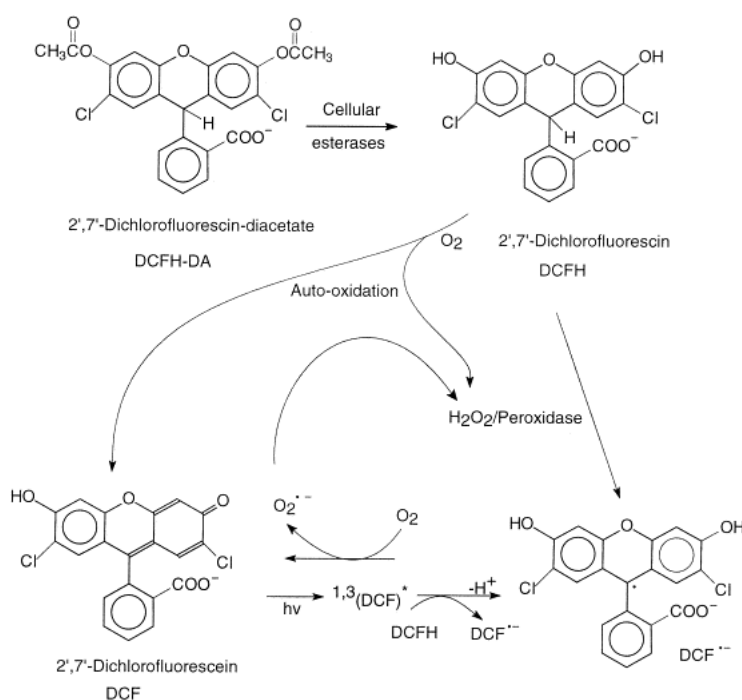


Figure 10. Scheme depicting the conversion of DCFH-DA into DCF (119).

Advantages and disadvantages

The DCFH-DA assay has the advantage of being sensitive to many ROS, while other probes can only be oxidized by one ROS (usually H_2O_2) and is also less expensive than other fluorescent probes. However, DCFH-DA is less sensitive and not as cost effective compared

to others. Besides this, the DCFH-DA is insoluble in water (109) and sensitive to UV radiation. A decrease in response in ROS generation when compared with the absence of UV was observed (111).

Reduced (GSH) and oxidised glutathione (GSSG) by DTNB-GSSG reductase recycling assay

As referred above, the reduced (GSH) and oxidised glutathione (GSSG) are part of the cellular antioxidant system, so their determination is important to study the ROS generation caused by irradiation of a compound. In the presence of GSH the compound can form (glutathion-S-yl)-adducts and the GSH conjugates remain redox active and can be oxidized, leading to the reductive addition of a second molecule of GSH to yield 2,5-bis-(glutathion- S-yl)- conjugates (112).

The assay for calculating the total GSH (GSH + GSSG, in GSH equivalents) is a specific and sensitive enzymatic procedure. GSH is oxidized by 5,5'-dithiobis(2-nitrobenzoic acid) (DTNB) (113) producing GSSG with stoichiometric formation of 5-thio-2-nitrobenzoic acid (TNB). Afterwards, GSSG is reduced to GSH through the highly specific glutathione reductase (GSSG reductase) and NADPH. Finally, the TNB (5-thio-2-nitrobenzoic acid) formation rate is evaluated at 412 nm (or 405 nm) and corresponds to the GSH and GSSG. The assay may be monitored at 340 nm by following NADPH consumption in the reaction (114).

1.7.5. *In vivo* assays

In vivo assays are also used to determine the potential phototoxicity of a chemical. However, as referred above, due to ethical restriction they are utilized with less frequency. A summary of these assays is provided (Table 6), including the advantages and disadvantages, the animal models used and the determinations that are possible to achieve with each assay.

Table 6. A comparison of different *in vivo* phototoxicity test.

Test	Advantages	Disadvantages	Models	Determinations
Animal	<ul style="list-style-type: none"> - Similarity with human condition, such as homeostatic mechanism. 	<ul style="list-style-type: none"> - Ethical issues; - 3R restrictions; - Without formal validation. 	<ul style="list-style-type: none"> - BALB/c mice; - Guinea pig; - OFA-Hr/hr hairless rats; - Rabbit; - Swine; - Squirrel monkey; - Hamster. 	<ul style="list-style-type: none"> - Phototoxicity; - Photoallergy; - Photogenotoxicity; - Photocarcinogenicity.
Photopatch	<ul style="list-style-type: none"> - Predict human condition; - Distinguish photoallergic from phototoxic response. 	<ul style="list-style-type: none"> - Difficulty in standardizing procedure; - Inter-individual variation; - Ethical issues. 	<ul style="list-style-type: none"> - Human. 	<ul style="list-style-type: none"> - Phototoxicity; - Photoallergy; - Photogenotoxicity; - Photocarcinogenicity.
Invertebrate animals	<ul style="list-style-type: none"> - Ideal initial biological screening method; - Rapid; - Simple; - Cheap. 	<ul style="list-style-type: none"> - Without formal validation; - Protocol is not well defined; - Does not predict the phototoxicity by itself 	<ul style="list-style-type: none"> - Crustaceans of genera <i>Artemia</i> and <i>Daphnia</i>. 	<ul style="list-style-type: none"> - Phototoxicity

1.8. Analyzed compounds

Despite the existence of set of antioxidant defenses that protect the skin against UV-induced oxidative stress, chronic and excessive exposure to UV-radiation can lead to oxidative stress and oxidative damage (23). As a solution to this, the topical application of antioxidants has been used (115-117), owing to their ability to prevent or minimize the UV induced-deleterious effects of reactive species on the skin (117).

In this work several compounds were analyzed: 1,2-Dihydroxyxanthone (1,2- DHX), 5-methoxypsoralen (5-MOP), Chlorogenic acid (CA) and chlorogenic acid persulfate (CAP), *Castanea sativa* leaf extract, Hydrogen peroxide (H₂O₂), resveratrol (RSV) and its derivatives, Avobenzone, Ethylhexyl Methoxycinnamate (EHMC), Acetylsalicylic acid (ASA), Chlorpromazine (CPZ), Diclofenac, Hexachlorophene, Quinine HCl and Sodium Lauryl Sulphate (SLS).

1.8.1. Positive controls

5-methoxypsoralen (5-MOP)

5-Methoxypsoralen (5-MOP, Bergapten) is a natural furocoumarin from several plant species ([118-121](#)) with antioxidant activity observed *in vitro* ([119](#)). The exposure to this compound can occur by food and drink ingestion and using perfumes and cosmetics with 5-MOP in their composition ([120, 121](#)). 5-MOP has been mainly used in photochemio therapy, such as psoriasis and vitiligo therapy due to its interaction with UV radiation, increasing the cutaneous photosensitivity ([118, 119, 121, 122](#)). For this reason, this compound is usually recommended as positive control in phototoxicity assays ([48](#)). It also shows anti-inflammatory, antidepressant, anticonvulsion and anticancer effects ([119, 121](#)). Since this compound has potential phototoxic properties ([59, 123](#)) 5-MOP was used as a positive control in this work.

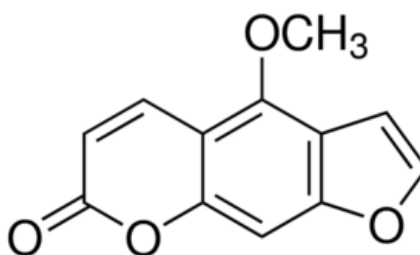


Figure 11. Chemical structure of 5-MOP.

Chlorpromazine (CPZ)

Chlorpromazine is as lipophilic drug ([124](#)) used in antipsychotic treatments ([125-127](#)), such as schizophrenia, the manic phase of bipolar disorders and other psychotic disorders. Studies revealed also antibacterial, anticancer, antiprionic, antiviral and multidrug resistance reversal activity ([126](#)). However, this drug can cause hepatotoxicity ([125, 126](#)), extrapyramidal effects, hyperprolactinemia, agranulocytosis, skin (e.g., jaundice and pigmentation, lichenoid, photosensitivity, pigmentation, subacute lupus erythematosus, toxic epidermal necrolysis, urticaria) and ocular (e.g., retinopathy, cataract) disorders. CPZ leads to oxidative stress ([125, 126](#)) which can cause tardive dyskinesia, cholestasis, cataract and retinopathy age-related macular degeneration. CPZ interferes with endogenous melanin causing hyperpigmentation and phototosensitivity, characterized by brown discoloration in skin sun-exposed areas and may even lead to a darker grayblue color ([126](#)).

Due to the photosensitivity of this compound it is frequently recommended as a positive control in phototoxicity assays (48).

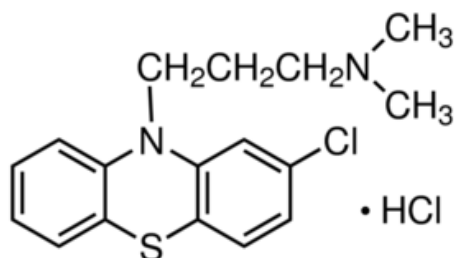


Figure 12. Chemical structure of CPZ.

Hydrogen peroxide (H₂O₂)

The use of commercial H₂O₂ is mainly in rocket propulsion. However, is also used as a conditioner, maturing and bleaching agent in food, as a strong oxidizer, anti-infective, clear and colorless liquid (128). The oxidative stress in cells leads to hydrogen peroxide formation, which glutathione peroxidase or catalase convert H₂O₂ in water and oxygen (129). Previous studies have shown that ROS can induce inflammatory conditions when the skin is exposed to UV radiation (13). In this work, hydrogen peroxide was used as positive control in ROS generation studies, so the cytotoxic and phototoxic evaluation must be performed to outwit its influence in ROS generation assay.

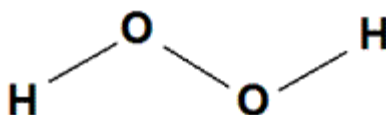


Figure 13. Chemical struture of H₂O₂.

Quinine HCl

Quinine is an alkaloid found in tree bark of genus *Cinchona* (130). This compound and its derivatives are frequently used in protozoal infection treatment like malaria (128, 130, 131) and nocturnal leg cramps. Due to the bitter taste of quinine, it is also used as bittering agent in tonic type drinks (131, 132). In street drugs, quinine is found as an adulterant of heroin, cocaine and other (133). Quinine causes photoallergic and phototoxic effects, the latter

probably via singlet oxygen production and interaction with intracellular targets (132). Quinine derivatives appear to be a photosensitizer for biological systems. Fluorescence events were also observed for quinine (130). Because quinine is a phototoxic compound, it is suggested as a positive control for phototoxicity assays (48).

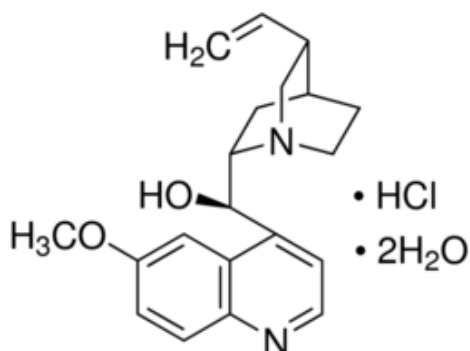


Figure 14. Chemical structure of Quinine HCl.

1.8.2. Negative controls

Acetyl salicylic acid (ASA)

Acetylsalicylic acid (ASA), most commonly known as Aspirin is a drug used for treatment of pain, fever, inflammation (134), heart attacks, thromboses (135, 136), strokes and ischemia prevention (137) and anticoagulant activity as a long-term treatment (135, 136). Recent studies showed that ASA might reduce the risk of cancer and reduction in metastasis (138). This compound is frequently recommended as a negative control in phototoxicity assays (139, 140).

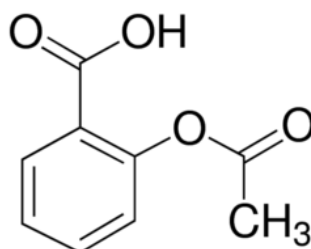


Figure 15. . Chemical structure of ASA.

Hexachlorophene

Hexachlorophene is an organochlorine compound, mainly used as an antiseptic in topical applications until the 1970s. Some studies have demonstrated that hexachlorophene can cause neurotoxicity in animal models ([141](#)). Because of its potential neurotoxicity in humans, its use has been regulated. Hexachlorophene is used in germicidal soaps as anti-infective, topical and detergent ([128](#)). The OCDE recommended this compound as a negative control in phototoxicity assays ([48](#)).

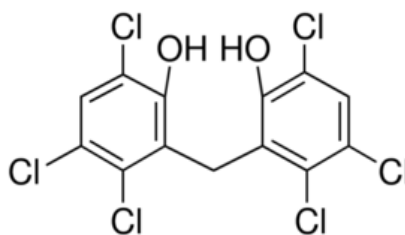


Figure 16. Chemical structure of hexachlorophene.

Sodium lauryl sulphate (SLS)

Sodium lauryl sulphate is an anionic surfactant especially used in several cosmetic products ([142](#), [143](#)). It is formed from lauryl alcohol, followed by neutralization with sodium carbonate and used in detergent, textile industry and toothpastes formulation ([128](#)). SLS is a not phototoxic compound used as a negative control in phototoxicity assays ([48](#), [144](#)).

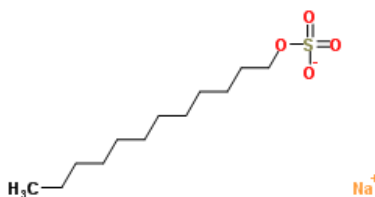


Figure 17. Chemical formula of SLS.

1.8.1. Raw compounds

1,2-Dihidroxyxanthone (1,2- DHX)

Chemically, xanthenes are a class of oxygenated heterocyclic compounds with a dibenzo- γ -pyrone scaffold (145). Many xanthenes with phenolic groups have been described for their antioxidant properties (115, 146, 147), being considered as one of the most important natural antioxidants (115, 147). These properties conduct to their anti-inflammatory, cancer chemopreventive (115, 147, 148), antibacterial and cardioprotective activities (115, 147). Xanthone and its derivatives have also been demonstrated to have antidepressant activity (149). In the present work, the phototoxicity of 1,2-DHX was assessed.

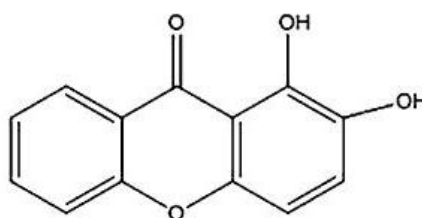


Figure 18. Chemical structure of 1,2-DHX.

Avobenzone

Avobenzone is a UV-filter and its use has been increasing over the last years due to its strong UVA attenuation, becoming probably the most important UVA filter. However the degradation of this active ingredient under UV exposition is significant (35, 79, 80) which may lead to photoproduct generation (35). For this reason, its use is usually combined with photostabilizers, including others UV-filters, in order to increase the efficacy of sunscreens. Avobenzone has been shown to have potential phototoxicity in 3T3 NRU with 3T3 BALB/c fibroblast (35, 80, 81), but some studies employing in human skin models considered it not phototoxic (80, 140). Considering the photo-instability and positive results in 3T3 NRU, its phototoxic potential in human keratinocytes is an interesting subject of study.

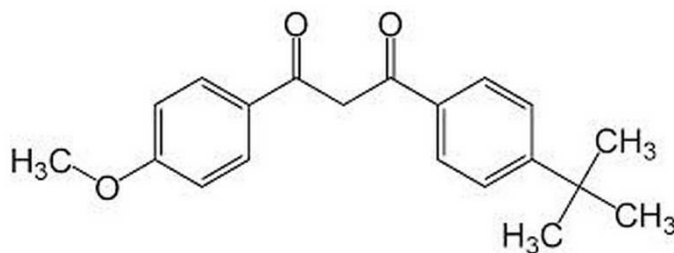


Figure 19. Chemical structure of Avobenzone.

Chlorogenic acid and chlorogenic acid persulfate

Chlorogenic acid (CA) is a polyphenolic component present in several plants and is very common in coffee. This compound has shown anti-inflammatory, cardioprotective, anti-tumor, lipid peroxidation inhibitory ([150](#), [151](#)), antioxidant ([150-152](#)), antibacterial, hypoglycemic, hypolipidemic and anti-hypertensive activities ([151](#)).

Chlorogenic acid persulfate (CAP) is obtained from chemical synthesis and has shown *in vitro* anticoagulant, antiplatelet and antioxidant activities ([153](#), [154](#)).

Due to antioxidant proprieties and because they are used as possible ingredients of cosmetic formulations, the phototoxic potential study of both compounds is an important factor.

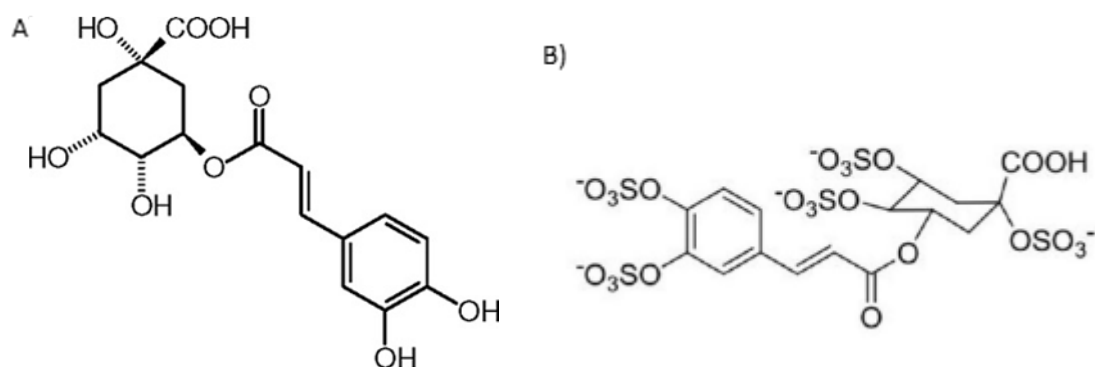


Figure 20. A) Chemical structure of CA B) Chemical structure of CAP.

Castanea sativa leaf extract

Castanea sativa (*C. sativa*) belongs to the *Fagaceae* family ([155](#), [156](#)), a flowering plant cultivated mainly in temperate regions such as Southern Europe, Asia and North of Africa

(156). *C. sativa* is a known source of phenolic active compounds (155, 157) and has several medicinal properties including antioxidant, chemopreventive, anti-inflammatory, neuroprotective, antiatherogenic, anti-thrombotic, antiangiogenic, cerebrovascular and peripheral vascular protective effects, being used in the treatment of various respiratory diseases (asthma, cold, cough, expectorating, bronchitis and bronchial affections), cardioprotective effects (155), diarrhea and rheumatic conditions, lower back pain, and stiff joints or muscles (156).

C. sativa extracts have the ability of scavenging different ROS, such as superoxide radical ($O_2^{\bullet-}$), hydroxyl radical (HO^{\bullet}), peroxy radical (ROO^{\bullet}), hydrogen peroxide (H_2O_2) and singlet oxygen (1O_2), which can lead to skin aging (157). The use of hydroalcoholic extracts from *C. sativa* leaves (which contain rutin, ellagic acid, hyperoside, isoquercitrin and chlorogenic acid) in cosmetic formulations has been considered safe and suitable for preventing and treating photoaging (158). *C. sativa* has in its composition chlorogenic acid at 2.23 mg/g of extract (22), so it is important to correlate its phototoxic potential with the amount in *C. sativa* extract. Besides that, since this extract releases ROS and its use has been increasing in cosmetic formulation against photoaging, its phototoxic potential is a determining factor in cosmetic safety.

Diclofenac

Diclofenac is a nonsteroidal anti-inflammatory drug (NSAID) (159, 160), used against pain, fever, and inflammation. This compound produces ROS leading to hepatotoxicity (159) and has potential photosensitizing in photohemolysis test (160, 161). Some studies have shown that its photosensitization is due to its photoproducts and not due to the parent drug (160). For these reasons, the study of the phototoxic potential in human keratinocytes was considered important.

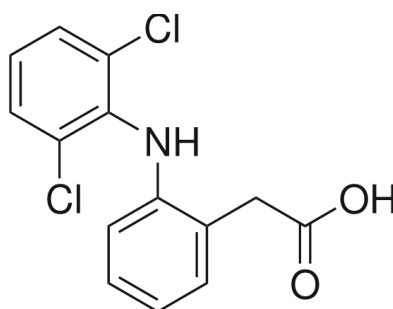


Figure 21. Chemical structure of Diclofenac.

Ethylhexyl methoxycinnamate (EHMC)

Ethylhexyl methoxycinnamate (EHMC) or octylmethoxycinnamate (OMC) ([162](#)) is an UVB filter ([80](#), [163](#)) with low cost, high compatibility with cosmetic formulations ([164](#)) and wide range of wavelengths ([165](#)), making it one of the most frequently used UV filters in the world ([162-166](#)), present in 90% of sun lotions ([167](#)) in 1:10 parts per weight ([162](#)). Due to its lipophilicity ([80](#), [168](#)), EHMC can bioaccumulate in fish, invertebrates and human breast milk ([168](#)), so the study of its toxicity is important, specially the phototoxicity study as it is constantly exposed to sun light. Several studies show that EHMC undergoes UV-mediated photodegradation and photoisomerization, making this compound photo-unstable ([164](#), [165](#), [169](#), [170](#)) by itself or in combination with other UV-filters ([170](#)). However, various studies have shown that EHMC in 3T3 Balb/c fibroblast was not phototoxic ([35](#), [79](#), [81](#), [171](#)). Therefore, the EHMC phototoxic potential is a point of interest.

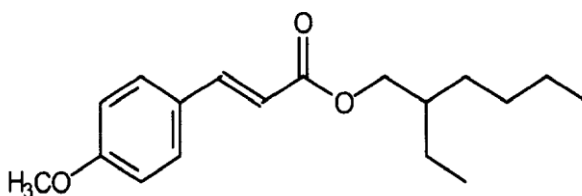


Figure 22. Chemical structure of EHMC.

Resveratrol and its derivatives

Resveratrol (RSV, 3, 5, 4' -trihydroxydystilbene) a natural antioxidant compound is a non flavonoid polyphenol ([172](#), [173](#)), present in different plants (peanuts, pistachio nuts, red grape seeds and skins, red wine, and other plant-derived food products) ([173](#)). This compound is present in Z- and E-isomeric forms ([172](#)). Several studies have shown the beneficial health effects of RSV and its use has been proposed in the treatment or prevention of different diseases ([174](#)), such as chemopreventive agent for skin cancer ([172](#)). Topical application of E-resveratrol (E-RSV) is known to prevent *in vivo* UV-induced skin damage and skin cancer ([172](#), [174](#)), treating *in vitro* melanoma inducing cellular apoptosis. However, E-RSV isomerizes under UV exposure, converting mostly in the less active Z-isomeric form ([172](#)).

The resveratrol glycoside sulfate (RGS, 3, 5, 4'-trihydroxydihydroxystilbene-3- β -D-glucopyranoside persulfate) was obtained by chemical synthesis and demonstrated an *in vitro* anticoagulant and antiplatelet activities ([153](#), [154](#)).

Due to UV isomerization of RSV, it is relevant to study the potential phototoxic of RSV and of its derivatives.

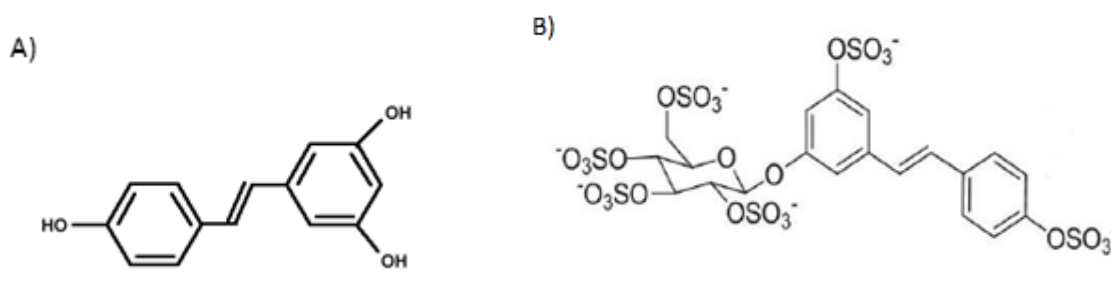


Figure 23. A) Chemical structure of RSV B) Chemical structure of RGS

Table 7. Summary of used compounds and their molecular weight.

Compounds	<u>Molecular weight</u> <u>(g/mol)</u>	Compounds	<u>Molecular weight</u> <u>(g/mol)</u>
1,2- DHX	228	DIC	296.15
5-MOP	216.19	EHMC	290.4
ASA	180.16	H₂O₂	34.01
Avobenzzone	310.39	Hexachlorophene	406.90
CA	354.31	Quinine HCl	396.91
CAP	864.53	RGS	1002.65
C. sativa leaf extract	NA	RSV	228.23
CPZ	318.86	SLS	288.372

NA- not applicable

2. Aim

The aim of this project was to implement a phototoxicity assay in a human keratinocyte cell line (HaCaT) based on the 3T3 Neutral Red Uptake Phototoxicity assay (3T3 NRU-PT) reported in OCDE432 guideline, using a UVA/UVB Osram lamp, and to evaluate the phototoxic potential of a series of raw materials for cosmetic and pharmaceutical products with the developed methodology. An additional aim was to perform preliminary tests regarding the implementation of a phototoxicity test using oxidative stress measures (tGSH and ROS generation) as endpoints.

3. Materials and methods

3.1. Materials

3.1.1. Raw materials

Resveratrol (RSV) was purchased from Fragon (Brazil). Ethanol (EtOH) was supplied by Aga (Portugal). Glycerin, acetyl salicylic acid (ASA) and sodium lauryl sulphate (SLS) were purchased from Acofarma (Spain). Acetic acid glacial and hydrogen peroxide (H₂O₂) 30% w/v were purchased from Panreac química SA (Spain). Avobenzone (butyl methoxydibenzoylmethane, eusolex 9020) and EHMC (octylmethoxycinnamate, ethylhexyl methoxycinnamate, eusolex 2292) were purchased from Merck (Germany). Hexachlorophene was purchased from Vaz Pereira (Portugal) and chlorogenic acid hemihydrate (CA) from Fluka (Switzerland). 1,2-Dihidroxyxanthone (1,2-DHX), chlorogenic acid persulfate (CAP), resveratrol glycoside sulfate (RGS) and *Castanea sativa* extract (*C. sativa*) were synthesized by the Laboratory of Organic and Pharmaceutical Chemistry (LQOF) of the Faculty of Pharmacy, University of Porto. Immortalized human keratinocyte (HaCaT) cell line was obtained from Cell Lines Service (CLS) (Germany). Dulbecco's Modified Eagles's Medium (DMEM) with 4,5 g/L D-glucose and pyruvate, DMEM with 4,5 g/L D-glucose, L-glutamine, 25mM HEPES and no phenol red, inactivated fetal bovine serum (FBS), penicillin-streptomycin solution, Dulbecco's Phosphate Buffered Saline (DPBS) without calcium chloride and magnesium chloride and 0,25% trypsin-ethylenediaminetetraacetic Acid (EDTA) solution were supplied by Gibco® Life Technologies (USA). Dimethyl sulfoxide (DMSO), trypan blue 0,4% solution, neutral red (NR) solution, quinine hydrochloride, chlorpromazine hydrochloride (CPZ), 5-methoxypsoralen (5-MOP), diclofenac and 2',7'-dichlorofluorescein diacetate (DCFH-DA)

were purchased from Sigma-Aldrich® (USA). The water used in all experiments was purified water obtained using a Direct-Q® Water Purification System (Merck Millipore, Darmstadt, Germany) with a reverse osmosis process.

3.1.2. Laboratory materials

The UVA/UVB lamp was an ultra vitalux 240V E27 from OSRAM (Germany), the heating ultrasonic baths used was a Bandelin Sonorex PK 100H and 96 well tissue culture plates flat were purchased from orange scientific (Belgium). The laminar flow chamber (HeraSafe, class II, model HS 12), the CO₂ incubator (HERAcell 150 Air-Jacketed) and the Centrifuge Series (Multifuge™ X1) were from Heraeus (Germany). The waterbath was from memmert and the Counting chambers, Neubauer improved bright-line (0,0025mm²) were purchased from Hirschmann (Germany). The inverted microscopes used was an AE2000 from Motic (Germany). The Microplate Reader (Synergy HT) and the Gen5 software used to read the microplates and transform the data in images were purchased from BioTek (United States). The spectrophotometer used was the Spectrophotometer Jasco UG50.

3.2. Methods

3.2.1. Cell culture

The *in vitro* experiments were conducted with the HaCaT cell line. These cells were originally obtained from Caucasian male aged 62 skin and are an immortal non-cancerous human keratinocyte cell line of adherent cells that form in monolayers.

Cells were maintained during all the assays at 37°C in a humidified atmosphere of 95% air and 5% CO₂ in the incubator in DMEM with 10% FBS and 1% antibiotics. Using an inverted microscope, cell confluence was observed and if the cells reached 70-80% confluence, subculture was done to prevent cell death. For this purpose, the culture medium was aspirated and the cells were washed with DPBS, 10 mL of trypsin-EDTA was added and incubated for 5 to 8 minutes at 37°C in a 5% CO₂ atmosphere. After cell detaching, medium was added in order to block the trypsin action and cell suspension was centrifuged at 416G for 5 minutes. The supernatant was discarded, the pellet resuspended in culture medium and cells were counted. For cell counting: 50 µL of cell suspension was added to 50 µL of trypan blue vital dye (1:10), resuspended, placed in a Neubauer chamber and the viable

cells were counted. The number of cells in the total volume was calculated with the following equation:

$$\text{Number of cells/mL} = \frac{n}{4} \times 10^4 \times \frac{1}{d^{-1}} \quad \text{Equation 1)}$$

where, n is the number of viable cells counted and d is the dilution coefficient.

For cell freezing, DMSO (5% v/v) was used as a cryo-preservative to prevent the formation of crystals during the storage phase.

HaCaT cell line

In order to characterize the cell line generation time, i.e., how long it is necessary for a population of cells to duplicate, five 25 cm² flasks with 1×10⁵ cells were seeded and incubated for 24 hours at 37°C in a 5% CO₂ atmosphere to a complete adherence. Then, the cells of each flasks were counted at different times using 50 µL of cell suspension added to 50 µL of 0.4% trypan blue vital dye (1:1) and the number total of cells in each flask was calculated using equation 1. The results were plotted in a graphic with cell number versus time, from which the generation time was calculated using linear regression analysis.

3.2.2. Implementation and optimization of phototoxicity *in vitro* test

Irradiation optimization

Irradiation dose and temperature control

Using a radiometer, the height of the UVA/UVB Osram lamp was adjusted in order to irradiate the cells with an irradiation dose of 1.7mW/cm².

Regarding temperature control over the irradiation time, DMEM without phenol red, at 37°C, was added to a 96-well plate and irradiated inside a Styrofoam recipient containing a water-cooling system. Medium and water temperature were measured during the irradiation at several times: 1, 3, 5, 7, 10, 12, 15, 17, 20, 23, 25 and 30 mins.

HaCaT sensitivity to radiation

The procedure, previously optimized, was used to study the cell sensitivity to radiation. For this purpose, 9 plates were irradiated, with an equivalent plate kept in the dark, at 9 irradiation times: 1, 3, 4, 5, 7, 10, 15, 20 and 30 mins. Then the cell viability was calculated for each time using the following calculation:

$$\text{Cell viability (\%)} = \left(\frac{\text{plate (+irr)}}{\text{plate (-irr)}} \right) \times 100 \quad \text{Equation 2)}$$

Optimization of neutral red uptake assay

In order to optimize the NR uptake assay several factors were tested, such as the optimal cell density, the concentration and the incubation time with the NR solution. With regard to cell density, 2.5×10^3 , 5×10^3 , 1×10^4 , 2×10^4 and 5×10^4 cells/well were seeded on 96-well tissue culture plates (150 $\mu\text{L/mL}$) and incubated at 37°C in a 5% CO_2 atmosphere for 24 hours. Afterwards the medium was removed, cells were washed with DPBS, and fresh culture medium was added and incubated under the same conditions for 24 hours. Since the NR could precipitate, the NR solutions were prepared every second day and incubated overnight at 37°C in a 5% CO_2 atmosphere protected from light. Before the addition to the wells, the NR solution was centrifuged at $1500 \times g$ for 10 minutes and filtered (5 μm). Finally, the medium of each plate was removed, cells were washed with DPBS and 33, 50, 100 and 330 $\mu\text{g/mL}$ NR solution in DMEM were added and incubated for 2, 3 or 4 hours. After this, NR solution was removed, the cells were washed once with DPBS previously heated at 37°C and a NR desorb solution (50% ethanol:1% acetic acid:49% distilled water) was added to extract the NR dye from the cells. For the reading procedure, each plate was placed in a microplate shaker for 10 minutes, at room temperature and protected from light, in order to extract all the NR from the cells and obtain a homogeneous solution. Finally, the absorbance was measured at 540 nm.

Optimization of ROS generation assay using DCFH-DA

In order to optimize the ROS generation assay several factors were tested, such as the optimal cell density, the concentration and the incubation time with the DCFH-DA. With regard to cell density, 2.5×10^3 , 5×10^3 , 1×10^4 , 2×10^4 and 5×10^4 cells/well were seeded on 96-well tissue culture plates and incubated at 37°C in a 5% CO_2 atmosphere for 24 hours.

Afterwards, the medium was removed, cells were washed with DPBS, and complete culture medium with different concentrations of DCFH-DA (5, 10, 25 and 50 μM) was added and incubated for two different times (30 min and 1 hour) under the same conditions. Afterwards, the DCFH-DA solution was removed, the cells were washed with DPBS and a solution of different concentrations of H_2O_2 , a positive control, and the negative control with only cells in DMEM without phenol red (400 and 700 μM) was added at different times: 1, 20 and 24h. Following thus incubation, the fluorescence was measured using a fluorescence plate reader with a baseline of 485 nm excitation and 530nm emission.

Optimization of a UV-mediated ROS generation assay using the DCFH-DA probe

The procedure, previously optimized in section 3.2.2.1.1 and 3.2.2.1.3, was used to study the radiation influence in the DCFH-DA, since this probe has been reported to be photolabile (111). For this purpose, the DCFH-DA was added before and after the irradiation, with or without a previous washing step of cells and the increase in fluorescence percentage was evaluated. A positive control (H_2O_2) was used before and after the incubation with the DCFH-DA after the irradiation. Another positive control (quinine hydrochloride) was also tested.

3.2.3. Phototoxicity study

Test compounds conditions

The phototoxicity and cytotoxicity of several compounds analysed, including compounds obtained by chemical synthesis with potential interest for topical application: 1,2-dihydroxyxanthone (1,2-DHX), chlorogenic acid persulfate (CAP) and resveratrol glycoside sulphate (RGS) synthesized at the Pharmaceutical Chemistry Laboratory, FFUP. Resveratrol (RSV), acetyl salicylic acid (ASA), sodium lauryl sulphate (SLS), hydrogen peroxide (H_2O_2), butyl methoxydibenzoylmethane (eusolex 9020 - Avobenzon), ethylhexyl methoxycinnamate (eusolex 2292 - EHMC), hexachlorophene, chlorogenic acid (CA), quinine hydrochloride, chlorpromazine hydrochloride (CPZ), 5-methoxypsoralen (5-MOP), diclofenac and *C. sativa* leaf extract were also studied. The concentrations tested and solvents are described in Table 8.

Table 8. Summary of used compounds, their solvents and concentrations.

Compounds	Solvents	Tested concentrations (Phototoxicity)	Tested concentrations (Cytotoxicity and ROS)
1,2- DHX	DMSO	12.5; 25; 50; 100; 200 μ M	12.5; 25; 50; 100; 200 μ M *
5-MOP	DMSO	10; 25; 50; 100; 300 μ M (no irradiate plate) 1; 2.5; 5; 7.5; 10 μ M (irradiate plate)	10; 25; 50; 100; 300 μ M
ASA	Ethanol 96%	1388; 2775; 5551; 8326; 11101 μ M	1388; 2775; 5551; 8326; 11101 μ M
Avobenzone	DMSO	10; 25; 50; 100; 200 μ M	10; 25; 50; 100; 200 μ M
CA	DMSO	10; 25; 50; 250; 500 μ M	NR
CAP	DMEM	115.7; 289.2; 578.3; 867.5; 1716.5 μ M	NR
C. sativa leaf extract	H ₂ O:Glycerin (1:1)	5; 50; 100; 250; 500 μ g/mL	5; 50; 100; 250; 500 μ g/mL *
CPZ	PBS	2.8; 28.2; 70.4; 140.9; 211.3; 281.7 μ M (no irradiated plate) 0.3; 2.8; 5.6; 8.5; 11.3; 14 μ M (irradiated plate)	10; 15; 25; 35; 50 μ M
Diclofenac	DMSO	10; 25; 50; 100; 500; 1000 μ M	10; 25; 50; 100; 500; 1000 μ M
EHMC	Ethanol 96%	3.4; 86.2; 172.4; 344.8; 517.2; 689.7 μ M	86.2; 172.4; 344.8; 517.2; 689.7 μ M
H₂O₂	DMEM	1; 100; 200; 400; 1000; 2000 μ M	1; 100; 200; 400; 1000; 2000 μ M
Hexachlorophene	DMSO	61.4; 122.9; 245.8; 307.2; 491.5 μ M (phototoxicity)	12.3; 24.6; 61.4; 122.9; 245.8; 307.2 μ M
Quinine HCl	Ethanol 96%	25.2; 125.9; 251.9; 503.9; 1259.7; 2519.5 μ M	25.2; 125.9; 251.9; 503.9; 1259.7; 2519.5 μ M
RGS	Water	10; 50; 100; 500; 1000 μ M	NR
RSV	DMSO	100; 500; 750; 1000; 2000 μ M	100; 500; 750; 1000; 2000 μ M *
SLS	DMEM	69.35; 138.7; 173.4; 260.1; 346.8; 866.9; 1733.9 μ M	69.35; 138.7; 173.4; 260.1; 346.8; 866.9; 1733.9 μ M

* Cytotoxicity previous studied at the host laboratory; NR- Not Realized.

To evaluate the cytotoxic and phototoxic effect of these compounds on the HaCaT cells, two assays were performed, the NRU and NRU-PT, after an initial optimization step. The ROS generation assay and total glutathione (tGSH) assay for each compound were performed as phototoxicity assay complement, since ROS are expected to be released when a phototoxic event happens. For all compounds, the cellular viability assessed through the lysosomal integrity was evaluated with and without irradiation and afterwards it was compared using the PIF index. The ROS generation was performed with the DCFH-DA assay. The cytotoxicity assays were conducted to assess the lysosomal integrity through the NRU assay. For some compounds, as referred in table 8, the cytotoxicity and the ROS generation were not evaluated, since it has been previously evaluated at the same laboratory and we ran out of ca and cap during the course of this study, respectively.

All experiments have at least three intra-day and inter-day replicas. All results from the cytotoxicity and phototoxicity assays were expressed in percentage of cell viability relative to positive control (cells treated with the solvent) and whenever possible the concentration able to reduce cell viability by 50% (IC₅₀) was calculated using linear regression analysis. In the ROS assay the difference between the fluorescence of treated cells and untreated cells was calculated and expressed as percentage.

Spectral absorption

Before performing the phototoxicity assays, the absorption spectra of all tested compounds were obtained. For this purpose, the tested substances were dissolved in the appropriate solvent at a concentration of 100 µg/mL. When this concentration was not appropriate a concentration of 10 µg/mL was used (e.g. EHMC, avobenzone, diclofenac, 5-MOP, 1,2-DHX and RSV). The absorbance was evaluated in the 250-700 nm range (covering UV and visible light wavelengths). Blanks with each solvent were performed to eliminate interferences. Solvents used for each compounds were the same used at assays mentioned in Table 8.

Study of the tested compounds phototoxic effect using the NR uptake assay

Using the optimized condition previously described, 2×10^4 cells/well (optimal cell density) were seeded and incubated for 24 hours at 37°C in a 5% CO₂ atmosphere. The medium was removed, cells washed once with DPBS and different test compounds solutions

in DMEM without phenol red were tested and incubated under the same conditions for 1h. After this, the plate was irradiated for 10 min at 29-32 °C, using as control an equivalent plate that was kept in the dark. The cells were then washed once again with DPBS and the medium was replaced with fresh DMEM without phenol red and incubated for 18-22h. At the third day, cells were washed with DPBS and complete DMEM containing 50 µg/mL NR (optimal concentration) previously incubate overnight, centrifuged at 1500 x g for 10 minutes and filtered (5 µm) was added to each well and incubated for 3 hours (optimal incubation time) protected from light. Finally, the NR solution was removed, cells washed and a desorb solution added. The plate was then shaken and absorbance measured at 540 nm as described above. The cell viability of solvent controls was evaluated using the same procedure.

The results were expressed as the absorbance ratio of treated to control cells, using the following calculation:

$$\text{Cell viability (\%)} = \left(\frac{\text{Treated cells absorbance}}{\text{Untreated cells absorbance}} \right) \times 100 \quad \text{Equation 3)}$$

Then, the IC₅₀ was determined using linear regression, to calculate the PIF.

Study of the tested compounds cytotoxic effect using the NR uptake assay

Using the procedure referred above, 2×10⁴ cells/well were seeded and incubated for 24 hours, the medium was removed, cells washed and different test compounds added and incubated for another 24 hours. At the third day, medium was removed, the cells were washed once with DPBS (37°C) and 50 µg/mL of NR solution previously incubated overnight, centrifuged at 1500 x g for 10 minutes and filtered (5 µm) was added to each well and incubated for 3 hours protected from light. After the incubation time, the NR solution was removed, cells were washed and the desorb solution added. The plates were then shaken as mentioned above and the absorbance measured at 540 nm. The cell viability of solvent controls was evaluated using the same procedure.

The results were expressed as the absorbance ratio of treated to control cells, using Equation 3.

Study of the tested compounds ROS generation using DCFH-DA

Using the optimized conditions, 2×10^4 cells/well were seeded and incubated at 37°C in a 5% CO_2 atmosphere. After 24 hours of incubation, the medium was removed, cells washed once with DPBS and complete DMEM containing $50\mu\text{M}$ DCFH-DA was added and incubated for 30min. Afterwards, the cells were washed once with DPBS and different test compounds were added and incubated for 24 hours. At the third day, the fluorescence was measured using a fluorescence plate reader with a baseline of 485 nm excitation and 530nm emission. A fluorescence interference of compounds without cells and a fluorescence of solvent controls studies were performed under the optimized procedure.

The results were calculated as the ratio between the fluorescence of treated cells and untreated cells and expressed in percentage as shown following:

$$\text{Fluorescence (\%)} = \left(\frac{\text{fluorescence of tretated cells}}{\text{fluorescence of untretated cells}} \right) \times 100 \quad \text{Equation 4)}$$

Validation of UV-mediated ROS generation assay using DCFH-DA with a positive control

Using the optimized conditions, 2×10^4 cells/well (optimal cell density) were seeded and incubated at 37°C in a 5% CO_2 atmosphere. After an incubation of 24 hours, the medium was removed, the cells washed once with DPBS and different test compound concentrations were added for 1h and irradiated for 10 min with a plate control kept in dark under the same conditions. Then, the cells were washed and complete DMEM contain $50\mu\text{M}$ of DCFH-DA was added and incubated for 30min. After this, the cells were washed once with DPBS, fresh medium added and incubated. The fluorescence was measured at different times (30min, 3h and 24h) using a fluorescence plate reader with a baseline of 485 nm excitation and 530nm emission.

The results were expressed as referred above (equation 4)

The effects of quinine HCl and irradiation in total GSH (tGSH) using (DTNB)-GSSG reductase-recycling assay

The cells was seeded into 6-well plates and incubated for 24h. Afterwards, the quinine HCl was added at $1260\mu\text{M}$ for 1h and irradiated for 10min with an equivalent plate kept in

dark. The cells were washed and after an incubation time of 22h, cells were lysed with 5% perchloric acid (HClO_4 , w/v) scrapped/precipitated and centrifuged at $13,000 \times g$ for 10 min at 4°C . Then, the supernatant of cell lysates was collected and stored at -80°C for further determination. The pellet obtained was resuspended in 0.3 M sodium hydroxide (NaOH) with 1:8 dilution for a final volume of 200 μL and used for protein quantification, determined by the Lowry assay. The thawed acidic supernatant, after a 1:8 dilution with HClO_4 (final volume of 200 μL), was neutralized with 0.76 M potassium bicarbonate (KHCO_3) in a 1:1 proportion and centrifuged for 5 min at $13,000 \times g$ at 4°C . To calculate the total glutathione (tGSH), 100 μL of the neutralized supernatants were transferred, in triplicate, to a 96-well plate. After this, 65 μL of freshly prepared reagent with 0.24 mM NADPH and 1.3 mM 5,5-dithio-bis(2-nitrobenzoic acid) (DTNB) in phosphate buffer (71.5 mM Na_2HPO_4 , 71.5 mM NaH_2PO_4 and 0.63 mM EDTA, pH 7.5) were added. Afterwards, the plates were incubated for 15 min, at 30°C and then 40 μL per well of a freshly prepared 10 IU/mL glutathione reductase solution in phosphate buffer were added. Finally, the stoichiometric formation of TNB was followed in kinetic mode (at 30°C), with pre-measurement mixing, every 10 s for 3 min at 415 nm, and compared with a standard curve. The results were normalized to the total protein amount, and the final results were expressed as nmol tGSH per mg protein.

Study of EHMC and TiO_2 combination under irradiation

An additional analysis was performed in partnership with FEUP research group, where photoproducts and compounds combinations was evaluated. An aqueous solutions of EHMC 8.0×10^{-5} M (10 % v/v in acetonitrile) were prepared in the absence and presence of TiO_2 -P25 (1 g/L, Evonik Degussa). Blank solutions of aqueous TiO_2 -P25 (1 g/L, 10% v/v in acetonitrile) and of water (10% v/v in acetonitrile) were also prepared. Aqueous solution of the mixture (EHMC+ TiO_2 -P25, 10% v/v in acetonitrile) was irradiated with one UV LED (10 W, emission at 385 nm) during 30 min. 5 mL of each solution was taken, filtered with 0.45 μm PTFT filters and EHMC was extracted with 5 mL of acetonitrile. These solutions were then used for NRU cytotoxicity assay.

3.2.4. Statistical analysis

All the data are presented as mean \pm standard deviation (SD) of at least three independent experiments. Statistical analysis was performed using the SPSS software (v

23.0; IBM, Armonk, NY, USA). To confirm the normality and homogeneity of variance Shapiro-Wilk and Levene tests were used, respectively, and after this the One-way analysis of variance (ANOVA) followed by the Dunnett post hoc test (comparison to negative control-cells with solvent) was performed. Graphs were generated with the software GraphPad Prism for Windows (version 6.0; GraphPad Software, Inc., USA).

4. Results and discussion

4.1. HaCat cell line characterization

According with the graph shown below (Figure 24), the doubling time for HaCaT cell line was 22.18 ± 4.47 h. A doubling time of 26 hours is reported in literature ([175](#)), thus confirming our results.

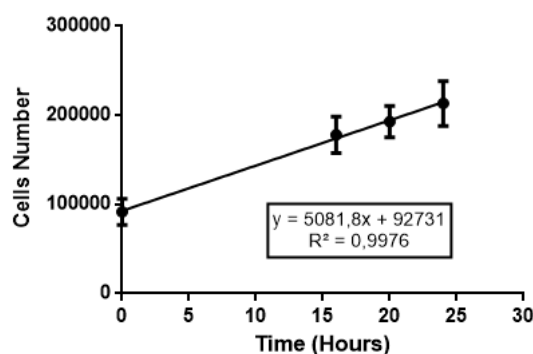


Figure 24. Determination of HaCaT cells doubling time by linear regression analysis. Data are presented as mean \pm SD ($n=3$).

4.2. ROS generation assay

4.2.1. Solvent control

The fluorescence range of all solvents used for the evaluation of ROS generation at 24h compound exposure is depicted in Figure 25. These solvent controls did not show a statistical significant difference relative to the negative controls (untreated cells; $p \geq 0.05$).

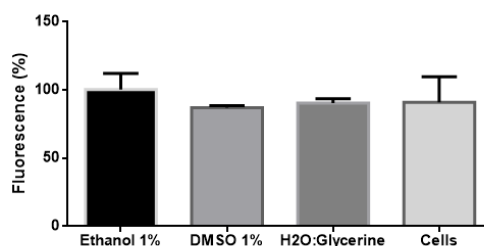


Figure 25. Fluorescence of HaCaT cell line exposed to solvent control by the Neutral Red by the DCFH-DA assay. Data are presented as mean \pm SD ($n=3$). Data were analysed using One-way ANOVA with Dunnett post hoc test.

4.2.2. ROS generation assay optimization

As referred above, an optimization of the ROS generation assay was performed by studying the optimal cell density, and the concentration and the incubation time with the DCFH-DA probe. From the results obtained (Figure 26) a density of 2×10^5 cells/well and a concentration of DCFH-DA of $50 \mu\text{M}$ seemed to be the ideal conditions for the ROS generation assay, since the fluorescence signal was high enough to ensure appropriate sensitivity. Regarding the incubation time with the DCFH-DA probe, a significant difference between the data at 30min and 1h was not evident so, in order to decrease the duration of the assay, 30 min incubations were chosen for the final procedure. The difference between the two positive control (H_2O_2) concentrations is not relevant, a slight increase of fluorescence with $400\mu\text{M}$ was observed.

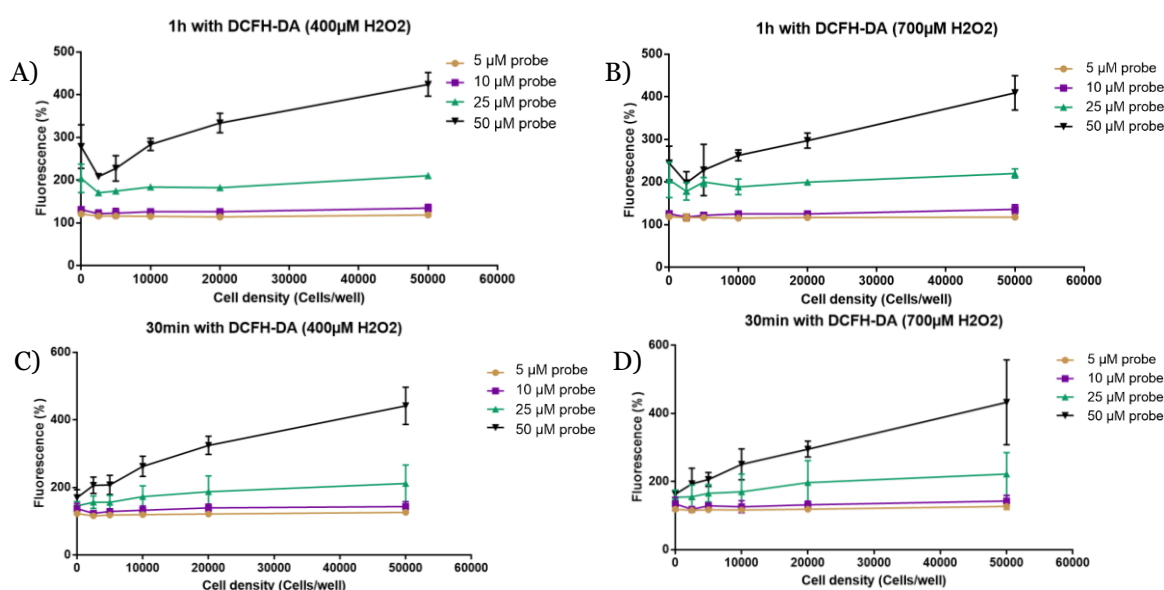


Figure 26. Optimization of ROS generation assay with fluorescence regarding cell density, DCFH-DA concentration, incubation time and positive control (H_2O_2) concentration. (A) 1h with DCFH-DA and H_2O_2 $400\mu\text{M}$ (B) 1h with DCFH-DA and H_2O_2 $700\mu\text{M}$ (C) 30min with DCFH-DA and H_2O_2 $400\mu\text{M}$ and (D) 30min with DCFH-DA and H_2O_2 $700\mu\text{M}$. Data are presented as mean \pm SD ($n=3$).

4.2.3. ROS generation using DCFH-DA

Positive controls

Hydrogen peroxide (H_2O_2)

H_2O_2 induced an increase in fluorescence, yet this increase was only statistically significant different from the solvent control at 2000 μM (Figure 27). These data should be interpreted with caution given that hydrogen peroxide can interact with the DCFH-DA probe as was observed in an exploratory assay realized. This result needs further confirmation.

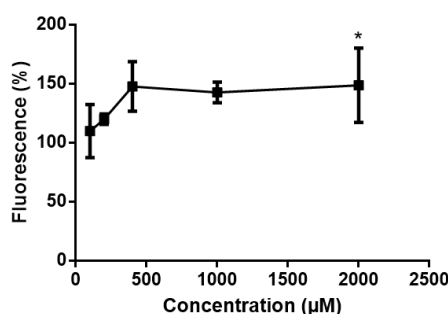


Figure 27. ROS detection in HaCaT cell line exposed to H_2O_2 by the DCFH-DA assay. Data are presented as mean \pm SD ($n=3$) relative to solvent control = 100 ± 20.8 ($n=3$). Data were analysed using One-way ANOVA with Dunnett post hoc test. * $P < 0.05$

Quinine HCl

Quinine led to a concentration dependent decrease in ROS generation with statistical significance difference relative to solvent control from 6.3 mM (Figure 28). However, it should be noted that quinine apparently quenches fluorescence at the tested emission wavelength as was observed in an exploratory study performed. This result needs further confirmation.

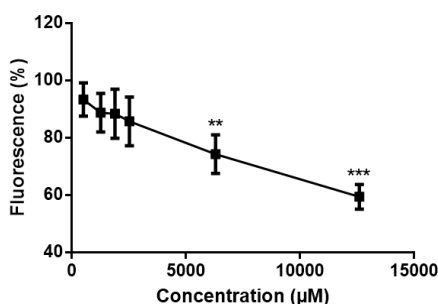


Figure 28. ROS detection in HaCaT cell line exposed to Quinine HCl by the DCFH-DA assay. Data are presented as mean \pm SD ($n=3-5$) relative to solvent control = 100 ± 11.7 ($n=3$). Data were analysed using One-way ANOVA with Dunnett post hoc test. ** $P < 0.01$, *** $P < 0.001$.

Raw materials under study

1,2-DHX

1,2-DHX did not present any significant increase in fluorescence signal relative to solvent control (Figure 29).

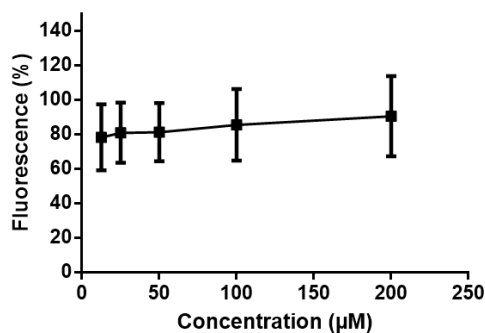


Figure 29. ROS detection in HaCaT cell line exposed to 1,2-DHX by the DCFH-DA assay. Data are presented as mean \pm SD ($n=3$) relative to solvent control = 100 ± 1.7 ($n=3$). Data were analyzed using One-way ANOVA with Dunnett post hoc test.

5-MOP

5-MOP did not promote ROS generation up to 300 µM with no statistical significance differences relative to solvent control (Figure 30).

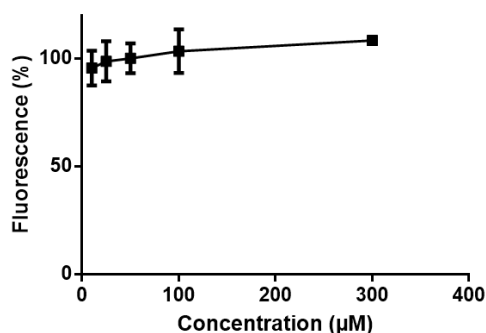


Figure 30. ROS detection in HaCaT cell line exposed to 5-MOP by the DCFH-DA assay. Data are presented as mean \pm SD ($n=3$) relative to solvent control = 100 ± 1.7 ($n=3$). Data were analysed using One-way ANOVA with Dunnett post hoc test.

Acetylsalicylic acid

ASA increased fluorescence up to 111101 μM (which was not concentration-dependent) with statistical significant difference relative to solvent control from 2775 μM (Figure 31). This result was possible due to interaction between ASA and the DCFH-DA probe and not due to an induced ROS generation in HaCaT cells as observed in an exploratory assay performed. However, this results needs further confirmation.

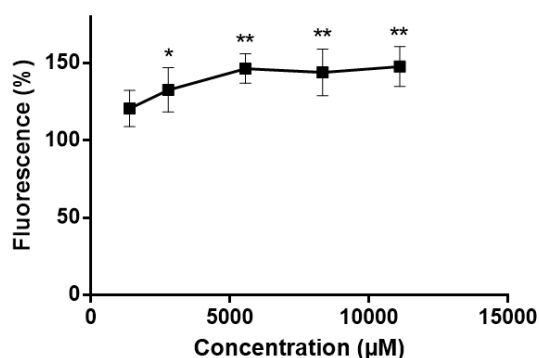


Figure 31. ROS detection in HaCaT cell line exposed to ASA by the DCFH-DA assay. Data are presented as mean \pm SD ($n=3$) relative to solvent control = 100 ± 11.7 ($n=3$). Data were analysed using One-way ANOVA with Dunnett post hoc test. * $P<0.05$, ** $P<0.01$.

Avobenzone

Avobenzone did not cause any alteration in fluorescence signal as can be observed on Figure 32, with no statistical significance difference in comparison with solvent control.

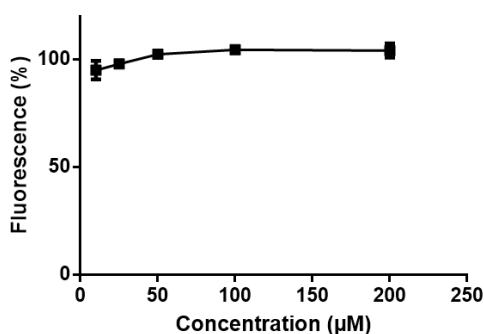


Figure 32. ROS detection in HaCaT cell line exposed to Avobenzone by the DCFH-DA assay. Data are presented as mean \pm SD ($n=4$) relative to solvent control = 100 ± 17 ($n=3$). Data were analysed using One-way ANOVA with Dunnett post hoc test.

C. sativa extract

The *C. sativa* extract demonstrated a concentration dependent fluorescence increase, with statistical significant difference relative to solvent control from 250 µg/mL (Figure 33). This result may be due to compound fluorescence interference as showed in an exploratory assay performed. This result must be confirmed in the future.

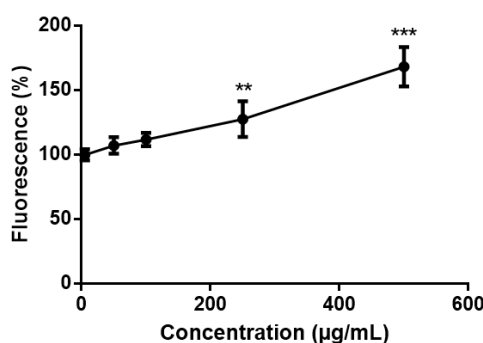


Figure 33. ROS detection in HaCaT cell line exposed to *C. sativa* extract by the DCFH-DA assay. Data are presented as mean \pm SD ($n=4$) relative to solvent control = 100 ± 3.7 ($n=3$). Data were analyzed using One-way ANOVA with Dunnett post hoc test. * $P<0.05$, ** $P<0.01$, *** $P<0.001$ data are significant.

Chlorpromazine

CPZ did not reveal fluorescence increases, with no statistical significance difference relative to solvent control (Figure 34).

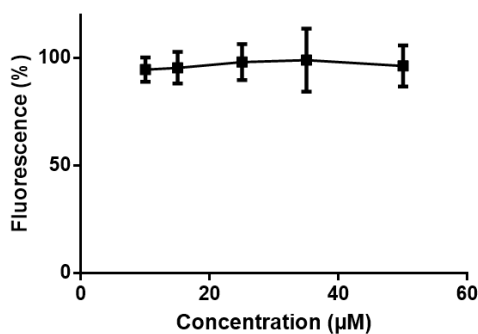


Figure 34. ROS detection in HaCaT cell line exposed to CPZ by the DCFH-DA assay. Data are presented as mean \pm SD ($n=4$) relative to solvent control = 100 ± 20.8 ($n=3$). Data were analysed using One-way ANOVA with Dunnett post hoc test.

Diclofenac

Diclofenac demonstrated a concentration dependent fluorescence increase, with statistical significance difference relative to solvent control from 500 μ M (Figure 35). This result can have a compound fluorescence interference as observed in an exploratory assay realized and needs further confirmation.

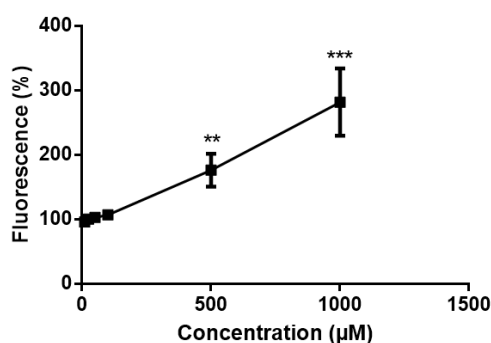


Figure 35. ROS detection in HaCaT cell line exposed to Diclofenac by the DCFH-DA assay. Data are presented as mean \pm SD ($n=4$) relative to solvent control = 100 ± 1.7 ($n=3$). Data were analysed using One-way ANOVA with Dunnett post hoc test. ** $P<0.01$, *** $P<0.001$

EHMC

EHMC did not promote an increase in fluorescence, with no statistical significance difference relative to solvent control (Figure 36).

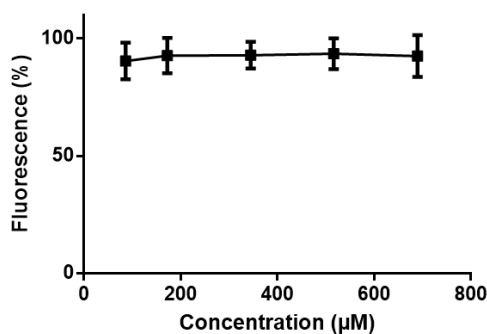


Figure 36. ROS detection in HaCaT cell line exposed to EHMC by the DCFH-DA assay. Data are presented as mean \pm SD ($n=3$) relative to solvent control = 100 ± 11.7 ($n=3$). Data were analysed using One-way ANOVA with Dunnett post hoc test.

Hexachlorophene

Hexachlorophene led to a concentration-dependent fluorescence increase, however only with statistical significance difference relative to solvent control from 245 μM (Figure 37). This increase may have a compound fluorescence interference and future confirmation must be realized.

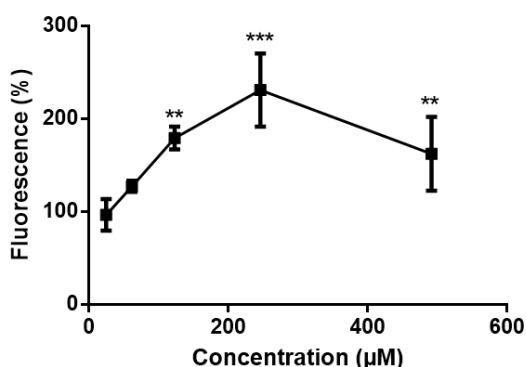


Figure 37. ROS detection in of HaCaT cell line exposed to Hexachlorophene by the DCFH-DA assay. Data are presented as mean \pm SD ($n=3-4$) relative to solvent control 100 ± 1.7 ($n=3$). Data were analysed using One-way ANOVA with Dunnett post hoc test. ** $P<0.01$, *** $P<0.001$.

Resveratrol

Resveratrol induced a decrease in ROS generation, with statistical significance difference relative to solvent control from 100 μM (Figure 38). However, this decrease may be related to interactions between RSV with medium and the DCFH-DA probe as observed in a exploratory assay performed. This result needs further confirmation.

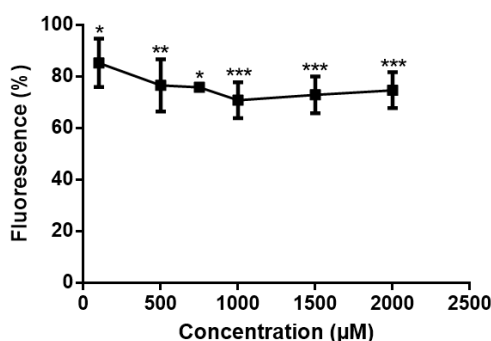


Figure 38. ROS detection in HaCaT cell line exposed to RSV by the DCFH-DA assay. Data are presented as mean \pm SD ($n=3-6$) relative to solvent control = 100 ± 1.7 ($n=3$). Data were analysed using One-way ANOVA with Dunnett post hoc test. * $P<0.05$, ** $P<0.01$, *** $P<0.001$.

Sodium lauryl sulphate

SLS evoked an increase in the measured fluorescence signal, with statistical significance difference relative to solvent control from 260 μM (Figure 39). However, also in this case, this result may result from an interaction of SLS with the DCFH-DA probe as observed in an exploratory assay preformed. Thus, this result needs further confirmation.

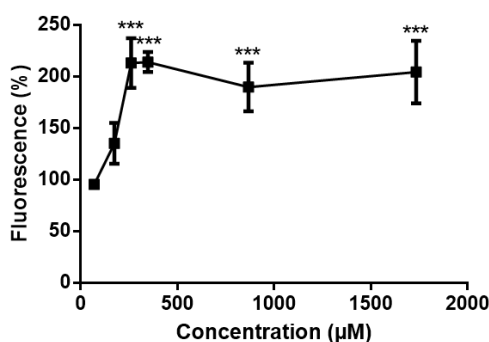


Figure 39. ROS detection in HaCaT cell line exposed to SLS by the DCFH-DA assay. Data are presented as mean \pm SD ($n=3-5$) relative to solvent control = 100 ± 20.8 ($n=3$). Data were analysed using One-way ANOVA with Dunnett post hoc test. *** $P < 0.001$.

4.3. Neutral red uptake assay

4.3.1. Solvent control

The cytotoxicity of all solvents used for the evaluation of phototoxic effects at 24h compound exposure is depicted in Figure 40. These solvent controls did not show a statistical significant difference relative to the negative controls (untreated cells; $p \geq 0.05$).

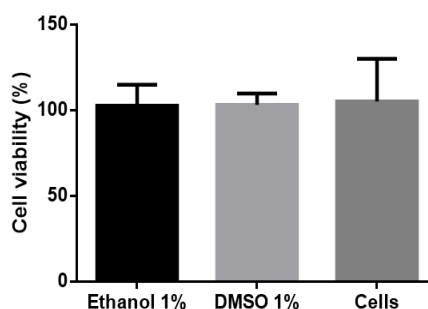


Figure 40. Cell viability of HaCaT cell line exposed to solvent control by the Neutral Red assay. Data are presented as mean \pm SD ($n=3$). Data were analysed using One-way ANOVA with Dunnett post hoc test.

4.3.2. Neutral red uptake assay optimization

As referred above, an optimization of NRU assay was performed, by studying the optimal cell density, NR concentration and incubation time with the NR solution. With regards to the NR concentration, the assay included macroscopic and microscopic observation. Crystal formation could be seen before filtering the 100 $\mu\text{g/mL}$ solution, so the final concentration was not the desired one. Crystal formation in the well could be observed at concentrations higher than 330 $\mu\text{g/mL}$, as shown in Figure 41.

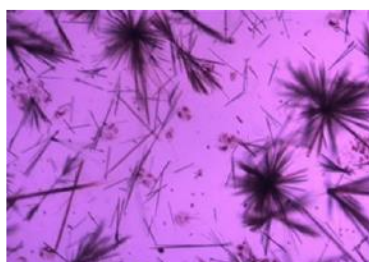


Figure 41. Observation under inverted microscope of HaCaT cells incubated with 100 $\mu\text{g/mL}$ NR solution (10X magnification).

From the results obtained (Figure 42) a density of 2×10^4 cells/well, NR concentration of 50 $\mu\text{g/mL}$ and 3h incubation with the NR solution were selected as the ideal test conditions. Under these conditions, no formation of NR crystals was observed and the absorbance was high enough to ensure appropriate assay sensitivity.

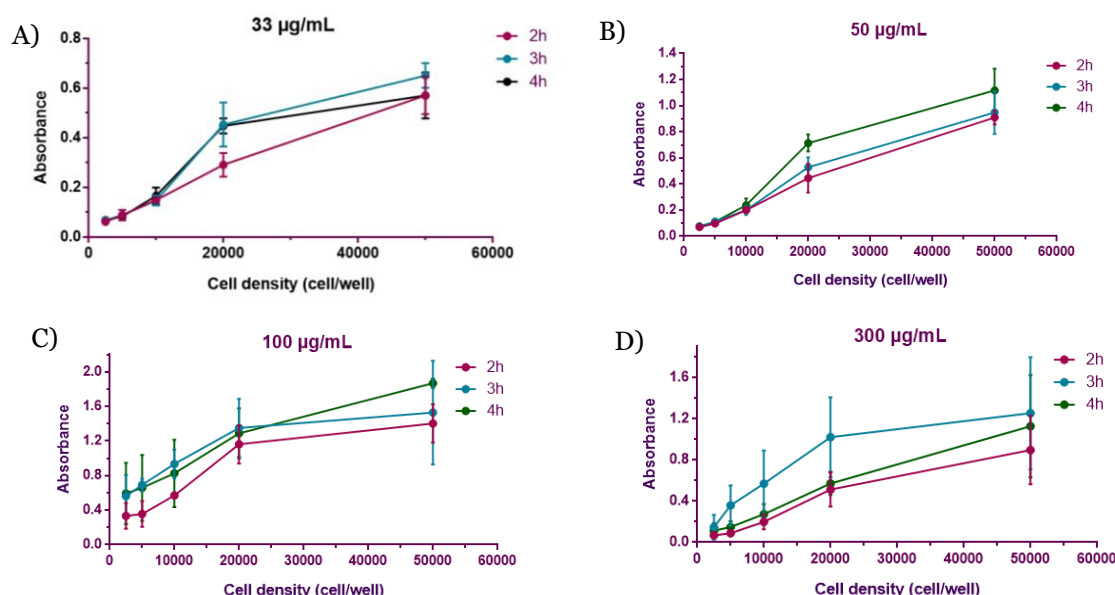


Figure 42. Optimization of NR uptake assay with absorbance regarding cell density, NR concentration and incubation time. (A) NR 33 $\mu\text{g/mL}$ (B) NR 50 $\mu\text{g/mL}$ (C) NR 100 $\mu\text{g/mL}$ and (D) NR 330 $\mu\text{g/mL}$. Data are presented as mean \pm SD (n=3-5).

Regarding the parameters optimized in a reported study, the NR concentration and incubation time, and exposure time of the tested compounds were identical to the majority of the studies conducted with this cell line. Cell densities varied from 5×10^3 /well to 1.5×10^5 /well which encompasses the cell density selected in this study (2×10^4 / well). The type of radiation source and irradiation doses vary widely in the literature reports, with the majority of the tests conducted solely with UVA (176).

4.3.3. Neutral red uptake cytotoxicity test

Raw materials under study

5-MOP

The cytotoxicity study demonstrated that 5-MOP does not cause cell death up to 300 μM after 24h exposure, with no significative differences relative to solvent control detected (Figure 43).

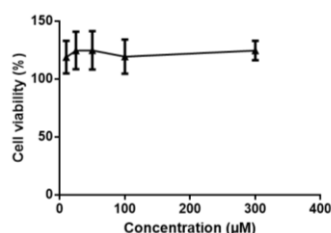


Figure 43. Cell viability of HaCaT cell line exposed to 5-MOP by the Neutral Red assay. Data are presented as mean \pm SD ($n=9-13$) relative to solvent control = 100 ± 6.3 . Data were analysed using One-way ANOVA with Dunnett post hoc test.

Acetyl salicylic acid

Acetyl salicylic acid (ASA) was found to be non cytotoxic to HaCaT cells until 1100 μM with no statistical significate difference relative to control (Figure 44).

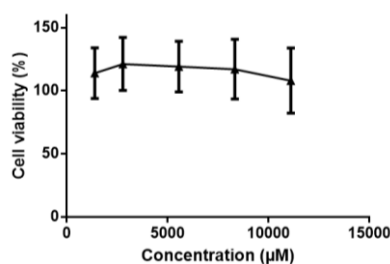


Figure 44. Cell viability of HaCaT cell line exposed to ASA by the Neutral Red assay. Data are presented as mean \pm SD ($n=5$) relative to solvent control = 100 ± 11.9 ($n=3$). Data were analysed using One-way ANOVA with Dunnett post hoc test.

Avobenzone

The UV-filter avobenzone did not demonstrate cytotoxic effects up to 200 μM . However it is possible to observe a decrease in cell viability between 10 and 100 μM and than a stabilization, but not with statistical significance relative to control (Figure 45).

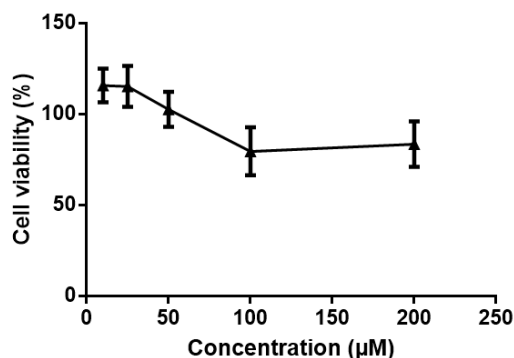


Figure 45. Cell viability of HaCaT cell line exposed to Avobenzone by the Neutral Red assay. Data are presented as mean \pm SD ($n=3$) relative to solvent control = 100 ± 6.3 ($n=3$). Data were analysed using One-way ANOVA with Dunnett post hoc test.

Chlorpromazine

CPZ promoted a decrease in HaCaT viability with an IC_{50} of 41.67 ± 2.62 μM , with statistical significance difference relative to solvent control from 35 μM (Figure 46).

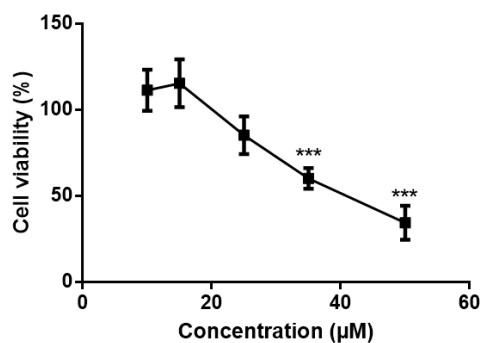


Figure 46. Cell viability of HaCaT cell line exposed to CPZ by the Neutral Red assay. Data are presented as mean \pm SD ($n=6$) relative to solvent control = 100 ± 12.5 ($n=3$). Data were analysed using One-way ANOVA with Dunnett post hoc test. *** $P < 0.001$.

Diclofenac

The cytotoxicity of diclofenac only presented a significant difference from controls from 500 μ M and the IC₅₀ could not be calculated (Figure 47).

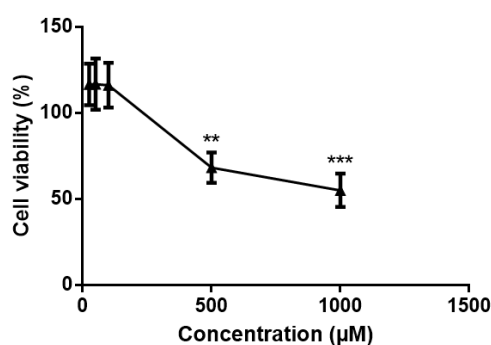


Figure 47. Cell viability of HaCaT cell line exposed to Diclofenac by the Neutral Red assay. Data are presented as mean \pm SD ($n=3$) relative to solvent control = 100 ± 6.3 ($n=3$). Data were analysed using One-way ANOVA with Dunnett post hoc test. ** $P<0.01$, *** $P<0.001$.

EHMC

EHMC had a IC₅₀ for cytotoxicity of 547.68 ± 88.48 μ M, with statistical significance difference relative to solvent control from 345 μ M (Figure 48).

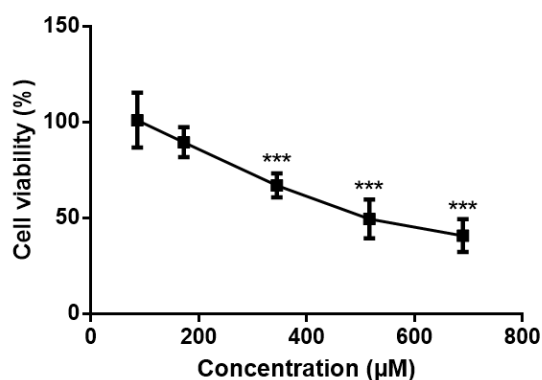


Figure 48. Cell viability of HaCaT cell line exposed to EHMC by the Neutral Red assay. Data are presented as mean \pm SD ($n=3-7$) relative to solvent control = 100 ± 11.9 ($n=3$). Data were analysed using One-way ANOVA with Dunnett post hoc test. *** $P<0.001$.

Hexachlorophene

Hexachlorophene presented an IC₅₀ of $156.66 \pm 19.27 \mu\text{M}$, with statistical significance difference relative to solvent control from $122 \mu\text{M}$ (Figure 49).

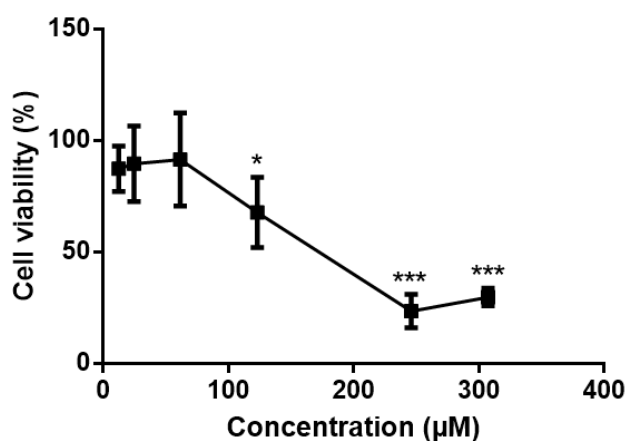


Figure 49. Cell viability of HaCaT cell line exposed to Hexachlorophene by the Neutral Red assay. Data are presented as mean \pm SD ($n=3-20$) relative to solvent control = 100 ± 6.3 ($n=3$). Data were analysed using One-way ANOVA with Dunnett post hoc test. * $P<0.05$, *** $P<0.001$.

Hydrogen peroxide

With respect to the study of the cytotoxicity of H_2O_2 the IC₅₀ determined was $243.31 \pm 59.64 \mu\text{M}$, with statistical significance difference relative to solvent control from $200 \mu\text{M}$ (Figure 50).

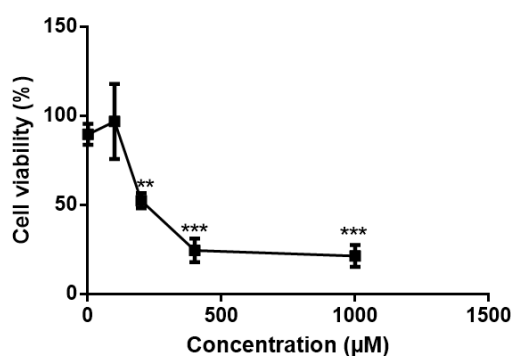


Figure 50. Cell viability of HaCaT cell line exposed to H_2O_2 by the Neutral Red assay. Data are presented as mean \pm SD ($n=3-8$) relative to solvent control = 100 ± 26.6 ($n=3$). Data were analysed using One-way ANOVA with Dunnett post hoc test. ** $P<0.01$, *** $P<0.001$.

Quinine HCl

The cytotoxicity study of quinine HCl present a IC_{50} of $787.75 \pm 222.73 \mu M$, with statistical significance difference relative to solvent control from $504 \mu M$ (Figure 51).

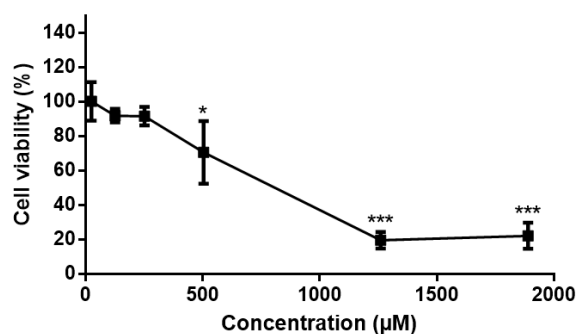


Figure 51. Cell viability of HaCaT cell line exposed to Quinine HCl by the Neutral Red assay. Data are presented as mean \pm SD ($n=5$) relative to solvent control = 100 ± 11.9 ($n=3$). Data were analysed using One-way ANOVA with Dunnett post hoc test. * $P<0.05$, *** $P<0.001$.

Sodium lauryl sulphate

SLS presented an IC_{50} of $221.09 \pm 26.13 \mu M$, with statistical significance difference relative to solvent control from $260 \mu M$ (Figure 52).

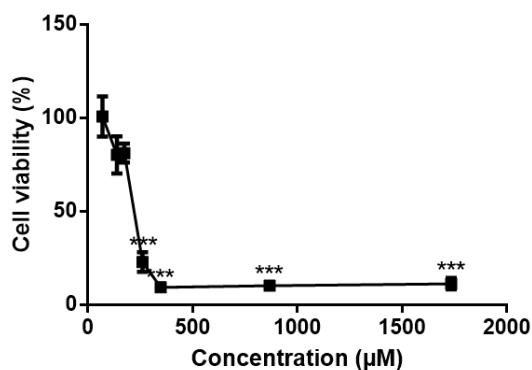


Figure 52. Cell viability of HaCaT cell line exposed to SLS by the Neutral Red assay. Data are presented as mean \pm SD ($n=3-6$) relative to solvent control = 100 ± 27.5 ($n=3$). Data were analysed using One-way ANOVA with Dunnett post hoc test. *** $P<0.001$.

4.4. Implementation and validation of a phototoxicity assay using HaCaT

4.4.1. Solvent control

The cytotoxicity of all solvents used for the evaluation of phototoxic effects, in the presence and absence of irradiation, with 1h of compound exposure is depicted in Figure 53. These solvent controls did not show a statistical significant difference relative to the negative controls (untreated cells; $p \geq 0.05$).

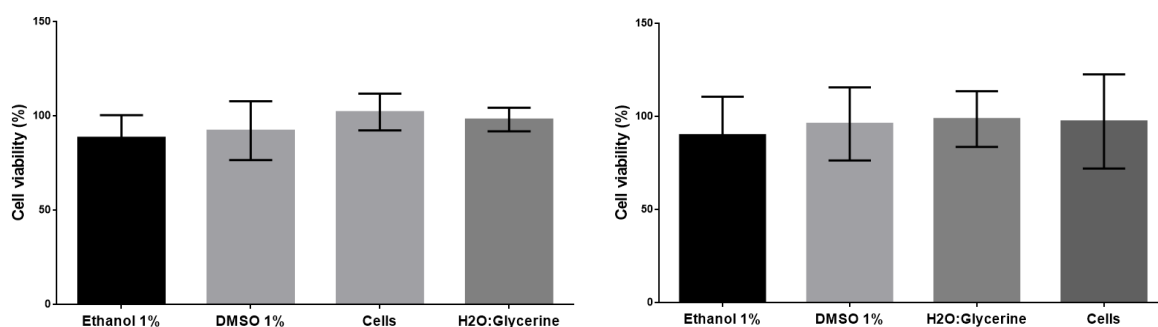


Figure 53. Cell viability of HaCaT cell line exposed to solvent control at plate A) not irradiate and B) irradiate by the Neutral Red assay. Data are presented as mean \pm SD ($n=3$). Data were analysed using One-way ANOVA with Dunnett post hoc test.

4.4.2. Spectral absorption

All the compounds exhibited absorption in the 290-700 nm range, which is a primary condition before conducting phototoxicity tests (Figures 54-67).

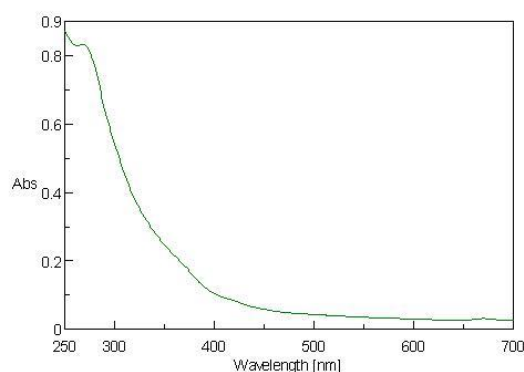


Figure 54. *C. sativa* spectral absorption

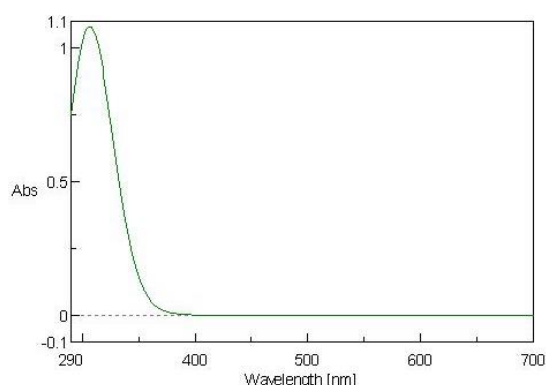


Figure 55. CPZ spectral absorption

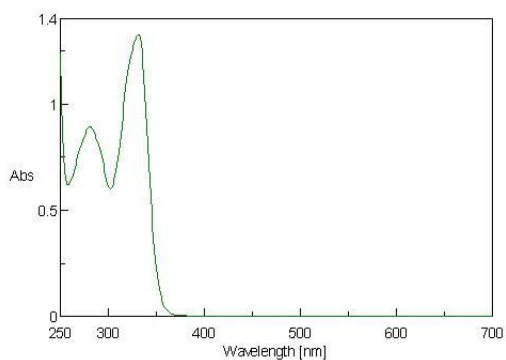


Figure 56. Quinine HCl spectral absorption

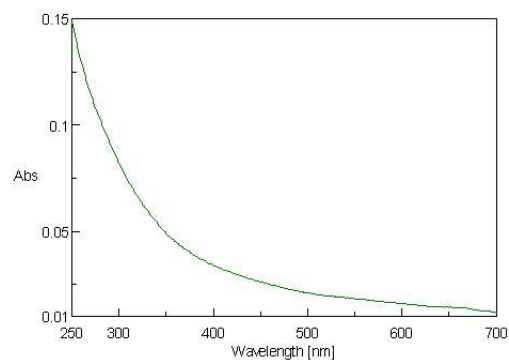


Figure 57. SLS spectral absorption

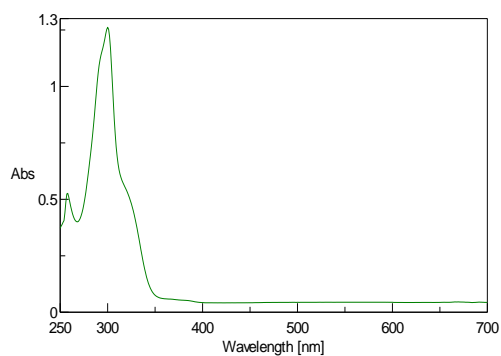


Figure 58. Hexachlorophene spectral absorption

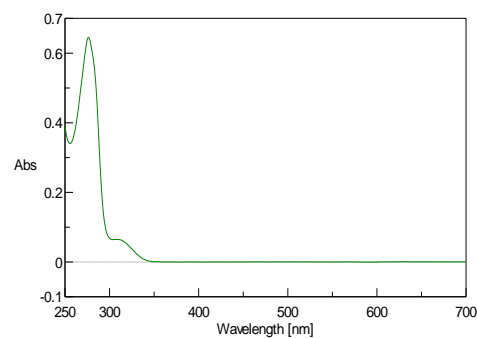


Figure 59. ASA spectral absorption

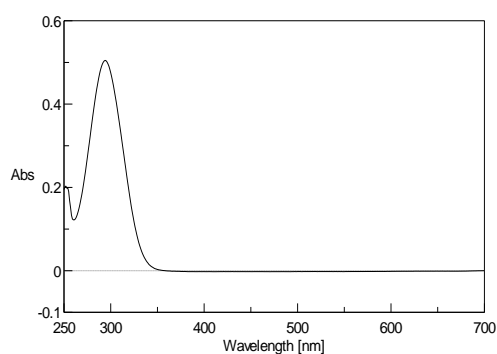


Figure 60. Diclofenac spectral absorption

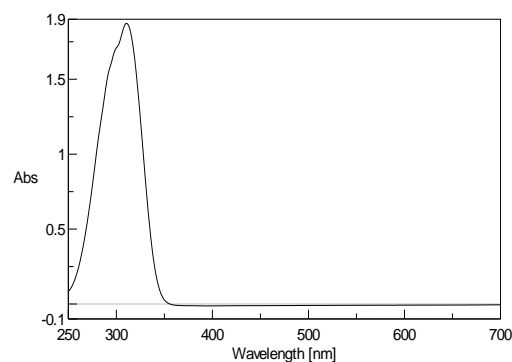


Figure 61. EHMC spectral absorption

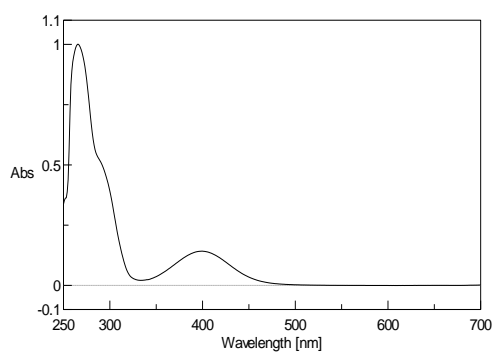


Figure 62. 1,2-DHX spectral absorption

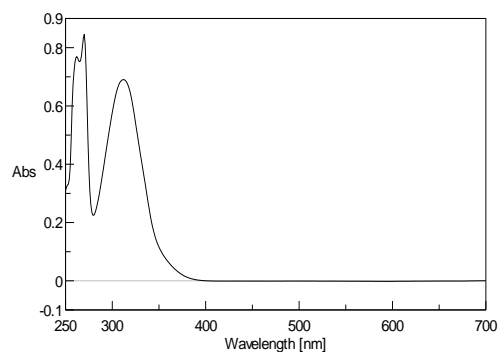


Figure 63. 5-MOP spectral absorption

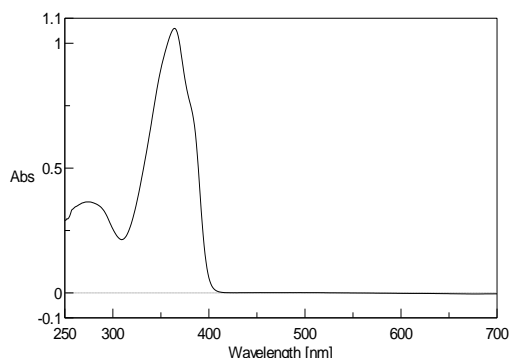


Figure 64. Avobenzone spectral absorption

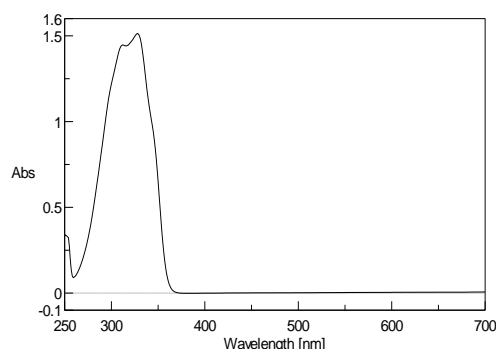


Figure 65. RSV spectral absorption.

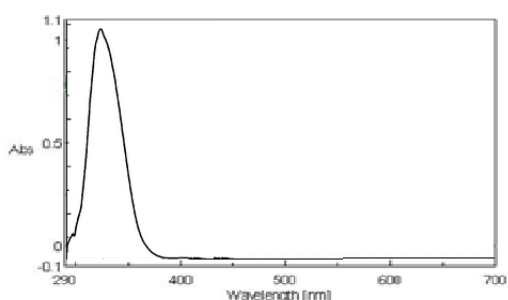
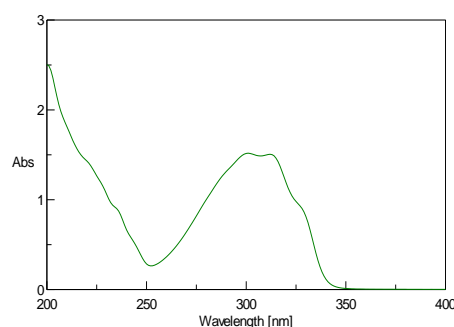
Figure 66. H₂O₂ spectral absorption

Figure 67. RGS spectral absorption

4.4.3. Optimization of irradiation conditions

The radiation intensity recommended by the OCDE 432 guideline is 1.7mW/cm², which corresponded to the irradiation obtained with the lamp positioned at 46.5cm height (Figure 68). During the irradiation period (1h), the temperature achieved using a water-cooling system varied between 29 and 32°C, maintaining the cell viability (Figure 69). Under these conditions, UV exposures longer than 15 min were cytotoxic for HaCaT cells. An irradiation period of 10 min was considered the optimal irradiation time, since it afforded cell viabilities of $77 \pm 2.94\%$ (Figure 70). Therefore, we assumed that this irradiation time provided evidence for the phototoxic potential of the test compounds without significantly compromising cell viability. The UVA/UVB lamp used has some advantages regarding the most commonly used UVA lamps, since it contemplates the UVA and UVB wavelength, better simulating the solar spectrum. Besides this, it is an inexpensive choice.



Figure 68. UVA/UVB Osram lamp and radiometer used in this work.

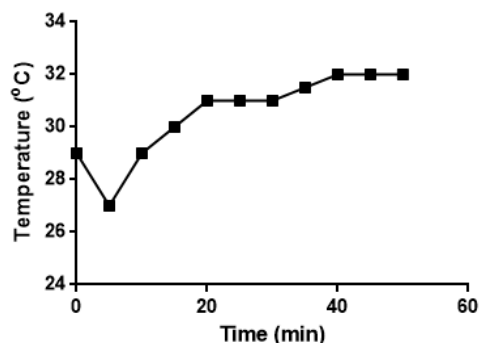


Figure 69. Temperature achieved using a water-cooling.

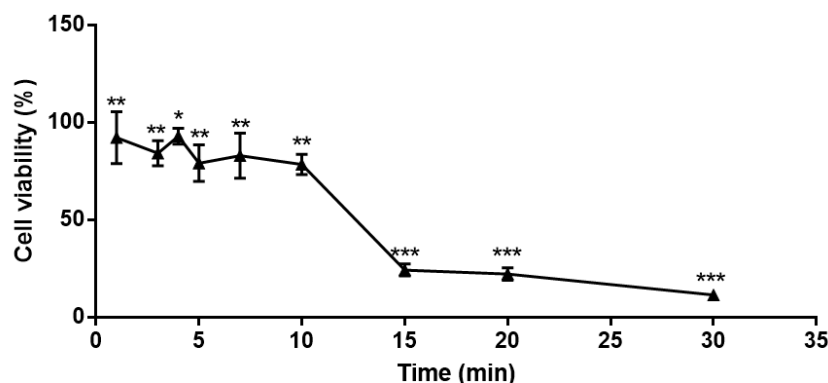


Figure 70. Viability of HaCaT cells exposed to UVA/UVB radiation, determined by the Neutral Red assay. Data are presented as mean \pm SD ($n=3-12$). Data were analysed using One-way ANOVA with Dunnett post hoc test. * $P<0.05$, ** $P<0.01$, *** $P<0.001$.

4.4.4. Neutral red uptake phototoxicity test

Positive controls

5-MOP

5-MOP is a positive control in phototoxicity testing. Under our test conditions, the IC₅₀(+irr) value determined was $3.8 \pm 0.24 \mu\text{M}$, with statistical significant differences relative to solvent control from $2.5 \mu\text{M}$. The IC₅₀(-irr) could not be obtained due to compound solubility limitations, therefore, it is possible to conclude that the IC₅₀(-irr) is higher than $300 \mu\text{M}$ (Figure 71). Thus, the PIF was calculated with the maximum concentration tested ($300 \mu\text{M}$), and not with the IC₅₀ values. With this calculation, the estimated PIF was 78.8 ± 5.11 , which it is in accordance with positive phototoxic potential.

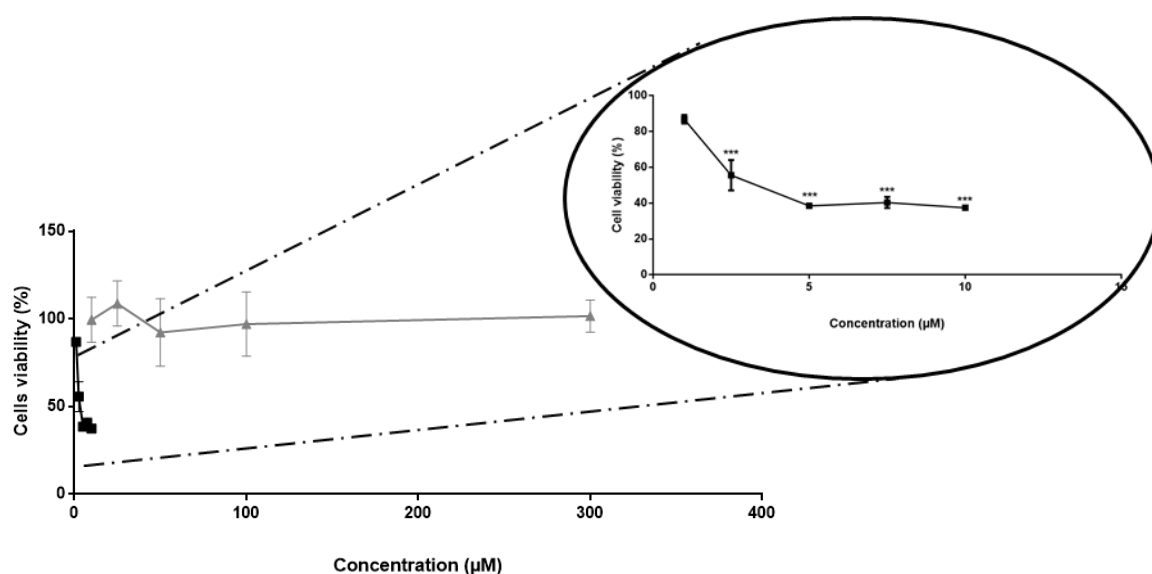


Figure 71. Cell viability of HaCaT cell line exposed to 5-MOP, determining the phototoxicity by the Neutral Red assay. -irr: plate not irradiate. +irr: plate irradiate. Data are presented as mean \pm SD ($n=4-5$) relative to solvent control, with (+irr)= 100 ± 20.5 ($n=3$) and (-irr)= 100 ± 16.9 ($n=3$). Data were analysed using One-way ANOVA with Dunnett post hoc test. *** $P<0.001$.

We have compared our data with the results reported for mice BALB/c 3T3 fibroblasts: IC₅₀(+irr) was 7.4 μ M, IC₅₀(-irr) could not be obtained, and PIF calculated as referred above, was 62.5 (123). It can be concluded that keratinocytes are probably more sensitive to 5-MOP phototoxicity than fibroblasts.

The NRU Phototoxicity test has already been performed with HaCaT cells (176, 177). In studies with 5-MOP and 250 mJ/cm² UVA, an IC₅₀(+irr) value of 190 μ M was obtained (178), which is markedly higher than the ones obtained in the present study (3.8 μ M). However in the mentioned study, it was used solely UVA light in a dose 4 times lower than the used in the present work.

Chlorpromazine

Chlorpromazine is the most used positive control for phototoxicity assays. The obtained results corroborate this fact. The IC₅₀(-irr) was 193.5 ± 13.74 μ M, with statistical significant difference relative to solvent control from 140.9 μ M and IC₅₀ (+irr) was 6.93 ± 1.46 μ M with statistical significant difference relative to solvent control from 8.5 μ M, thereby obtaining a PIF of 23.30 ± 2.69 (Figure 72).

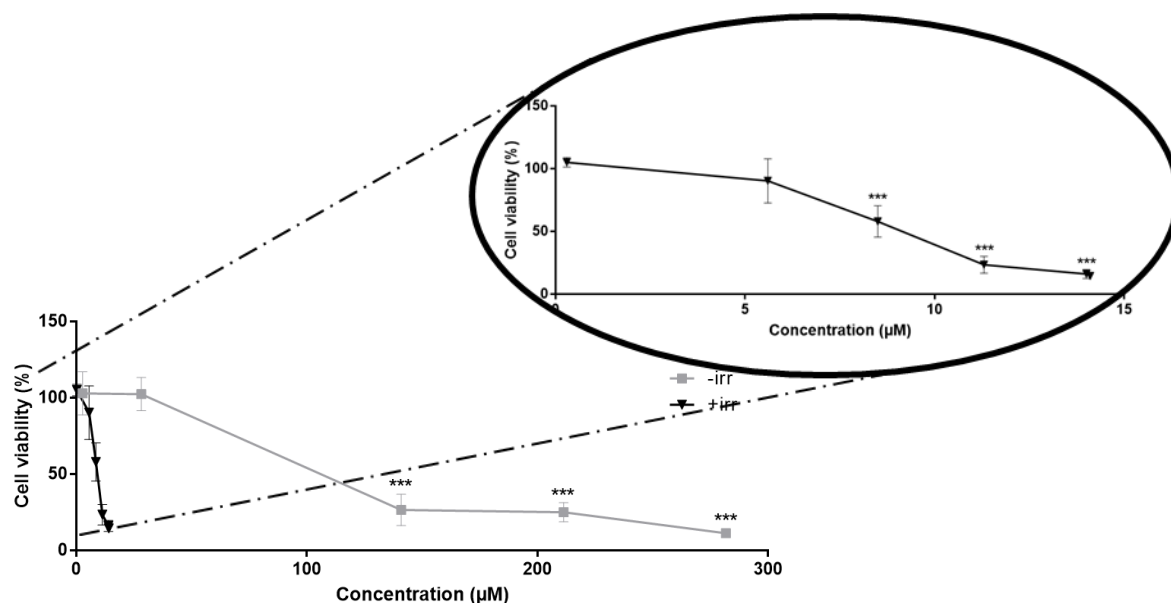


Figure 72. Cell viability of HaCaT cell line exposed to CPZ, determining the phototoxicity by the Neutral Red assay. -irr: plate not irradiate. +irr: plate irradiate Data are presented as mean \pm SD ($n=3-6$) relative to solvent control, with afforded a cell viability of (+irr)= 100 ± 15.2 % ($n=3$) and (-irr)= 100 ± 7.8 ($n=3$). Data were analysed using One-way ANOVA with Dunnett post hoc test. *** $P<0.001$.

Comparing these results with those already reported for BALB/c 3T3 fibroblasts, when $IC_{50}(-irr)$ was $34.49 \mu M$, $IC_{50}(+irr)$ was $1.2 \mu M$ and PIF was 9.2 (123), the human keratinocyte cell line manifested less sensitivity to chlorpromazine, which may be due to the powerful antioxidant system of these cells, since ROS generation with CPZ was reported in literature to mitochondrial membrane potential assay.

In another HaCaT study reported in literature, the $IC_{50}(+irr)$ was $15.82 \mu M$ with 250 mJ/cm^2 UVA (178), which is markedly higher than the values obtained in the present study ($6.93 \mu M$). However the mentioned study used solely UVA light in a dose 4 times lower than the one used in the present work. The PIF values described in literature were 49 (179) and 16.7 (180). Taking together, these findings support the validity of the methodology implemented herein but reinforce the importance of careful comparisons when different test conditions such as cell density, irradiation sources and doses are used.

Quinine HCl

Quinine is a positive control in phototoxicity assays. In the present study its $IC_{50}(-irr)$ was $4269.88 \pm 734.08 \mu M$, its $IC_{50}(+irr)$ was $1293.42 \pm 240.97 \mu M$, both with statistical significance difference relative to solvent control from $1259 \mu M$ and a PIF of 2.09 ± 0.85 . Quinine was thus classify as probably phototoxic (Figure 73).

In a study conducted with BALB/c 3T3 fibroblasts the PIF was 15.7 (59). Also in this case, the differences observed in our keratinocytes may be possibly justified by their powerful antioxidant system, since quinine was reported to produce 6-methoxy-quinoline-4-ylmethyl-oxonium as photoproduct and to generate ROS, such as 1O_2 , $O_2(\bullet-)$ and $(\bullet)OH$ under UV exposure (181). Finally, this conclusion can be corroborated by the GSH assay data reported in section 4.4.7.

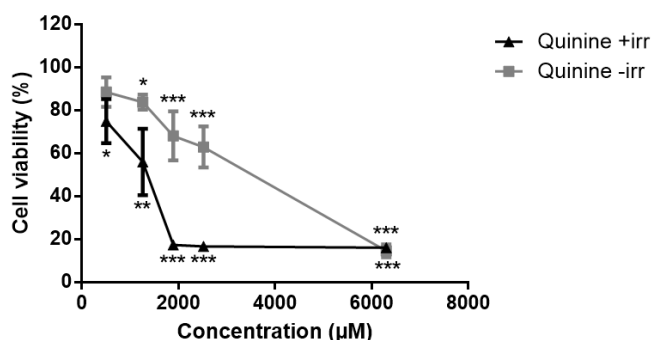


Figure 73. Cell viability of HaCaT cell line exposed to Quinine HCl, determining the phototoxicity by the Neutral Red assay. -irr: plate not irradiate. +irr: plate irradiate Data are presented as mean \pm SD ($n=3-5$) relative to solvent control, with (+irr)= 100 ± 20.7 ($n=3$) and (-irr)= 100 ± 12.0 ($n=3$). Data were analysed using One-way ANOVA with Dunnett post hoc test. * $P<0.05$, ** $P<0.01$, *** $P<0.001$.

Negative controls

Acetyl salicylic acid (ASA)

This compound is commonly used as a negative control in phototoxicity evaluations. Our data corroborat this fact (Figure 74). However, the IC_{50} and PIF could not be determinated since no statistically significant differences relative to control were observed at any of the tested concentrations. As an alternative, the MPE determination could provide relevant information.

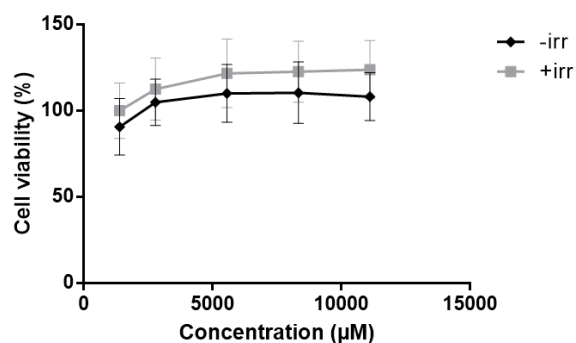


Figure 74. Cell viability of HaCaT cell line exposed to ASA, determining the phototoxicity by the Neutral Red assay. -irr: plate not irradiate. +irr: plate irradiate Data are presented as mean \pm SD ($n=5$) relative to solvent control, with (+irr)= 100 ± 20.7 ($n=3$) and (-irr)= 100 ± 12.0 ($n=3$). Data were analysed using One-way ANOVA with Dunnett post hoc test.

Hexachlorophene

Hexachlorophene is also a negative control commonly used in phototoxicity assays. In this study, the $IC_{50}(-irr)$ for this compound was 356.61 ± 49.41 μ M, with statistical significance difference relative to solvent control from 307 μ M and $IC_{50}(+irr)$ was 327.18 ± 47.26 μ M, with statistical significance difference relative to solvent control from 491 μ M, with a calculated PIF value of 1.03 ± 0.08 (Figure 75). Thus it was confirmed that hexachlorophene is not phototoxic also in our keratinocyte cell model.

In 3T3 NRU-PT with BALB/c 3T3 fibroblasts, $IC_{50}(-irr)$ was 27.03 μ M, $IC_{50}(+irr)$ was 22.86 and a PIF of 1.2, indicating that human keratinocytes are less sensitive to Hexachlorophene than fibroblasts.

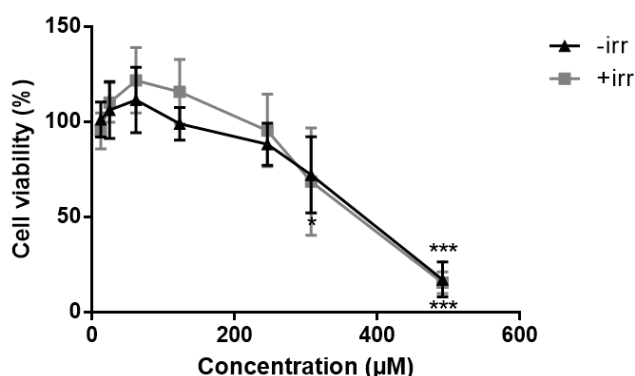


Figure 75. Cell viability of HaCaT cell line exposed to Hexachlorophene, determining the phototoxicity by the Neutral Red assay. -irr: plate not irradiate. +irr: plate irradiate Data are presented as mean \pm SD ($n=3-8$) relative to solvent control, with (+irr)= 100 ± 20.5 ($n=3$) and (-irr)= 100 ± 16.9 ($n=3$). Data were analysed using One-way ANOVA with Dunnett post hoc test. * $P<0.05$, ** $P<0.01$, *** $P<0.001$.

Sodium Lauryl Sulphate

The most commonly used negative control in the NRU-PT assay is SLS and the present study confirmed its negative phototoxicity. The $IC_{50}(-irr)$ was $559.92 \pm 57.74 \mu M$, $IC_{50}(+irr)$ was $519.73 \pm 231.94 \mu M$, both with statistical significance difference relative to solvent control from $347 \mu M$. The corresponding PIF was 1.25 ± 0.53 (Figure 76).

From data reported in the literature for SLS with BALB/c 3T3 fibroblasts, an $IC_{50}(-irr)$ of $124.84 \mu M$, an $IC_{50}(+irr)$ of $112.7 \mu M$ and a PIF of 1.2 were found, which may reflect a lower sensitivity of HaCaT to SLS.

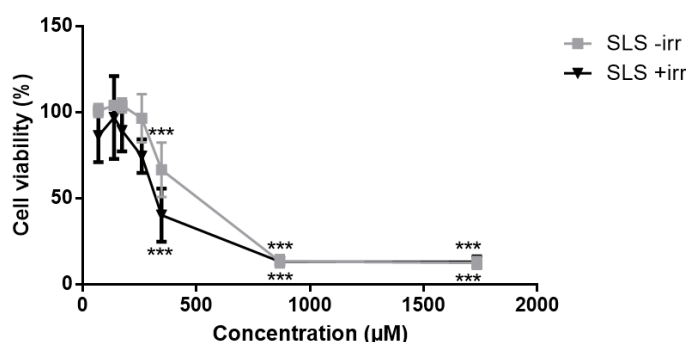


Figure 76. Cell viability of HaCaT cell line exposed to SLS, determining the phototoxicity by the Neutral Red assay. -irr: plate not irradiate. +irr: plate irradiate Data are presented as mean \pm SD ($n=3-6$) relative to solvent control, with (+irr)= 100 ± 27.4 ($n=3$) and S-irr)= 100 ± 22.3 ($n=3$). Data were analysed using One-way ANOVA with Dunnett post hoc test. *** $P < 0.001$.

Overall, the positive and negative controls validate the established procedure for the NRU-PT assay with HaCat cell line. However, as mentioned above, the Quinine HCl is not an adequate positive control.

Raw materials

1,2-DHX

In the 1,2-DHX phototoxicity assay the IC_{50} values and consequently the PIF could not be obtained, and no statistical significant difference relative to solvent control was observed. The compound does not seem to be phototoxic up to $200 \mu M$ (Figure 77). Also in this case MPE determination could provide additional confirmation of the lack of phototoxic properties.

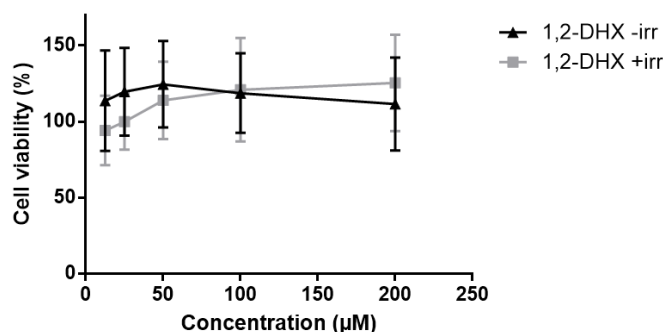


Figure 77. Cell viability of HaCaT cell line exposed to 1,2-DHX, determining the phototoxicity by the Neutral Red assay. -irr: plate not irradiate. +irr: plate irradiate Data are presented as mean \pm SD ($n=3$) relative to solvent control, with (+irr)= 100 ± 20.5 ($n=3$) and (-irr)= 100 ± 16.9 ($n=3$). Data were analysed using One-way ANOVA with Dunnett post hoc test.

Avobenzone

Avobenzone is a UV- filter with a positive result in 3T3 NRU-PT with fibroblasts but not in human tests (140). The obtained results did not allow to determine the IC₅₀ and PIF, yet the data seem to indicate the absence of phototoxicity up to 200 µM, with no statistical significant differences relative to solvent control detected (Figure 78). Therefore, these results can further support a good correlation of the procedure conducted with HaCaT cells to *in vivo* tests. Again for this compound the MPE calculation would be recommended.

The results reported with BALB/c 3T3 fibroblasts correspond to these results, when the IC₅₀s and PIF could not be obtained (123).

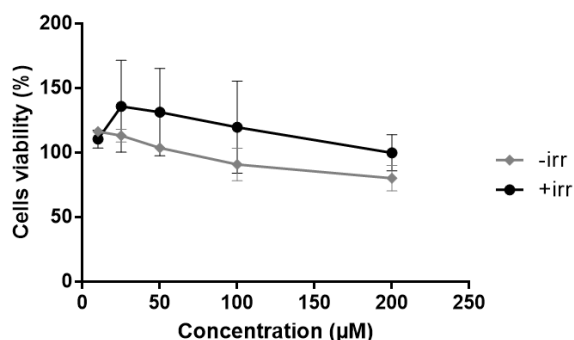


Figure 78. Cell viability of HaCaT cell line exposed to Avobenzone, determining the phototoxicity by the Neutral Red assay. -irr: plate not irradiate. +irr: plate irradiate Data are presented as mean \pm SD ($n=3$) relative to solvent control, with (+irr)= 100 ± 20.5 ($n=3$) and (-irr)= 100 ± 16.9 ($n=3$). Data were analysed using One-way ANOVA with Dunnett post hoc test.

C. sativa leaf extract

The study of *C. sativa* phototoxicity revealed a $IC_{50}(-irr)$ of $419.97 \pm 76.91 \mu\text{g/mL}$, with statistical significance difference relative to solvent control from $250 \mu\text{g/mL}$ and a $IC_{50}(+irr)$ of $193.22 \pm 3.82 \mu\text{g/mL}$ with statistical significance difference relative to solvent control from $100 \mu\text{g/mL}$ (Figure 79). A PIF of $2.18 \pm 0.42 \mu\text{g/mL}$ was obtained. In conclusion this is a probable phototoxic agent. Nevertheless, the MPE should be calculated to confirm this result.

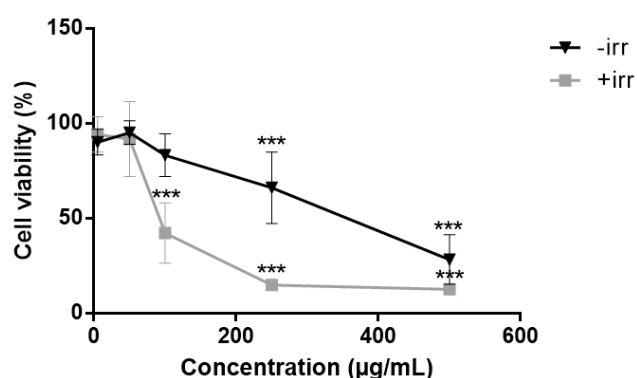


Figure 79. Cell viability of HaCaT cell line exposed to *C. sativa*, determining the phototoxicity by the Neutral Red assay. -irr: plate not irradiate. +irr: plate irradiate Data are presented as mean \pm SD ($n=3-4$) relative to solvent control, with (+irr)= 100 ± 14.9 ($n=3$) and (-irr)= 100 ± 6.3 ($n=3$). Data were analysed using One-way ANOVA with Dunnett post hoc test. *** $P < 0.001$.

Chlorogenic acid (CA)

A preliminary test ($n=1$) was conducted for CA where it was possible to observe differences between the irradiate and non irradiation conditions yet these were not very marked. It is impossible determine the IC_{50} at this concentration range and consequently the PIF. In conclusion, CA is possibly not phototoxic up to $500 \mu\text{M}$, but additional assays should be performed, followed by calculation of MEP (Figure 80).

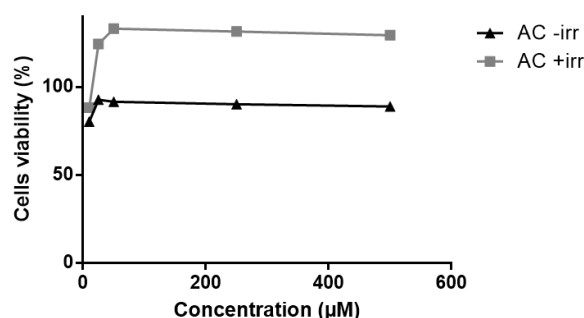


Figure 80. Cell viability of HaCaT cell line exposed to CA, determining the phototoxicity by the Neutral Red assay. -irr: plate not irradiate. +irr: plate irradiate. Data are presented as mean ($n=1$).

Comparing these results with concentration in *C. sativa* extract, which has 2.23 mg/g of CA and this value correspond to 1.115 μg in 500 μg (maximum concentration evaluated) of extract. CA was tested up to 500 μM that correspond to 177.16 $\mu\text{g/mL}$, thus the CA present in *C. sativa* extract may not be responsible by phototoxic potential of extract. To confirm this more phototoxicity assays with CA must be performed, as well as evaluated the phototoxic potential of another constituents of *C. sativa* extract and MPE calculation.

Chlorogenic acid persulfate (CAP)

A preliminary test ($n=2$) was conducted for CAP where it was observed a small difference between irradiate and non irradiation conditions. It was impossible to calculate the IC_{50} at this concentration range, and therefore it can only be concluded that CAP is possibly not phototoxic at these concentrations and under the present test conditions (Figure 81). To confirm these results, additional assays must be performed and the MPE index should be calculated.

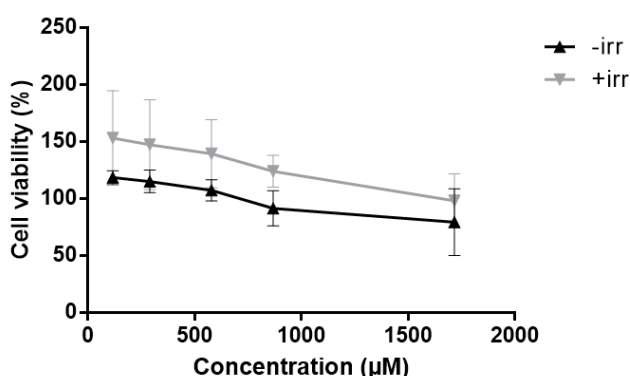


Figure 81. Cell viability of HaCaT cell line exposed to CAP, determining the phototoxicity by the Neutral Red assay. -irr: plate not irradiate. +irr: plate irradiate Data are presented as mean \pm SD ($n=2$).

Diclofenac

As referred above, this compound is known as photosensitizer and was expected to perform as a phototoxic compound in this study. However, the IC_{50} values could not be obtained and consequently the PIF value was not calculated. However, our data analysis showed that the compound does not seem to present phototoxic potential up to 1000 μM , since no statistical significance difference relative to solvent control was observed (Figure 82). To confirm this assumption the MPE determination should be performed.

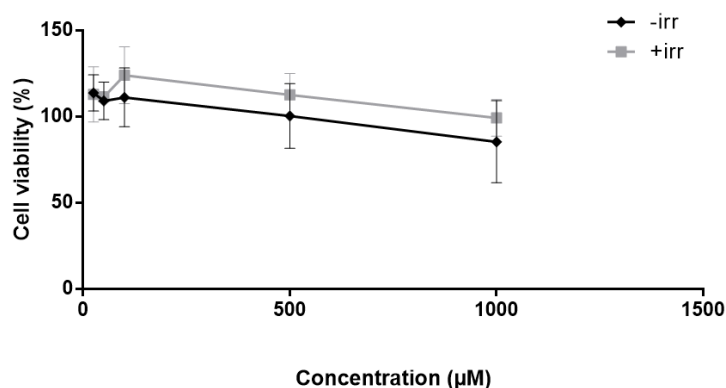


Figure 82. Cell viability of HaCaT cell line exposed to Diclofenac, determining the phototoxicity by the Neutral Red assay. -irr: plate not irradiate. +irr: plate irradiate Data are presented as mean \pm SD ($n=3$) relative to solvent control, with (+irr)= 100 ± 20.5 ($n=3$) and (-irr)= 100 ± 16.9 ($n=3$). Data were analysed using One-way ANOVA with Dunnett post hoc test.

EHMC

The UV-filter EHMC is a photo-unstable compound that can form photoproducts under UV irradiation. In the present phototoxicity assay the $IC_{50}(-irr)$ obtained was 635.6 ± 47.85 μ M and $IC_{50}(+irr)$ was 437.84 ± 129.5 μ M, both with statistical significance difference relative to solvent control from 5160 μ M, which led to a PIF of 1.58 ± 0.45 (Figure 83). In conclusion, EHMC was not a phototoxic compound under our test conditions.

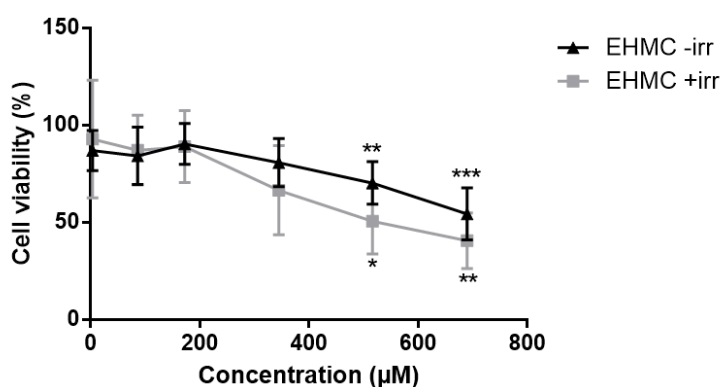


Figure 83. Cell viability of HaCaT cell line exposed to EHMC, determining the phototoxicity by the Neutral Red assay. -irr: plate not irradiate. +irr: plate irradiate Data are presented as mean \pm SD ($n=3-7$) relative to solvent control, with (+irr)= 100 ± 20.7 ($n=3$) and (-irr)= 100 ± 12.0 ($n=3$). Data were analysed using One-way ANOVA with Dunnett post hoc test. * $P < 0.05$, ** $P < 0.01$, *** $P < 0.001$.

A negative result has been already obtained with BALB/c 3T3 fibroblasts, but the IC_{50} values and PIF could not be obtained in that study, where the maximum concentration tested was 344 μ M (123).

In order to study the cytotoxicity of EHMC photoproducts the NRU assay was performed for EHMC irradiated in the presence of TiO₂ P25, a known photocatalist and a UV-filter frequently used in combination with EHMC (182). This assay was performed twice, with two different compounds production, corresponding to two different graphs present below.

It can be concluded that the solvent (acetonitrile- ACN) does not affect cell viability and that 100x, 30x and 15x dilutions did not present significant differences relative to solvent control. At the 10x dilution and when TiO₂ is present, the cellular viability decreased significantly relative to solvent control. In the absence of TiO₂ this effect did not occur (Figure 84 and 85). Therefore, is possible to conclude that citotoxicity is caused by TiO₂ or its photoproducts and not by EHMC or its phototproducts, ensuring the safety of EHMC as sunscreen.

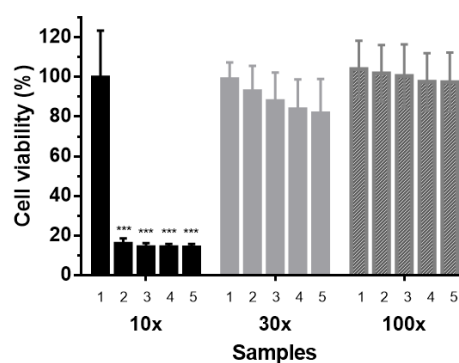


Figure 84. Cell viability of HaCaT cell line exposed to first analysed samples by the Neutral Red assay. Data are presented as mean \pm SD ($n=3-7$). Data were analysed using One-way ANOVA with Dunnett post hoc test. X- dilution; 1-10% ACN. (solvent control); 2- EHMC + 10% ACN.; 3- EHMC + P25 (TiO₂) + 10% ACN. (0 min irr); 4- EHMC + P25 (TiO₂) + 10% ACN. (30 min irr); 5- P25 (TiO₂) + 10% ACN; *** $P<0.001$.

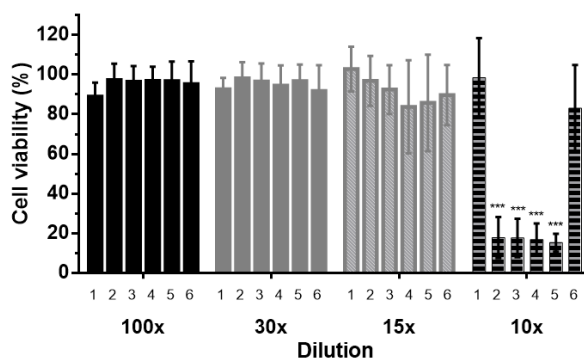


Figure 85. Cell viability of HaCaT cell line exposed to second analysed samples by the Neutral Red assay. Data are presented as mean \pm SD ($n=3-6$). Data were analysed using One-way ANOVA with Dunnett post hoc test. X- dilution; 1- EHMC + 10% ACN.; 2- EHMC + P25 (TiO₂) + 10% ACN. (0 min irr); 3- EHMC + P25 (TiO₂) + 10% ACN. (30 min irr); 4- EHMC + P25 (TiO₂) + 10% ACN. (60 min irr); 5- P25 (TiO₂) + 10% ACN; 6- 10% ACN. (solvent control)*** $P<0.001$.

Hydrogen peroxide

Since H₂O₂ was used as a positive control in the ROS assay, the phototoxicity of H₂O₂ was also evaluated. The IC₅₀(-irr) was $302.42 \pm 177.57 \mu\text{M}$ and the IC₅₀(+irr) was $178.52 \pm 52.27 \mu\text{M}$, both with statistical significance difference relative to solvent control from 100 μM , leading to a PIF of 1.37 ± 0.82 (Figure 86). It was concluded that hydrogen peroxide is a not phototoxic compound.

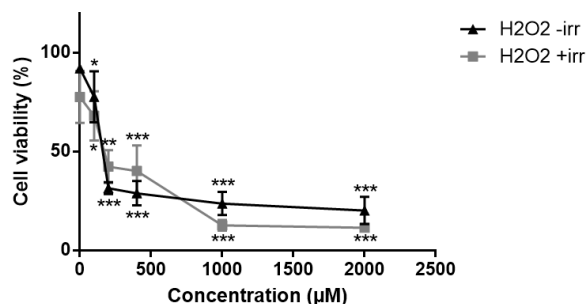


Figure 86. Cell viability of HaCaT cell line exposed to H₂O₂, determining the phototoxicity by the Neutral Red assay. -irr: plate not irradiate. +irr: plate irradiate Data are presented as mean \pm SD (n=3-9) relative to solvent control, with (+irr)= 100 ± 40.2 (n=3) and (-irr)= 100 ± 32.9 (n=3). Data were analysed using One-way ANOVA with Dunnett post hoc test. * $P < 0.05$, ** $P < 0.01$, *** $P < 0.001$.

RSV and its derivatives

RSV isomerizes after UV exposure. Regrading its phototoxicity, is a not phototoxic compound, since the IC₅₀(-irr) was $1187 \pm 186.54 \mu\text{M}$, yet with no statistical significance difference relative to solvent control and IC₅₀(+irr) was $821 \pm 142.24 \mu\text{M}$, with statistical significance difference relative to solvent control from 750 μM , leading to a PIF of 1.48 ± 0.19 (Figure 87). Thus, the RSV isomeres formation did not influence the phototoxic potential.

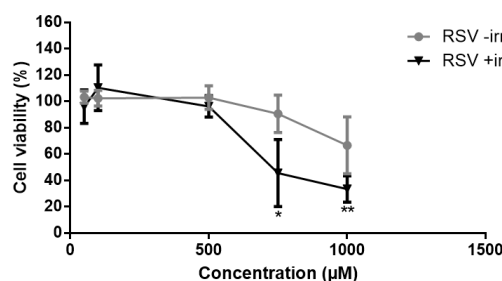


Figure 87. Cell viability of HaCaT cell line exposed to RSV, determining the phototoxicity by the Neutral Red assay. -irr: plate not irradiate. +irr: plate irradiate Data are presented as mean \pm SD (n=3-6) relative to solvent control, with (+irr)= 100 ± 20.5 (n=3) and (-irr)= 100 ± 16.9 (n=3). Data were analysed using One-way ANOVA with Dunnett post hoc test. * $P < 0.05$, ** $P < 0.01$.

A preliminary test (n=1) was conducted for RGS where the observation of differences between the irradiate and non irradiation conditions was possible, yet these were not very marked. The IC₅₀ calculation is not possible at this concentration range and consequently the same to PIF. Therefore, RGS is possibly not phototoxic up to 500 μ M, but additional assays should be performed, followed by calculation of MEP (Figure 88).

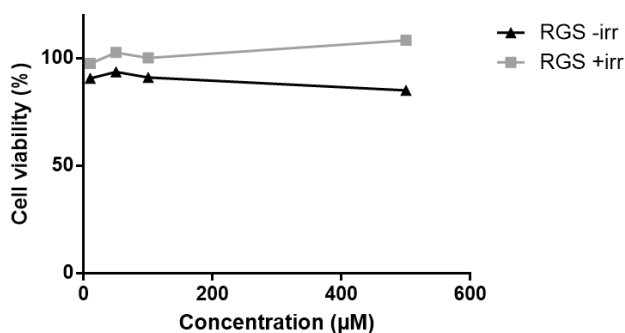


Figure 88. Cell viability of HaCaT cell line exposed to RGS, determining the phototoxicity by the Neutral Red assay. -irr: plate not irradiate. +irr: plate irradiate.

HaCat keratinocytes were less sensitive to photo-irritant compounds when compared to 3T3 fibroblasts, as was previously reported ([176](#)). However, for some specific purposes, like cosmetic's safety assays, keratinocytes are preferred since they are the first cells exposed to topical formulations and to the sun light. The 3T3 NRU phototoxicity test has been however validated by the ECVAM (European Centre for the Validation of Alternative Methods) in 3T3 mouse fibroblasts due to the high correlation with *in vivo* tests. The modified neutral red assay developed herein was found to be a simple and reliable method for detecting phototoxic effects of reference agents.

A photosafety survey has found that 85% of *in vitro* 3T3-NRU phototoxicity assay positives were negative when tested *in vivo* ([183](#)). A 86 % reduction in positive 3T3 NRU phototoxicity tests was also described by Liebsch et al ([184](#)) when using 3-D skin models. Based on our results, one possible explanation is the over-sensitivity of 3T3 fibroblasts when comparing with human keratinocytes.

Table 9. Summary of phototoxicity, cytotoxicity and ROS generation results

Compound	IC ₅₀ (-irr)	IC ₅₀ (+irr)	PIF	IC ₅₀ (24h)	Fluorescence (%)
1,2-DHX	> 200 μ M *	> 200 μ M *	NA	NR	=
5-MOP	3.8 \pm 0.24 μ M *	> 300 μ M *	78.8 \pm 5.11 **	> 300 μ M *	=
ASA	> 1000 μ M *	> 1000 μ M	NA	> 1000 μ M *	↑
Avobenzone	> 200 μ M *	> 200 μ M *	NA	> 200 μ M *	=
C. sativa	419.97 \pm 76.91 μ g/mL	193.22 \pm 3.82 μ g/mL	2.18 \pm 0.42	NR	↑
CA	> 500 μ M *	> 500 μ M *	NA	NR	NR
CAP	> 1700 μ M *	> 1700 μ M *	NA	NR	NR
CPZ	193.5 \pm 13.74 μ M	6.93 \pm 1.46	23.30 \pm 2.69	41.67 \pm 2.62 μ M	=
Diclofenac	> 1000 μ M *	> 1000 μ M *	NA	> 1000 μ M *	↑
EHMC	635.6 \pm 47.85 μ M	437.84 \pm 129.5 μ M	1.58 \pm 0.45	547.68 \pm 88.48 μ M	=
H₂O₂	302.42 \pm 177.57 μ M	178.52 \pm 52.27 μ M	1.37 \pm 0.82	243.31 \pm 59.64 μ M	↑
Hexochlorophene	356.61 \pm 49.41 μ M	327.18 \pm 47.26 μ M	1.03 \pm 0.08	156.66 \pm 19.27 μ M	↓
Quinine HCl	4269.88 \pm 734.08 μ M	1293.42 \pm 240.97 μ M	2.09 \pm 0.85	787.75 \pm 222.73 μ M	↓
RSV	1187 \pm 186.54 μ M	821 \pm 142.24 μ M	1.48 \pm 0.19	NR	↑
SLS	559.92 \pm 57.74 μ M	519.73 \pm 231.94 μ M	1.25 \pm 0.53	221.09 \pm 26.13 μ M	↑

NA- Not applicable. NR- Not Realized; ↑ : increase in fluorescence; ↓ : decrease in fluorescence; =- not different from negative control; *Tested at maximum solubility **IC₅₀(-irr) could not be obtained

4.4.5. Optimization of UV-mediated ROS generation assay using DCFH-DA with a positive control

Since the DCFH-DA is sensitive to light ([111](#)), the probe was incubated before or after the irradiation and the ROS generation was evaluated using H₂O₂ as positive control. If the probe would be inactivated by the irradiation, then no ROS generation after H₂O₂ would be observed, as observed in Figure 89. In order to the washing and not washing steps with PBS again no fluorescence was detected. This is likely due to the cytotoxic effect induced by the

H₂O₂ test concentration or to the permeability of DCF (the fluorescent product of DCFH), which can leak out of cells ([185](#)).

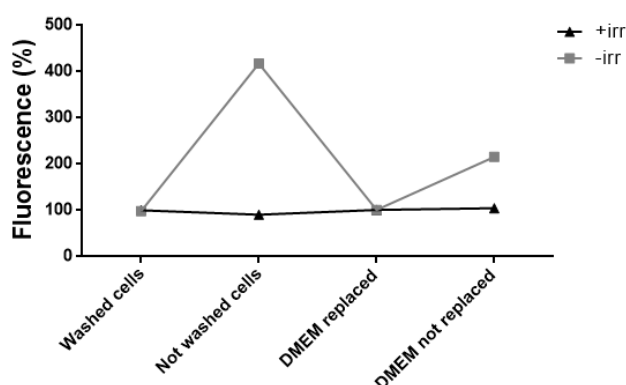


Figure 89. Fluorescence of HaCaT cell line exposed to positive control by the DCFH-DA assay with and without fresh medium replacement steps. DCFH-DA incubated before irradiation. +irr= plate irradiated. -irr= plate not irradiated (n=1).

When the DCFH-DA was added after the irradiation, no fluorescence increase was detected in the presence of cells (Figure 90). This result was difficult to interpret and can have many explanations such as the cell death at this H₂O₂ concentration mentioned above or the phenomenon of self-propagating redox-cycling reactions induced by the DCF radical ([186](#)) and the adducts formed by ROS with biological targets, both associated with losses of fluorescence signal ([58](#), [59](#)). Therefore, this result requires future studies. In order to the fluorescence increase in non replaced fresh medium can be justified by interference of H₂O₂ with DCFH-DA observed in an exploratory assay.

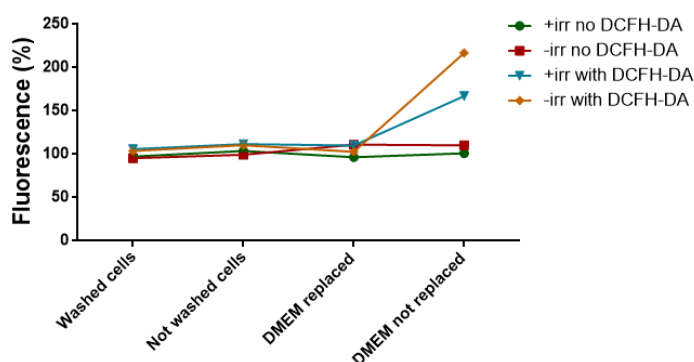


Figure 90. Fluorescence of HaCaT cell line exposed to positive control by the DCFH-DA assay with and without fresh medium replacement steps. DCFH-DA incubated after irradiation. +irr= plate irradiate. -irr= plate not irradiate (n=1).

For the purpose of increasing the fluorescence signal, an incubation time with DCFH-DA of 1h30m was studied. However, the fluorescence signal only increased slightly (Figure 91). Following this result, the DCFH-DA proper functioning was evaluated by testing the positive control addition before and after the incubation with DCFH-DA, which is incubated after irradiation. Beside that, the fluorescence was measured at different times (3, 8 and 24h) (Figure 92 A).

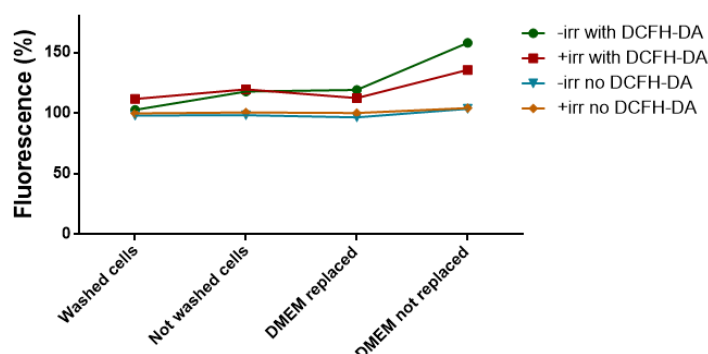


Figure 91. Fluorescence of HaCaT cell line exposed to positive control by the DCFH-DA assay with and without fresh medium replacement steps. DCFH-DA incubated for 1h30 after irradiation. +irr= plate irradiate. -irr= plate not irradiate (n=1).

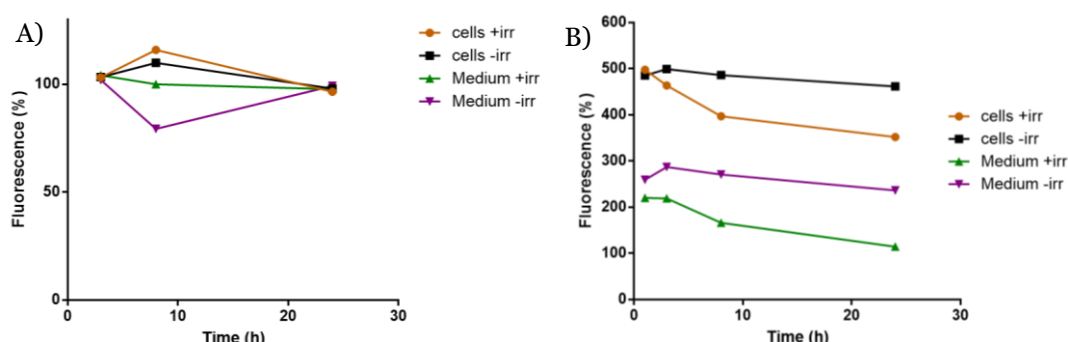


Figure 92. Fluorescence of HaCaT cell line exposed to positive control by the DCFH-DA assay A) before and B) after the DCFH-DA incubation. +irr= plate irradiate. -irr= plate not irradiate (n=1).

The addition of positive control before DCFH-DA did not demonstrate marked differences between irradiation and no irradiation conditions (Figure 92 A). However, the fluorescence reading at 8h showed a transient increase, which can suggest a relevant influence of time in probe oxidation. The addition of H_2O_2 after the DCFH-DA incubation demonstrated that DCFH-DA was performing well and able to detect reactive oxygen species (Figure 92 B).

Overall, these results may indicate cell death with the H_2O_2 concentration used or unsuitability of DCFH-DA to this assay. With the aim of clarify this result and optimize the UV-mediated ROS generation assay, a DCFH-DA kinetics assay should be performed, once the reading at 24h can not be maximum fluorescence range. The use of another probe, such as versions of H_2DCFDA must be evaluated. An increase in cell density may also increase the assay sensibility.

4.4.6. Validation of UV-mediated ROS generation assay using DCFH-DA with a positive control

The validation of the UV-mediated ROS generation assay as a phototoxic measure was performed by analysing a known phototoxic and ROS generator compound, quinine. Taking into account Figure 93 it is possible observe a slight increase in fluorescence, only about the 20% at the maximum time of fluorescence measure up to $\sim 2000 \mu\text{M}$. Afterwards, the fluorescence begins to decrease until 100%. This decrease correponde to the concentration when cell death begins to be significant as can be confirmed by the Figure 73 (section 4.4.4.). During apoptosis, cytochrome c is released from mitochondria to the cytosol, which is capable to oxidize DCFH directly or indirectly through a peroxidase-type mechanism, forming DCF, leading to fluorescence emissions (186). Thus the fluorescence increase observed after $2500 \mu\text{M}$ may be caused by a related phenomenon or others such as ROS released with cell death. This increase was more evident in the irradiated plate and fluorescence reading at 24h. Therefore, the increase in fluorescence is not sufficiently marked, considering quinine is expected to perform as a positive control. Thus, the increase of cell density and/or the exposure area (related to width of well) could be tested in future studies to allow for a increase in fluorescence signal. Another explication it the low sensitivity of human keratinocytes to quinine HCl mentionated above, thus supporting the use of another positive control.

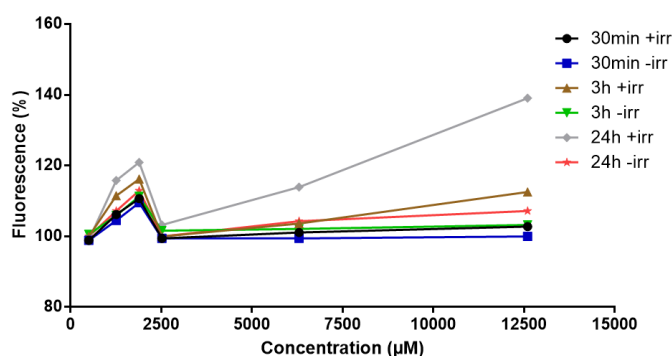


Figure 93. Fluorescence of HaCaT cell line exposed to Quinine HCl by the DCFH-DA assay. +irr= plate irradiate. -irr= plate not irradiate.

4.4.7. Study of quinine HCl in total glutathione (tGSH)) by DTNB-GSSG reductase recycling assay with irradiation

The study of GSH corroborated the previous hypothesis, since GSH production is increased in response to oxidative. Thus, the HaCaT exposure to quinine HCl may have increased glutathione synthesis, due to powerfull antioxidative system present in keratinocytes. It is also noteworthy, although without statistical significative difference, the tGSH difference between irradiated and non irradiated plate, suggesting that exposure to both UV radiation and quinine HCl may have caused more cell injury (Figure 94).

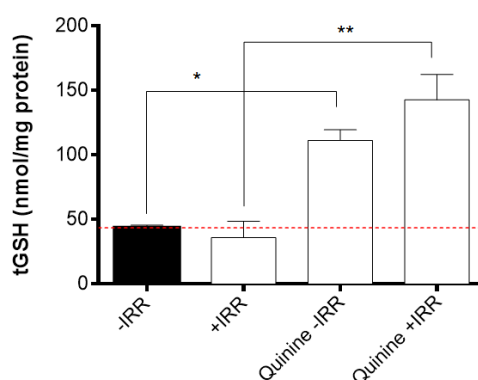


Figure 94. tGSH of HaCaT cell line exposed to 1260 μ M of Quinine HCl normalized by protein using Lowry Protocol. +irr= irradiate plate –irr= not irradiate plate. Data are presented as mean \pm SD (n=35-69). Data were analysed using One-way ANOVA with Dunnett post hoc test.

5. Conclusions

Regulatory authorities demand the photosafety evaluation of pharmaceutical and cosmetic products before being placed on the market. Regarding the evaluation of cosmetic products or ingredients, testing on animals was banned in Europe since 2009, which fostered the development of alternative *in vitro* methodologies. An *in vitro* phototoxicity test (3T3 NRU-PT) is currently recommended by the OECD and officially accepted by the European Union in Directive 2010/63/EU). Among its limitations, the use of a mouse cell line and the reports of over-sensitivity are particularly relevant.

The implementation of the methodology was based on 3T3 NRU-PT but using a human keratinocyte cell line (HaCaT), which can represent a more realistic model since these cells are abundantly present in the most external layer of skin, where the topical compounds are applied, and is also more exposed to solar radiation.

The HaCaT NRU-PT methodology implemented in this work was based on the official test (3T3 NRU-PT) and was optimized with respect to a number of parameters (cell density, radiation dose, Neutral Red concentration and incubation time, temperature control) in order to obtain a harmonized and robust method. The developed method was validated following the phototoxic evaluation of known phototoxic agents and also of non-phototoxic compounds. The use of a light source comprising an UVA/UVB Osram lamp is a simple and inexpensive choice which has the benefit of more closely resembling the UV solar spectrum in comparison with UVA lamps that are routinely used in photosafety tests.

The optimized test conditions were defined as follows: UVA/UVB Osram lamp positioned at 46.5cm height, 10 min irradiation, cell density of 2×10^4 cell/well, neutral red dye concentration of 50 $\mu\text{g/mL}$ (with 3h incubation time). During the irradiation, the temperature achieved in the wells using a water-cooling system varied between 29 and 32°C, and cell viability was maintained under these conditions.

Validation of the HaCaT NRU-PT assay was conducted with three positive controls, (CPZ, quinine HCl and 5-MOP) and three negative controls (ASA, hexachlorophene and SLS). For all negative controls PIFs were close to 1, while for CPZ and 5-MOP were above 5 thus confirming the validity of the HaCaT NRU-PT assay developed in this work. Noteworthy, for quinine the obtained PIF was not as high as expected. This result may be justified by powerful antioxidant system of keratinocytes.

The optimized assay was applied to several raw materials of pharmaceutical and cosmetic formulations. For 1,2-DHX, avobenzone, diclofenac, H₂O₂, EHMC, RSV and RGS no phototoxic effects were observed, although in some cases the PIF could not be calculated. Only *C. sativa* extract was shown to be a probable phototoxic agent, presenting a PIF of 2.18 ± 0.42 . For future studies, the MPE could be calculated, specially for the test substances for which the IC₅₀ values could not be obtained.

In an attempt to find alternative endpoints and gain mechanistic insight, another phototoxicity test was implemented based on stress oxidative markers: ROS generation and intracellular glutathione quantification.

In order to study ROS generation induced by the test compounds using DCFH-DA as probe, the cell density, the DCFH-DA concentration and its incubation time were optimized. A density of 2×10^4 cells/well and a concentration of DCFH-DA of 50 μ M were considered the ideal conditions, since the fluorescence signal was high enough to ensure appropriate sensitivity. Regarding the incubation time with the DCFH-DA probe, to decrease the length of the assay, a 30 min incubation was chosen for the final procedure. The results showed that none of the test compounds led to a marked ROS generation after 24h incubation. In the future, a detailed study of these and the fluorescence signal should be carried out.

In order to implement a procedure that evaluates ROS generation after irradiation, DCFH-DA was tested as a suitable probe and several test conditions were analysed. However, this methodology presented high complexity and an optimized procedure could not be obtained. As an alternative oxidative stress endpoint we measured intracellular total GSH levels, using quinine in an exploratory assay that revealed an increase in tGSH in HaCaT cells after quinine incubation. This result allowed us to speculate that the low PIF value found with the HaCaT NRU-PT could be due to an adaptive response of keratinocytes to oxidative stress.

In future studies, alternative probes to DCFH-DA and other positive controls should be evaluated. A more comprehensive evaluation of tGSH, GSSH and GSH levels after UV exposure of known phototoxic agents should also be carried out. The HaCaT NRU-PT methodology implemented in this work could be of use to evaluate the phototoxicity of potential photosensitizers especially if they are intended for topical application.

6. References

1. Celleno L, Tamburi F. Chapter 1 - Structure and Function of the Skin. In: Blair ATM, editor. Nutritional Cosmetics. Boston: William Andrew Publishing; 2009. p. 3-45.
2. Proksch E, Brandner JM, Jensen JM. The skin: an indispensable barrier. *Experimental dermatology*. 2008;17(12):1063-72.
3. Zhai H, Maibach HI. *Dermatotoxicology*, Sixth Edition: CRC Press; 2004.
4. Food and Drug Administration. Guidance For Industry- Photosafety Testing. Center for Drug Evaluation and Research (CDER), U.S. Department of Health and Human Services Food and Drug Administration, editors. Fishers Ln, Rockville, USA2003.
5. Kornhauser A, Wamer WG, Lambert LA. Cellular and Molecular Events Following Ultraviolet Irradiation of Skin. In: Francis Ta, editor. *Dermatotoxicology*. Washington, DC1996. p. 189-230.
6. Moan J, Dahlback A, Setlow RB. Epidemiological support for an hypothesis for melanoma induction indicating a role for UVA radiation. *Photochem Photobiol*. 1999;70(2):243-7.
7. Nakpiban C. LESSON 6-01 – Skin Structure and Function 2010 [Available from: <http://cosbiology.pbworks.com/w/page/11556260/LESSON%206-01%20%E2%80%93%20Skin%20Structure%20and%20Function>.
8. Gartner LP, Hiatt JL. *Tratado de Histologia em Cores*. 8 ed2003.
9. Mayes M. Your skin: Absorption: Musings From The Farm. Comfortable living in your own skin; 2013 [cited 2015. Available from: <http://thealabublog.com/2013/11/skin-absorption/>.
10. Black AT, Gray JP, Shakarjian MP, Laskin DL, Heck DE, Laskin JD. Increased oxidative stress and antioxidant expression in mouse keratinocytes following exposure to paraquat. *Toxicology and Applied Pharmacology*. 2008;231(3):384-92.
11. Ferrario DF. Curso rápido de la histología de la piel 2012 [Available from: <http://www.medicinabc.com/2012/10/curso-rapido-de-la-histologia-de-la-piel.html#axzz3elzGiZ1d>.
12. Junqueira L, Carneiro J. *Histologia Básica*. 10 ed. Rio de Janeiro: Guanabara Koogan;2004.
13. Seo S-H, Jeong G-S. Fisetin inhibits TNF- α -induced inflammatory action and hydrogen peroxide-induced oxidative damage in human keratinocyte HaCaT cells through PI3K/AKT/Nrf-2-mediated heme oxygenase-1 expression. *International Immunopharmacology*. 2015;29(2):246-53.
14. Szychowski KA, Rybczynska-Tkaczyk K, Leja ML, Wojtowicz AK, Gminski J. Tetrabromobisphenol A (TBBPA)-stimulated reactive oxygen species (ROS) production in cell-free model using the 2',7'-dichlorodihydrofluorescein diacetate (H2DCFDA) assay-limitations of method. *Environmental science and pollution research international*. 2016;23(12):12246-52.
15. Halliwell B, Cross CE. Oxygen-derived species: their relation to human disease and environmental stress. *Environmental health perspectives*. 1994;102 Suppl 10:5-12.

16. Chamulitrat W, Stremmel W, Kawahara T, Rokutan K, Fujii H, Wingler K, et al. A constitutive NADPH oxidase-like system containing gp91phox homologs in human keratinocytes. *J Invest Dermatol*. 2004;122(4):1000-9.
17. Beak SM, Lee YS, Kim JA. NADPH oxidase and cyclooxygenase mediate the ultraviolet B-induced generation of reactive oxygen species and activation of nuclear factor-kappaB in HaCaT human keratinocytes. *Biochimie*. 2004;86(7):425-9.
18. Hornig-Do HT, von Kleist-Retzow JC, Lanz K, Wickenhauser C, Kudin AP, Kunz WS, et al. Human epidermal keratinocytes accumulate superoxide due to low activity of Mn-SOD, leading to mitochondrial functional impairment. *J Invest Dermatol*. 2007;127(5):1084-93.
19. Vessey DA. The cutaneous antioxidant system. In: Fa P, editor. *Oxidative stress in dermatology*. Nova Iorque: Marcel Dekker; 1993. p. 81-104.
20. Marrot L, Jones C, Perez P, Meunier JR. The significance of Nrf2 pathway in (photo)-oxidative stress response in melanocytes and keratinocytes of the human epidermis. *Pigment cell & melanoma research*. 2008;21(1):79-88.
21. Bulteau AL, Moreau M, Nizard C, Friguet B. Impairment of proteasome function upon UVA- and UVB-irradiation of human keratinocytes. *Free radical biology & medicine*. 2002;32(11):1157-70.
22. Almeida IF. Desenvolvimento de um sistema semi-sólido contendo fitocompostos captadores de espécies reativas. Porto: Faculdade de Farmácia da Universidade do Porto; 2009.
23. Nichols JA, Katiyar SK. Skin photoprotection by natural polyphenols: anti-inflammatory, antioxidant and DNA repair mechanisms. *Archives of dermatological research*. 2010;302(2):71-83.
24. Zheng R, Heck DE, Mishin V, Black AT, Shakarjian MP, Kong A-NT, et al. Modulation of keratinocyte expression of antioxidants by 4-hydroxynonenal, a lipid peroxidation end product. *Toxicology and Applied Pharmacology*. 2014;275(2):113-21.
25. Aquilano K, Baldelli S, Ciriolo MR. Glutathione: new roles in redox signaling for an old antioxidant. *Frontiers in Pharmacology*. 2014;5:196.
26. Yeh MY, Burnham EL, Moss M, Brown LAS. Chronic Alcoholism Alters Systemic and Pulmonary Glutathione Redox Status. *American Journal of Respiratory and Critical Care Medicine*. 2007;176(3):270-6.
27. Prista N, Bahia M, Vilar E. *Dermofarmácia e Cosmética*. Porto: Associação Nacional das Farmácias; 1992.
28. Kanebo. Basic knowledge of the skin: Structure and function of the skin Kanebo Cosmetics [Available from: <http://www.kanebo.com/science/skin/struct.html>].
29. Junqueira L CJ. *Histologia Básica*. 10, editor2004.
30. Russell R. *The Multispectral Sun: Windows2universe*
National Earth Science Teachers Association; 2007 [Available from: http://www.windows2universe.org/sun/spectrum/multispectral_sun_overview.html].

31. Wilhelm KP, Zhai H, Maibach HI. Dermatotoxicology: CRC Press; 2007.
32. Butcher G. Tour of the Electromagnetic Spectrum. (NASA) NAaSA, editor: NASA; 2010.
33. ISO. Space environment (natural and artificial) — Process for determining solar irradiances 2007.
34. Dinies. UV-irradiation Villingendorf, Germany: Dinies Technologies GmbH; [Available from: <http://www.dinies.com/uv-technik/uv-wissen.html>].
35. Kawakami CM, Gaspar LR. Mangiferin and naringenin affect the photostability and phototoxicity of sunscreens containing avobenzene. *Journal of Photochemistry and Photobiology B: Biology*. 2015;151:239-47.
36. Nigam PK. Adverse reactions to cosmetics and methods of testing. *Indian journal of dermatology, venereology and leprology*. 2009;75(1):10-8; quiz 9.
37. Smith E, Kiss F, Porter RM, Anstey AV. A review of UVA-mediated photosensitivity disorders. *Photochemical & Photobiological Sciences*. 2012;11(1):199-206.
38. Anderson DM, Keith J, Novac P, Elliott MA. *Dorland's Illustrated Medical Dictionary*. 28th, editor. Philadelphia: W. B. Saunders Company; 1994.
39. Smith KC, Ed. *The Science of Photobiology*. Plenum Press: New York. 1989;2nd ed.
40. Megaw JM, Drake LA. *Photobiology of the Skin and Eye*. Marcel Dekker: New York. 1986.
41. Spielmann H, Muller L, Averbeck D, Balls M, Brendler-Schwaab S, Castell JV, et al. The second ECVAM workshop on phototoxicity testing. The report and recommendations of ECVAM workshop 42. *Altern Lab Anim*. 2000;28(6):777-814.
42. Incorvaia C, Fuiano N, Megali R, Riario-Sforza GG. Skin reaction to inhaled tiotropium bromide: a case report. *J Med Case Rep*. 2011;5:119.
43. Zigman S. Ocular light damage. *Photochem Photobiol*. 1993;57(6):1060-8.
44. Klaassen C. Casarett and Doull's toxicology : the basic science of poisons In: Education L-H, editor. 8 ed. New York 2013.
45. (CPMP) TEAFoMPEoMfHUECfmp. Note for Guidance on Photosafety Testing. 2002.
46. EMA. ICH guideline S10 .Guidance on photosafety evaluation of pharmaceuticals. Step 3. European Medicines Agency | Science medicines agency. Committee for medicinal products for human use (CHMP) 2012.
47. Chobot V, Vytlačilová J, Jahodár L. Phototoxic Activity And The Possibilities of this Testing. *Cent Eur J Publ Health*. 2004;12:S31-S3.
48. OCDE. Guideline for Testing of Chemicals 432. In Vitro 3T3 NRU phototoxicity test 2004.
49. IIVS. In Vitro Phototoxicity Assays. Institute for in Vitro Sciences. Gaithersburg.
50. Smith E, Kiss F, Porter RM, Anstey AV. A review of UVA-mediated photosensitivity disorders. *Photochem Photobiol Sci*. 2012;11(1):199-206.

51. Kutlubay Z, Sevim A, Engin B, Tuzun Y. Photodermatoses, including phototoxic and photoallergic reactions (internal and external). *Clin Dermatol*. 2014;32(1):73-9.
52. Ferguson J. Photosensitivity due to drugs. *Photodermatology, photoimmunology & photomedicine*. 2002;18(5):262-9.
53. Gonalo M. Phototoxic and Photoallergic Reactions. In: Johansen JD, Frosch PJ, Lepoittevin J-P, editors. *Contact Dermatitis*: Springer Berlin Heidelberg; 2011. p. 361-76.
54. Kolle S. Genotoxicity and Carcinogenicity. BASF The Chemical Company. 2012.
55. Robbins, Cotran. *Patologia: Base patol3gica da doena*. 7 ed. Rio de Janeiro: Elsevier; 2010.
56. Ceridono M, Tellner P, Bauer D, Barroso J, Alepee N, Corvi R, et al. The 3T3 neutral red uptake phototoxicity test: practical experience and implications for phototoxicity testing--the report of an ECVAM-EFPIA workshop. *Regul Toxicol Pharmacol*. 2012;63(3):480-8.
57. Group IEW, editor *Photosafety Evaluation of Pharmaceuticals*. S10. International conference on harmonisation of technical requirements for registration of pharmaceuticals for human use; 2013.
58. Uemura MT, Lopes PS, Genesi BP, Mathor MB, Kaneko TM, Bara MTF, et al. Phototoxicity Evaluation of Sucupira Extract: A Potential New Cosmetic Ingredient. *IFSCC MAGAZINE*. 2013.
59. Onoue S, Suzuki G, Kato M, Hirota M, Nishida H, Kitagaki M, et al. Non-animal photosafety assessment approaches for cosmetics based on the photochemical and photobiochemical properties. *Toxicology in Vitro*. 2013;27(8):2316-24.
60. Daniels Jr F, Brophy D, Lobitz Jr WC. Histochemical Responses of Human Skin Following Ultraviolet Irradiation1. *The Journal of Investigative Dermatology*. 1961;37(5):351-7.
61. Grossman D, Kim PJ, Blanc-Brude OP, Brash DE, Tognin S, Marchisio PC, et al. Transgenic expression of survivin in keratinocytes counteracts UVB-induced apoptosis and cooperates with loss of p53. *Journal of Clinical Investigation*. 2001;108(7):991-9.
62. Woodcock A, Magnus IA. The sunburn cell in mouse skin: preliminary quantitative studies on its production. *The British journal of dermatology*. 1976;95(5):459-68.
63. Marzulli FN, Maibach HI. *Dermatotoxicology*. 4, editor. New York1991.
64. Baynes RE, Brownie C, Freeman H, Riviere JE. In vitro percutaneous absorption of benzidine in complex mechanistically defined chemical mixtures. *Toxicol Appl Pharmacol*. 1996;141(2):497-506.
65. Anderson RR, Parrish JA. The optics of human skin. *J Invest Dermatol*. 1981;77(1):13-9.
66. Serup J, Winther A, Blichmann C. A Simple Method for the Study of Scale Pattern and Effects of a Moisturizer--Qualitative and Quantitative Evaluation by DSquame Tape Compared With Parameters of Epidermal Hydration. *Clin Experiment Dermatol*. 1989;14:277-82.
67. Kaidbey K, Kligman A. Topical Photosensitizers: Influence of Vehicles on Penetration. *Arch Dermatol*. 1974;110:868-70.

68. Dearman RJ, Cumberbatch M, Hilton J, Clowes HM, Fielding I, Heylings JR, et al. Influence of dibutyl phthalate on dermal sensitization to fluorescein isothiocyanate. *Fundam Appl Toxicol*. 1996;33(1):24-30.
69. Asker AF, Harris CW. Influence of Certain Additives on the Photostability of Physostigmine Sulfate Solutions. *Drug Development and Industrial Pharmacy*. 1988;14:733-46.
70. Islam MS, Asker AF. Photoprotection of daunorubicin hydrochloride with sodium sulfite. *PDA J Pharm Sci Technol*. 1995;49(3):122-6.
71. Marti-Mestres G, Fernandez G, Parsotam N, Nielloud F, Mestres JP, Maillols H. Stability of UV Filters in Different Vehicles: Solvents and Emulsions, Drug Development Industry. *Pharmacy* 1997;23:647-55.
72. Gibbs NK, Young AR, Magnus IA. FAILURE OF UVR DOSE RECIPROCITY FOR SKIN TUMORIGENESIS IN HAIRLESS MICE TREATED WITH 8-METHOXYPSORALEN. *Photochemistry and Photobiology*. 1985;42(1):39-42.
73. Council. Directive 76/768/EEC Official Journal of the European Communities; 1976. 169-200 p.
74. Colipa. Guidelines for the Safety Assessment of a Cosmetic Product. The European Cosmetic, Toiletry and Perfumery Association. Brussels: S. Marx; 1997.
75. Chen W, Wang C, Cheng Y, Xue Y, Zhang Q. [Simultaneous determination of 8-methoxypsoralen and 5-methoxypsoralen in cosmetics using LC-MS/MS]. *Se Pu*. 2007;25(5):768-9.
76. Blaas W, Kellert M, Krull L, Schramm M, Weber R. [Determination of 5-methoxypsoralen in suntan cosmetics]. *Z Lebensm Unters Forsch*. 1985;180(3):230-3.
77. EuropeanCommission. Furocoumarins in cosmetic products. SCIENTIFIC COMMITTEE ON CONSUMER PRODUCTS (SCCP): Health & Consumer Protection Directorate- General; 2005.
78. Polonini HC, Dias RMP, Souza IO, Gonçalves KM, Gomes TBB, Raposo NRB, et al. Quinolines derivatives as novel sunscreens agents. *Bioorganic & Medicinal Chemistry Letters*. 2013;23(16):4506-10.
79. Gaspar LR, Tharmann J, Maia Campos PM, Liebsch M. Skin phototoxicity of cosmetic formulations containing photounstable and photostable UV-filters and vitamin A palmitate. *Toxicology in vitro : an international journal published in association with BIBRA*. 2013;27(1):418-25.
80. Nash JF, Tanner PR. Relevance of UV filter/sunscreen product photostability to human safety. *Photodermatology, photoimmunology & photomedicine*. 2014;30(2-3):88-95.
81. Benevenuto CG, Guerra LO, Gaspar LR. Combination of retinyl palmitate and UV-filters: Phototoxic risk assessment based on photostability and in vitro and in vivo phototoxicity assays. *European Journal of Pharmaceutical Sciences*. 2015;68:127-36.
82. Rodil R, Moeder M, Altenburger R, Schmitt-Jansen M. Photostability and phytotoxicity of selected sunscreen agents and their degradation mixtures in water. *Analytical and Bioanalytical Chemistry*. 2009;395(5):1513-24.
83. FD&C-Act. Chapter 1 e 2, Subchapter 2, Sec. 201. In: Federal Food D, and Cosmetic Act (FD&C-Act), editor.

84. Johnson BE. Light Sensitivity Associated With Drugs and Chemicals. *Physiol Pathophysiol Skin*. 1984; 8:2542-606.
85. Hölzle E, Neumann N, Hausen B, Przybilla B, Schauder S, Hönigsmann H, et al. Photopatch testing: The 5-year experience of the German, Austrian, and Swiss Photopatch Test Group. *Journal of the American Academy of Dermatology*. 1991;25(1, Part 1):59-68.
86. Henderson VC, Kimmelman J, Fergusson D, Grimshaw JM, Hackam DG. Threats to validity in the design and conduct of preclinical efficacy studies: a systematic review of guidelines for in vivo animal experiments. *PLoS Med*. 2013;10(7):e1001489.
87. Schumann J, Boudon S, Ulrich P, Loll N, Garcia D, Schaffner R, et al. Integrated Preclinical Photosafety Testing Strategy for Systemically Applied Pharmaceuticals. *Toxicological Sciences*. 2014;139(1):245-56.
88. EuropeanCommission. GUIDANCE ON THE SAFETY ASSESSMENT OF NANOMATERIALS IN COSMETICS. Safety SCoC, editor2012.
89. Teunis M. 3R methods: Innovative Testing in Life Sciences & Chemistry (INT); 2013 [Available from: <http://www.innovativetesting.nl/alternatives>].
90. EuropeanCommission. Directive 2010/63/eu of the european parliament and of the council of 22 september 2010 on the protection of animals used for scientific purposes. *Official Journal of the European Union* 2010;276/33.
91. EMEA. Note for guidance on non-clinical local tolerance testing of medicinal products. CPMP/SWP/2145/00. 2001.
92. Kienapfel A. A review of the advancements in photosafety testing with regard to ICH's new topic S10: Photosafety evaluation of pharmaceuticals [Drug Regulatory Affairs]. Hamburg: Rheinischen Friedrich-Wilhelms-Universität Bonn; 2013.
93. Learn DB, Donald FP, Sambuco CP. Chapter 16 - Photosafety: Current Methods and Future Direction. In: Faqi AS, editor. *A Comprehensive Guide to Toxicology in Preclinical Drug Development*: Academic Press; 2013. p. 395-422.
94. MIN-A K, HYEONG-U S, CHEOL-SIK Y, SUNG-HEE N, YOUNG-CHEOL C, SANG-HAN L. Comparison of in vitro and in vivo phototoxicity tests with S-(-)-10,11-dihydroxyfarnesic acid methyl ester produced by *Beauveria bassiana* KACC46831. *Biomedical Reports*. 2014;2:659-63.
95. EuropeanCommission. REGULATION (EC) No 1223/2009. COUNCIL TEPAOT, editor2009. 59 p.
96. SCCS. THE SCCS'S NOTES OF GUIDANCE FOR THE TESTING OF COSMETIC INGREDIENTS AND THEIR SAFETY EVALUATION 7TH REVISION: Scientific Committee on Consumer Safety; 2010.
97. EuropeanCommission. DIRECTIVE 2003/15/EC OF THE EUROPEAN PARLIAMENT AND OF THE COUNCIL of 27 February 2003 amending Council Directive 76/768/EEC on the approximation of the laws of the Member States relating to cosmetic products. *official Journal of the European Union*. Brussels2003.
98. Gonçalo M. Photopatch Testing. In: Johansen JD, Frosch PJ, Lepoittevin J-P, editors. *Contact Dermatitis*. 1: Springer Berlin Heidelberg; 2010.

99. Hjorth N, Moller H. Phototoxic textile dermatitis (bikini dermatitis). *Arch Dermatol.* 1976;112:1445-7.
100. Jeanmougin M, Pedreiro J, Bouchet J, Civatte J. [Phototoxic activity of 5% benzoyl peroxide in man. Use of a new methodology]. *Dermatologica.* 1983;167(1):19-23.
101. Bjellerup M. Medium-wave ultraviolet radiation (UVB) is important in doxycycline phototoxicity. *Acta Derm Venereol.* 1986;66(6):510-4.
102. European Commission. EURL ECVAM Recommendation on the 3T3 Neutral Red Uptake Cytotoxicity Assay for Acute Oral Toxicity Testing. Joint Research Centre Scientific and Policy Reports. Luxembourg: European Union; 2013.
103. Borenfreund E, Puerner JA. A simple quantitative procedure using monolayer cultures for cytotoxicity assays (HTD/NR-90). *Journal of tissue culture methods.* 1985;9(1):7-9.
104. Sigma, inventor. In vitro toxicology assay kit neutral red based. USA.
105. Sciences IfIV. 3T3 Neutral Red Uptake Phototoxicity 2015 [Available from: <http://www.iivs.org/scientific-services/laboratory-services/phototoxicity/neutral-red-uptake/>].
106. Kyadarkunte A, Patole M, Pokharkar V. In Vitro Cytotoxicity and Phototoxicity Assessment of Acylglutamate Surfactants Using a Human Keratinocyte Cell Line. *Cosmetics.* 2014;1(3):159-70.
107. Liebsch M, Spielmann H, Pape W, Krul C, Deguercy A, Eskes C. UV-induced effects. In: Project JDEE, editor. Establishment of timetables for the phasing out of animal experiments for cosmetics:.
108. Clothier R, Willshaw A, Cox H, Garle M, Bowler H, Combes R. The Use of Human Keratinocytes in the EU/COLIPA International In Vitro Phototoxicity Test Validation Study and the ECVAM/COLIPA Study on UV Filter Chemicals. *Altern Lab Anim.* 1999;27(2):247-59.
109. Bland EJ, Keshavarz T, Bucke C. Using 2', 7'-dichlorodihydrofluorescein-diacetate to assess polysaccharides as immunomodulating agents. *Molecular biotechnology.* 2001;19(2):125-31.
110. Ciapetti G, Granchi D, Verri E, Savarino L, Cenni E, Savioli F, et al. Fluorescent microplate assay for respiratory burst of PMNs challenged in vitro with orthopedic metals. *Journal of biomedical materials research.* 1998;41(3):455-60.
111. Boulton S, Anderson A, Swalwell H, Henderson JR, Manning P, Birch-Machin MA. Implications of using the fluorescent probes, dihydrorhodamine 123 and 2',7'-dichlorodihydrofluorescein diacetate, for the detection of UVA-induced reactive oxygen species. *Free radical research.* 2011;45(2):139-46.
112. Anderson ME. Determination of glutathione and glutathione disulfide in biological samples. *Methods in enzymology.* 1985;113:548-55.
113. Nakchat O, Nalinratana N, Meksuriyen D, Pongsamart S. Tamarind seed coat extract restores reactive oxygen species through attenuation of glutathione level and antioxidant enzyme expression in human skin fibroblasts in response to oxidative stress. *Asian Pacific Journal of Tropical Biomedicine.* 2014;4(5):379-85.

114. Dias da Silva D, Silva MJ, Moreira P, Martins MJ, Valente MJ, Carvalho F, et al. In vitro hepatotoxicity of 'Legal X': the combination of 1-benzylpiperazine (BZP) and 1-(m-trifluoromethylphenyl)piperazine (TFMPP) triggers oxidative stress, mitochondrial impairment and apoptosis. *Archives of toxicology*. 2016.
115. Naksuriya O, Okonogi S. Comparison and combination effects on antioxidant power of curcumin with gallic acid, ascorbic acid, and xanthone. *Drug discoveries & therapeutics*. 2015;9(2):136-41.
116. Cai Y, Luo Q, Sun M, Corke H. Antioxidant activity and phenolic compounds of 112 traditional Chinese medicinal plants associated with anticancer. *Life sciences*. 2004;74(17):2157-84.
117. Bogdan Allemann I, Baumann L. Antioxidants used in skin care formulations. *Skin therapy letter*. 2008;13(7):5-9.
118. McNeely W, Goa KL. 5-Methoxypsoralen. A review of its effects in psoriasis and vitiligo. *Drugs*. 1998;56(4):667-90.
119. Liu WX, Jia FL, He YY, Zhang BX. Protective effects of 5-methoxypsoralen against acetaminophen-induced hepatotoxicity in mice. *World journal of gastroenterology*. 2012;18(18):2197-202.
120. Konda S, Maibach HI. Percutaneous penetration of 5-methoxypsoralen in rhesus monkeys. *Food and Chemical Toxicology*. 2011;49(5):1092-5.
121. Lee YM, Wu TH, Chen SF, Chung JG. Effect of 5-methoxypsoralen (5-MOP) on cell apoptosis and cell cycle in human hepatocellular carcinoma cell line. *Toxicology in Vitro*. 2003;17(3):279-87.
122. Honigsmann H, Jaschke E, Gschnait F, Brenner W, Fritsch P, Wolff K. 5-Methoxypsoralen (Bergapten) in photochemotherapy of psoriasis. *The British journal of dermatology*. 1979;101(4):369-78.
123. Okamoto Y, Ryu A, Ohkoshi K. In vitro alternatives and phototoxicity testing. I. Evaluation of in vitro phototoxicity assays. *Altern Lab Anim*. 1999;27(4):639-64.
124. Broeders JJ, Blaauboer BJ, Hermens JL. In vitro biokinetics of chlorpromazine and the influence of different dose metrics on effect concentrations for cytotoxicity in Balb/c 3T3, Caco-2 and HepaRG cell cultures. *Toxicology in vitro : an international journal published in association with BIBRA*. 2013;27(3):1057-64.
125. Bachour-El Azzi P, Sharanek A, Abdel-Razzak Z, Antherieu S, Al-Attrache H, Savary CC, et al. Impact of inflammation on chlorpromazine-induced cytotoxicity and cholestatic features in HepaRG cells. *Drug metabolism and disposition: the biological fate of chemicals*. 2014;42(9):1556-66.
126. Otreba M, Zdybel M, Pilawa B, Beberok A, Wrzesniok D, Rok J, et al. EPR spectroscopy of chlorpromazine-induced free radical formation in normal human melanocytes. *European biophysics journal : EBJ*. 2015;44(5):359-65.
127. Broeders JJW, Parmentier C, Truisi GL, Jossé R, Alexandre E, Savary CC, et al. Biokinetics of chlorpromazine in primary rat and human hepatocytes and human HepaRG cells after repeated exposure. *Toxicology in Vitro*. 2015;30(1, Part A):52-61.

128. Marletta MA. The merck index. An encyclopedia of chemicals, drugs, and biologicals. Tenth Edition. Martha Windholz, Editor; Susan Budavari, Co-Editor; Rosemary F. Blumetti, Associate Editor, Elizabeth S. Otterbein, Assistant Editor. 2, 067 pp. (including tables and index). Rahway, New Jersey: Merck & Co., Inc., 1983. \$28.50. *Hepatology*. 1985;5(1):165-.
129. Förster D, Reiser G. Nucleotides protect rat brain astrocytes against hydrogen peroxide toxicity and induce antioxidant defense via P2Y receptors. *Neurochemistry International*. 2016;94:57-66.
130. Spikes JD. Photosensitizing properties of quinine and synthetic antimalarials. *Journal of Photochemistry and Photobiology B: Biology*. 1998;42(1):1-11.
131. Awasthi S, Srivastava A, Singla ML. Voltammetric determination of citric acid and quinine hydrochloride using polypyrrole–pentacyanonitrosylferrate/platinum electrode. *Synthetic Metals*. 2011;161(15–16):1707-12.
132. Gould JW, Mercurio MG, Elmetts CA. Cutaneous photosensitivity diseases induced by exogenous agents. *Journal of the American Academy of Dermatology*. 1995;33(4):551-73.
133. Huertas A, Wessinger WD, Kucheryavykh YV, Sanabria P, Eaton MJ, Skatchkov SN, et al. Quinine enhances the behavioral stimulant effect of cocaine in mice. *Pharmacology Biochemistry and Behavior*. 2015;129:26-33.
134. Khan SA, Chatterjee SS, Kumar V. Low dose aspirin like analgesic and anti-inflammatory activities of mono-hydroxybenzoic acids in stressed rodents. *Life sciences*. 2016;148:53-62.
135. Julian DG, Chamberlain DA, Pocock SJ. A comparison of aspirin and anticoagulation following thrombolysis for myocardial infarction (the AFTER study): a multicentre unblinded randomised clinical trial. *BMJ : British Medical Journal*. 1996;313(7070):1429-31.
136. Krumholz HM, Radford MJ, Ellerbeck EF, Hennen J, Meehan TP, Petrillo M, et al. Aspirin in the Treatment of Acute Myocardial Infarction in Elderly Medicare Beneficiaries. *Circulation*. 1995;92(10):2841.
137. Johnston SC, Amarenco P, Albers GW, Denison H, Easton JD, Evans SR, et al. Ticagrelor versus Aspirin in Acute Stroke or Transient Ischemic Attack. *The New England journal of medicine*. 2016;375(1):35-43.
138. Algra AM, Rothwell PM. Effects of regular aspirin on long-term cancer incidence and metastasis: a systematic comparison of evidence from observational studies versus randomised trials. *The Lancet Oncology*. 2012;13(5):518-27.
139. Onoue S, Hosoi K, Wakuri S, Iwase Y, Yamamoto T, Matsuoka N, et al. Establishment and intra-/inter-laboratory validation of a standard protocol of reactive oxygen species assay for chemical photosafety evaluation. *Journal of Applied Toxicology*. 2013;33(11):1241-50.
140. Onoue S, Hosoi K, Toda T, Takagi H, Osaki N, Matsumoto Y, et al. Intra-/inter-laboratory validation study on reactive oxygen species assay for chemical photosafety evaluation using two different solar simulators. *Toxicology in Vitro*. 2014;28(4):515-23.
141. Narayan M, Peralta DA, Gibson C, Zitnyar A, Jinwal UK. An optimized InCell Western screening technique identifies hexachlorophene as a novel potent TDP43 targeting drug. *Journal of Biotechnology*. 2015;207:34-8.

142. Siva M, Ramamurthy K, Dhamodharan R. Sodium salt admixtures for enhancing the foaming characteristics of sodium lauryl sulphate. *Cement and Concrete Composites*. 2015;57:133-41.
143. Jung HJ, Ahn HI, Park JY, Ho MJ, Lee DR, Cho HR, et al. Improved oral absorption of tacrolimus by a solid dispersion with hypromellose and sodium lauryl sulfate. *International Journal of Biological Macromolecules*. 2016;83:282-7.
144. Lelièvre D, Justine P, Christiaens F, Bonaventure N, Coutet J, Marrot L, et al. The episkin phototoxicity assay (EPA): Development of an in vitro tiered strategy using 17 reference chemicals to predict phototoxic potency. *Toxicology in Vitro*. 2007;21(6):977-95.
145. Pinto MM, Sousa ME, Nascimento MS. Xanthone derivatives: new insights in biological activities. *Current medicinal chemistry*. 2005;12(21):2517-38.
146. Panda SS, Chand M, Sakhuja R, Jain SC. Xanthoness as potential antioxidants. *Current medicinal chemistry*. 2013;20(36):4481-507.
147. Kondo M, Zhang L, Ji H, Kou Y, Ou B. Bioavailability and antioxidant effects of a xanthone-rich Mangosteen (*Garcinia mangostana*) product in humans. *Journal of agricultural and food chemistry*. 2009;57(19):8788-92.
148. Pedro M, Cerqueira F, Sousa MEI, Nascimento MSJ, Pinto M. Xanthoness as inhibitors of growth of human cancer cell lines and Their effects on the proliferation of human lymphocytes In Vitro. *Bioorganic & Medicinal Chemistry*. 2002;10(12):3725-30.
149. Zhao X, Chen Q, Liu Y, Xia C, Shi J, Zheng M. Effect of xanthone derivatives on animal models of depression. *Current therapeutic research, clinical and experimental*. 2014;76:45-50.
150. Taram F, Winter AN, Linseman DA. Neuroprotection comparison of chlorogenic acid and its metabolites against mechanistically distinct cell death-inducing agents in cultured cerebellar granule neurons. *Brain Research*. 2016;1648, Part A:69-80.
151. Yang Z, Tan Z, Li F, Li X. An effective method for the extraction and purification of chlorogenic acid from ramie (*Boehmeria nivea* L.) leaves using acidic ionic liquids. *Industrial Crops and Products*. 2016;89:78-86.
152. Budryn G, Zaczynska D, Oracz J. Effect of addition of green coffee extract and nanoencapsulated chlorogenic acids on aroma of different food products. *LWT - Food Science and Technology*. 2016;73:197-204.
153. Correia-da-Silva M, Cidade H, Sousa E, Pinto M. Searching for Small Molecules with Antioxidant and Anticoagulant Properties to Fight Thrombosis. Columbia International Publishing. 2014;1(1)(43-50).
154. Correia-da-Silva M, Sousa E, Duarte B, Marques F, Cunha-Ribeiro LM, Pinto MM. Dual anticoagulant/antiplatelet persulfated small molecules. *European journal of medicinal chemistry*. 2011;46(6):2347-58.
155. Chiarini A, Micucci M, Malaguti M, Budriesi R, Ioan P, Lenzi M, et al. Sweet Chestnut (*Castanea sativa* Mill.) Bark Extract: Cardiovascular Activity and Myocyte Protection against Oxidative Damage. *Oxidative Medicine and Cellular Longevity*. 2013;2013:10.

156. Díaz Reinoso B, Couto D, Moure A, Fernandes E, Domínguez H, Parajó JC. Optimization of antioxidants – Extraction from *Castanea sativa* leaves. *Chemical Engineering Journal*. 2012;203:101-9.
157. Almeida IF, Fernandes E, Lima JL, Costa PC, Bahia MF. Protective effect of *Castanea sativa* and *Quercus robur* leaf extracts against oxygen and nitrogen reactive species. *Journal of photochemistry and photobiology B, Biology*. 2008;91(2-3):87-95.
158. Díaz-Reinoso B, Moure A, Domínguez H, Parajó JC. Membrane concentration of antioxidants from *Castanea sativa* leaves aqueous extracts. *Chemical Engineering Journal*. 2011;175:95-102.
159. Huang J, Nguyen V, Tang X, Wei J, Lin X, Lai Z, et al. Protection from diclofenac-induced liver injury by Yulangsan polysaccharide in a mouse model. *Journal of Ethnopharmacology*. 2016;193:207-13.
160. Encinas S, Bosca F, Miranda MA. Phototoxicity associated with diclofenac: a photophysical, photochemical, and photobiological study on the drug and its photoproducts. *Chemical research in toxicology*. 1998;11(8):946-52.
161. Ioele G, Tavano L, De Luca M, Ragno G, Picci N, Muzzalupo R. Photostability and ex-vivo permeation studies on diclofenac in topical niosomal formulations. *International Journal of Pharmaceutics*. 2015;494(1):490-7.
162. Klammer H, Schlecht C, Wuttke W, Schmutzler C, Gotthardt I, Köhrle J, et al. Effects of a 5-day treatment with the UV-filter octyl-methoxycinnamate (OMC) on the function of the hypothalamo-pituitary–thyroid function in rats. *Toxicology*. 2007;238(2–3):192-9.
163. Montenegro L, Carbone C, Puglisi G. Vehicle effects on in vitro release and skin permeation of octylmethoxycinnamate from microemulsions. *International Journal of Pharmaceutics*. 2011;405(1–2):162-8.
164. Puglia C, Damiani E, Offerta A, Rizza L, Tirendi GG, Tarico MS, et al. Evaluation of nanostructured lipid carriers (NLC) and nanoemulsions as carriers for UV-filters: Characterization, in vitro penetration and photostability studies. *European Journal of Pharmaceutical Sciences*. 2014;51:211-7.
165. Huong SP, Andrieu V, Reynier J-P, Rocher E, Fourneron J-D. The photoisomerization of the sunscreen ethylhexyl p-methoxy cinnamate and its influence on the sun protection factor. *Journal of Photochemistry and Photobiology A: Chemistry*. 2007;186(1):65-70.
166. Klammer H, Schlecht C, Wuttke W, Jarry H. Multi-organic risk assessment of estrogenic properties of octyl-methoxycinnamate in vivo: A 5-day sub-acute pharmacodynamic study with ovariectomized rats. *Toxicology*. 2005;215(1–2):90-6.
167. Brown J. Health concerns place sunscreen ingredients under scrutiny. 2000.
168. Jentzsch F, Olsson O, Westphal J, Reich M, Leder C, Kümmerer K. Photodegradation of the UV filter ethylhexyl methoxycinnamate under ultraviolet light: Identification and in silico assessment of photo-transformation products in the context of grey water reuse. *Science of The Total Environment*. 2016.

169. MacManus-Spencer LA, Tse ML, Klein JL, Kracunas AE. Aqueous photolysis of the organic ultraviolet filter chemical octyl methoxycinnamate. *Environmental science & technology*. 2011;45(9):3931-7.
170. Gonzalez H, Tarras-Wahlberg N, Stromdahl B, Juzeniene A, Moan J, Larko O, et al. Photostability of commercial sunscreens upon sun exposure and irradiation by ultraviolet lamps. *BMC Dermatol*. 2007;7:1.
171. Struwe M, Greulich K-O, Suter W, Plappert-Helbig U. The photo comet assay—A fast screening assay for the determination of photogenotoxicity in vitro. *Mutation Research/Genetic Toxicology and Environmental Mutagenesis*. 2007;632(1–2):44-57.
172. Detoni CB, Souto GD, da Silva ALM, Pohlmann AR, Guterres SS. Photostability and Skin Penetration of Different E-Resveratrol-Loaded Supramolecular Structures. *Photochemistry and Photobiology*. 2012;88(4):913-21.
173. Scognamiglio I, De Stefano D, Campani V, Mayol L, Carnuccio R, Fabbrocini G, et al. Nanocarriers for topical administration of resveratrol: A comparative study. *International Journal of Pharmaceutics*. 2013;440(2):179-87.
174. Baur JA, Sinclair DA. Therapeutic potential of resveratrol: the in vivo evidence. *Nature reviews Drug discovery*. 2006;5(6):493-506.
175. Rekus MT. haracterization of growth and differentiation of a spontaneously immortalized keratinocyte cell line (HaCaT) in a defined, serum-free culture system 2000.
176. Zanatta CF, Mitjans M, Urgatondo V, Rocha-Filho PA, Vinardell MP. Photoprotective potential of emulsions formulated with Buriti oil (*Mauritia flexuosa*) against UV irradiation on keratinocytes and fibroblasts cell lines. *Food and chemical toxicology : an international journal published for the British Industrial Biological Research Association*. 2010;48(1):70-5.
177. Rai V, Dayan N, Michniak-Kohn B. A comparative evaluation of photo-toxic effect of fractionated melanin and chlorpromazine hydrochloride on human (dermal fibroblasts and epidermal keratinocytes) and mouse cell line/s (fibroblast Balb/c 3T3). *Toxicology in vitro : an international journal published in association with BIBRA*. 2011;25(2):538-44.
178. Wilhelm KP, Biel S, Siegers CP. Role of flavonoids in controlling the phototoxicity of *Hypericum perforatum* extracts. *Phytomedicine : international journal of phytotherapy and phytopharmacology*. 2001;8(4):306-9.
179. Woods JA, Ferguson JS, Kalra S, Degabriele A, Gardner J, Logan P, et al. The phototoxicity of vemurafenib: An investigation of clinical monochromator phototesting and in vitro phototoxicity testing. *Journal of photochemistry and photobiology B, Biology*. 2015;151:233-8.
180. Rajnochova Svobodova A, Zalesak B, Biedermann D, Ulrichova J, Vostalova J. Phototoxic potential of silymarin and its bioactive components. *Journal of photochemistry and photobiology B, Biology*. 2016;156:61-8.
181. Yadav N, Dwivedi A, Mujtaba SF, Kushwaha HN, Singh SK, Ray RS. Ambient UVA-induced expression of p53 and apoptosis in human skin melanoma A375 cell line by quinine. *Photochem Photobiol*. 2013;89(3):655-64.

182. Kim EJ, Kim MJ, Im NR, Park SN. Photolysis of the organic UV filter, avobenzene, combined with octyl methoxycinnamate by nano-TiO₂ composites. *Journal of Photochemistry and Photobiology B: Biology*. 2015;149:196-203.
183. Lynch AM, Wilcox P. Review of the performance of the 3T3 NRU in vitro phototoxicity assay in the pharmaceutical industry. *Experimental and Toxicologic Pathology*. 2011;63(3):209-14.
184. Liebsch M, Traue D, Barrabas C, Spielmann H, Gerberick GF, Cruse L, et al. Prevalidation of the EpiDerm™ Phototoxicity Test. In: D. G. Clark SGLaRM, editor. *Alternatives to Animal Testing II*. Brussels: COLIPA; 1999. p. 160-7.
185. Eruslanov E, Kusmartsev S. Identification of ROS using oxidized DCFDA and flow-cytometry. *Methods in molecular biology* (Clifton, NJ). 2010;594:57-72.
186. Kalyanaraman B, Darley-Usmar V, Davies KJA, Dennery PA, Forman HJ, Grisham MB, et al. Measuring reactive oxygen and nitrogen species with fluorescent probes: challenges and limitations. *Free Radical Biology and Medicine*. 2012;52(1):1-6.